



D4.2: Intermediate deployment of beyond 5G RAN, core, and open-source networks, disruptive RAN technologies and trial controller

Revision: 1.0

Work package	WP 4
Task	T4.1, T4.2, T4.3, T4.4
Due date	30/11/2024 (M23)
Submission date	28/11/2024
Deliverable lead	NOKIA
Version	1.0
Authors	Nokia: Olli Liinamaa VTT: Jarno Pinola, Olli Apilo Vicomtech: Roberto Viola CGE: Javier Godas, Aurora Ramos I2CAT: Daniel Camps Mur, Amr Abdelnabi UOULU: Antti Pauanne, Jussi Haapola, Mahdi Salmani, Jani Pellikka, Sabbir Ahmed, Marko Leinonen IT: Hemalatha Vulchi Interdigital: Javier Lorca Hernando Ericsson: Diego San Cristobal IMEC: Miguel Glassee, Björn Debaille
Reviewers	IT: Mohammed Al-Rawi, Telefonica: Fernando Pargas Nieto / Telefonica
Abstract	This document outlines the design and initial performance of XR XR enablers 3GPP, O-RAN and Disruptive paths towards 6G. It also reports a first implementation of the Trial Controller.

Keywords	Extended Reality (XR), 5G/6G, Holographic Communications, 3D Digital Twin, Energy optimization, Network Slicing, Resolution adaptation, Control plane optimization, O-RAN, disruptive RAN, Trial controller, Network controlled repeaters, Reconfigurable intelligent surfaces, ATSSS.
-----------------	--

Document Revision History

Version	Date	Description of change	List of contributor(s)
V0.1	21/05/2024	1st version of the ToC for comments	See Authors
V0.2	10/11/2024	Version for External Review	Olli Liinamaa, Daniel Camps Mur
V1.0	27/11/2024	Version for publishing	Olli Liinamaa

DISCLAIMER



Co-funded by the European Union



Project funded by

Schweizerische Eidgenossenschaft
Confédération suisse
Confederazione Svizzera
Confederaziun svizra
Swiss Confederation

Federal Department of Economic Affairs,
Education and Research EAER,
State Secretariat for Education,
Research and Innovation SERI

6G-XR (6G eXperimental Research infrastructure to enable next-generation XR services) project has received funding from the [Smart Networks and Services Joint Undertaking \(SNS JU\)](#) under the European Union’s [Horizon Europe research and innovation programme](#) under Grant Agreement No 101096838. This work has received funding from the [Swiss State Secretariat for Education, Research, and Innovation \(SERI\)](#).

Views and opinions expressed are however those of the author(s) only and do not necessarily reflect those of the European Union. Neither the European Union nor the granting authority can be held responsible for them.

COPYRIGHT NOTICE

© 2023 - 2025 6G-XR Consortium

Project co-funded by the European Commission in the Horizon Europe Programme		
Nature of the deliverable:	R	
Dissemination Level		
PU	Public, fully open, e.g. web (Deliverables flagged as public will be automatically published in CORDIS project’s page)	✓
SEN	Sensitive, limited under the conditions of the Grant Agreement	
Classified R-UE/ EU-R	EU RESTRICTED under the Commission Decision No2015/ 444	
Classified C-UE/ EU-C	EU CONFIDENTIAL under the Commission Decision No2015/ 444	
Classified S-UE/ EU-S	EU SECRET under the Commission Decision No2015/ 444	

* R: Document, report (excluding the periodic and final reports)

DEM: Demonstrator, pilot, prototype, plan designs

DEC: Websites, patents filing, press & media actions, videos, etc.

DATA: Data sets, microdata, etc.

DMP: Data management plan

ETHICS: Deliverables related to ethics issues.

SECURITY: Deliverables related to security issues

OTHER: Software, technical diagram, algorithms, models, etc.

EXECUTIVE SUMMARY

This is 2nd deliverable of Work Package 4 (WP4) – “Experimental RAN infrastructure”. WP4 focuses on the deployment of 6G-XR beyond 5G cellular network infrastructure. D4.1 identified innovative XR enabler technologies and created initial design with related KPIs for XR solution assuming B5G networks with three evolution paths: 3GPP, OPEN-RAN (O-RAN) and DISRUPTIVE.

Deliverable D4.2 describes initial deployment and first performance evaluation of 5 3GPP enablers, 3 ORAN enablers, and 3 Disruptive enablers. Next steps are discussed for each enabler. The deliverable also reports on a first implementation of the Trial Controller, which has been made available both for the south node and the north node. defines interim deployments for enablers allowing XR services assuming mentioned evolution paths. New enablers are to be integrated and tested at the project’s north node (UOULU’s 5GTN and VTT’s 5GTN) and south node (i2CAT’s 5GBarcelona and Capgemini’s 5TONIC), and performance results are also documented if available. Deployment includes also XR trial controller meant to ease the automatic deployment of XR-related experimentations and remote use of testbed.

TABLE OF CONTENTS

DISCLAIMER	3
COPYRIGHT NOTICE	3
1 INTRODUCTION	13
1.1 OBJECTIVE OF THE DELIVERABLE.....	13
1.2 Structure of the deliverable.....	13
1.3 target audience OF THE DELIVERABLE	14
2 3GPP XR ENABLERS	15
2.1 Summary of proposed 3gpp enablers in D4.1	15
2.2 3GPP XR proposed ENABLERS: DESIGN AND INITIAL IMPLEMENTATION RESULTS	16
2.2.1 Network-Controlled Repeaters in indoor environment	16
2.2.2 Network assisted Rate Control API	19
2.2.3 ATSSS based capacity enhancement	23
2.2.4 Energy and Application aware management of 3GPP infrastructure	25
2.2.5 Upgrade and evaluation of experimental RAN infrastructure in SN and NN	29
3 O-RAN XR ENABLERS	35
3.1 SUMMARY of ORAN ENABLERS in D4.1	35
3.2 O-RAN XR proposed ENABLERS	36
3.2.1 Congestion aware load balancing	36
3.2.2 Energy-aware E2E resource management.....	39
3.2.3 O-RAN enabled slicing to support XR services	43
4 6G DISRUPTIVE XR ENABLERS	49
4.1 SUMMARY of DISRUPTIVE ENABLERS proposed in D4.1	49
4.2 6G DISRUPTIVE XR Proposed ENABLERS	50
4.2.1 High-Frequency Transceivers for THz-RIS and ISAC	50
4.2.2 Baseband implementation for THz-RIS and ISAC based on SC-FDE	56
4.2.3 Deep Reinforcement Learning for THz-RIS	60
5 6G-XR TRIAL CONTROLLER	64
5.1 Update Trial CONTROLLER architecture	64
5.2 Initial trial CONTROLLER implementation	65
5.2.1 Common Trial Engine components	65
5.2.2 South Node Trial Engine Components.....	67
5.2.3 North Node Trial Engine Components	72
6 SUMMARY	80



7 REFERENCES..... 81

LIST OF FIGURES

FIGURE 1. DEPLOYMENT SCENARIO FOR INDOOR XR APPLICATIONS WITH NCR-ASSISTED NETWORK ARCHITECTURE FOR XR 17

FIGURE 2. PERFORMANCE ANALYSIS: ECDF OF SNR AND THROUGHPUT FOR NCR AND NON-NCR CONFIGURATIONS..... 18

FIGURE 3. NETXRATE COMPONENTS INTERACTION AND SIGNALLING MESSAGES. USAGE SCENARIO FOR XR NETWORK ASSISTED RATE CONTROL API ENabler 19

FIGURE 4. NETWORK ASSISTED RATE CONTROL API ARCHITECTURE (NETXRATE) WITH RED ARROW INDICATING THE NEW PROPOSED ANALYTICS. 20

FIGURE 5. NETXRATE COMPONENTS INTERACTION AND SIGNALLING MESSAGES..... 21

FIGURE 6. (A) NETXRATE OUTAGE VS NUMBER OF CLUSTERS (LEFT) AND (B) NETXRATE AGGREGATED THROUGHPUT VS NUMBER OF CLUSTERS (RIGHT)..... 22

FIGURE 7. ATSSS ENabler TO AGGREGATE PUBLIC 5G WITH INDOOR WI-FI 23

FIGURE 8. ENVISIONED ATSSS ENabler ARCHITECTURE, FEATURING OPENVSWITCH AND A 5G/WI-FI CAPACITY ESTIMATION FUNCTION 24

FIGURE 9. VALIDATION OF I2CAT'S HOLOMIT APPLICATION TRANSMITTING EACH HOLOGRAM IN DIFFERENT TCP PORTS IN A 3-PARTY CALL 25

FIGURE 10. USAGE AND TEST SCENARIO FOR ENERGY EFFICIENT XR SERVICES IN 3GPP INFRASTRUCTURE. 26

FIGURE 11. 3GPP RAN INFRASTRUCTURE SETUP UTILISED IN THE VTT 5GTN TEST FACILITY. 27

FIGURE 12: SOLUTION DESIGN INCLUDING FR1+FR2 RADIOS AND UPF FOR LOCAL BREAKOUT (LEFT) AND RACK DEPLOYED IN 5TONIC DURING THE PREPARATION PHASE (RIGHT) 30

FIGURE 13: RACK DEPLOYED IN I2CAT 30

FIGURE 14: OUTDOOR 5G AT OULU 5GTN 31

FIGURE 15. UPGRADED FR2 CAPABILITIES DEPLOYED AT THE VTT 5GTN TEST FACILITY..... 32

FIGURE 16. USAGE SCENARIO FOR O-RAN CONGESTION AWARE LOAD BALANCING ENabler..... 36

FIGURE 17. DESIGN OF ORAN CDF FUNCTION TO ENFORCE HO UPON CONGESTION 37

FIGURE 18. UE REPORTING RAPP SIGNALLING MESSAGES 38

FIGURE 19. CONGESTION REPORTING RAPP SIGNALLING MESSAGES 38

FIGURE 20. VALIDATING AMARISFOT HO XAPP 39

FIGURE 21. USAGE AND TEST SCENARIO FOR ENERGY EFFICIENT XR SERVICES IN O-RAN INFRASTRUCTURE. 40

FIGURE 22. O- RAN INFRASTRUCTURE DEPLOYED AT THE VTT 5GTN TEST FACILITY. 40

FIGURE 23. O-RAN TEST SETUP OVERVIEW SHOWN THROUGH THE ACCELLERAN DRAX DASHBOARD... 42

FIGURE 24. E2 NODE COMPONENTS SHOWN THROUGH THE ACCELLERAN DRAX DASHBOARD. 42

FIGURE 25. O-RAN DISAGGREGATED NETWORK ARCHITECTURE BROUGHT BY THE OC1 6G-SLICE PROJECT TO 5GTN FACILITY. 44

FIGURE 26. TEST SETUP IN THE UNIVERSITY OF OULU LABORATORY 45

FIGURE 27. URLLC AND EMBB SLICE DATA LOAD AND LATENCIES IN NORMAL LOAD 46

FIGURE 28. URLLC AND EMBB SLICE DATA LOAD AND LATENCIES WHEN EMBB IS OVERLOADED WITH DATA..... 47

FIGURE 29. 140 GHZ BEAMSTEERING TRANSMITTER SCHEMATIC..... 51

FIGURE 30. 140 GHZ TX EVALUATION SET-UP. 52

FIGURE 31 SCREENSHOT OF 5G-NR MODULATION ANALYSIS 53

FIGURE 32. RF ARCHITECTURE OF THE DESIGNED 300 GHZ SLIDING IFRECEIVER AND PHOTOGRAPH OF THE MANUFACTURED RFIC []..... 54

FIGURE 33. SINEWAVE SIGNAL MEASUREMENT SETUP AND 300 GHZ RECEIVER’S GAIN CURVE..... 55

FIGURE 34. MODULATED SIGNAL MEASUREMENT SETUP FOR 300 GHZ RECEIVER TESTING [] 55

FIGURE 35. MEASUREMENT SETUP FOR 300 GHZ RECEIVER TESTING 56

FIGURE 36: BUILDING BLOCKS OF THE EXPERIMENTAL PLATFORM COMPRISING THE BASEBAND AND HIGH-FREQUENCY TRANSCEIVER IMPLEMENTATION..... 57

FIGURE 37: UNCODED BER COMPARISON BETWEEN SC-FDE AND CP-OFDM FOR CDL-E CHANNEL..... 59

FIGURE 38: CODED BLER COMPARISON BETWEEN SC-FDE AND CP-OFDM FOR CDL-E CHANNEL. 59

FIGURE 39. CODED BLER COMPARISON BETWEEN SC-FDE AND CP-OFDM FOR CDL-B CHANNEL. 60

FIGURE 40. INDOOR XR MEETING ENABLED BY DRL-AIDED THZ-RIS 61

FIGURE 41. COMPARISON OF AVERAGE SPECTRAL EFFICIENCY (SE) WITH NUMBER OF RIS ELEMENTS FOR IN MULTI-USER XR SCENARIOS TYPICALLY USING 28GHZ AND 140GHZ. 62

FIGURE 42. DRL ALGORITHM CURVE FOR DIFFERENT TIME STEPS. 63

FIGURE 43. INITIAL ARCHITECTURE DESIGN OF 6G-XR TRIAL CONTROLLER..... 64

FIGURE 44. TRIAL CONTROLLER ARCHITECTURE..... 65

FIGURE 45. UNIFIED WEB PORTAL..... 66

FIGURE 46. SOUTH NODE TRIAL CONTROLLER COMPONENTS 68

FIGURE 48. CREATION OF A NST IN THE SOUTH NODE WEB PORTAL 69

FIGURE 49. LIST OF NSTS IN THE SOUTH NODE WEB PORTAL..... 70

FIGURE 50. WORKFLOW AMONG SOUTH NODE TRIAL CONTROLLER COMPONENTS..... 71

FIGURE 51. NORTH WEB PORTAL. 73

FIGURE 52. NORTH WEB PORTAL (NST MANAGEMENT) 74

FIGURE 53. ARCHITECTURE OF NNA. 74

FIGURE 54. INTERACTION BETWEEN NNA AND QOSIUM. 75

FIGURE 55. INITIALIZATION PHASE OF NNA OPERATION. 77

FIGURE 56. EXECUTION PHASE OF NNA OPERATION..... 78

FIGURE 57. TERMINATION PHASE OF NNA OPERATION..... 79



LIST OF TABLES

TABLE 1. SUMMARY OF PROPOSED 6G-XR ENABLERS IN THE 3GPP PATH 15

TABLE 2. MAIN SIMULATION SETTINGS FOR THE NCR-BASED INDOOR COVERAGE MODEL..... 18

TABLE 3. MEASURED MAXIMUM POWER CONSUMPTION REDUCTIONS AT 3GPP RAN INFRASTRUCTURE LEVEL WITH DIFFERENT ENERGY SAVING METHODS..... 28

TABLE 4: PARAMETERS CONFIGURED IN 5TONIC TESTING 33

TABLE 5: PERFORMANCE RESULTS OBTAINED AT 5TONIC LAB 33

TABLE 6: PRELIMINARY APPLICATION-LEVEL KPI RESULTS MEASURED WITH THE FR2 OUTDOOR RADIOS AT THE VTT 5GTN TEST FACILITY 33

TABLE 7. SUMMARY OF PROPOSED 6G-XR ENABLERS IN THE O-RAN PATH..... 35

TABLE 8. SUMMARY OF PROPOSED 6G-XR ENABLERS IN THE DISRUPTIVE PATH..... 49

TABLE 9: 5G NR PUSCH EVM CONFORMANCE SPECIFICATIONS 52

TABLE 10. EVM MEASUREMENTS RESULTS SUMMARY 53

TABLE 11 : SIMULATION ASSUMPTIONS FOR EVALUATION OF THE SW-BASED LINK LEVEL SIMULATOR OF THE BASEBAND PROCESSING BLOCKS. 58

ABBREVIATIONS

6G	6 th generation mobile network
5G	5th generation mobile network
5GTN	5G Test Network
3D	3 Dimensional
3GPP	Third Generation Partnership Project
ADC	Analog to Digital Converter
AF	Application Function
AMC	Adaptive Modulation and Coding
ANBR	Access Network Bitrate Recommendation
API	Application Programable Interface
AS	Application Server
ATSSS	Adaptive Traffic Switching Steering Splitting
BLER	Block Error Rate
BSoTA	Beyond-state-of- the-art
SoTA	State of the art
CAD	Computer Aided Design
CEF	Capacity Estimation Function
CCC	Cell Configuration and Control
CDF	Congestion Detection Function
CG	Cloud Gaming
C-Link	Control Link
CNC	Computerized Numerical Control
CO ₂	Carbon Dioxide
COTS	Commercial Off-the-Shelf
CP	Control Plane
CPU	Central Processing Unit
CSS	Cascading Style Sheets
CU	Central Unit
DAC	Digital to Analog Converter
DC	Data Channel
DCS	Data Channel Server
DDPG	Deep Deterministic Policy Gradient
DF	Decode and Forward
DL	Downlink
DNN	Deep Neural Network
DRL	Deep Reinforcement Learning
DRX	Discontinuous Reception
DSP	Digital Signal Processing
DT	Digital Twin
DTX	Discontinuous Transmission
DU	Distributed Unit
DWDM	Dense Wavelength Division Multiplexing
E-UTRA	Evolved Universal Terrestrial Radio Access
E2E	End-to-End
EARFCN	E-UTRA Absolute Radio Frequency Channel Number
EI	External Interface
eMBB	enhanced Mobile Broadband
EPC	Evolved Packet Core

ETSI	European Telecommunications Standards Institute
FoV	Field of View
FMI	Finnish Meteorological Institute
FPS	Framerate Per Second
FRx	Frequency Range x
gNB	5G NodeB
GPS	Global Positioning System
GPU	Graphics Processing Unit
GUI	Graphical User Interface
HMD	Head-Mounted Display
HW	Hardware
IAB	Integrated Access and Backhaul
IF	Intermediate Frequency
InH	Indoor Hotspot
ISAC	Integrated Sensing and Communications
KPI	Key Performance Indicator
KPM	Key Performance Measurements
L1/L2	Layer 1/Layer 2
LO	Local Oscillator
LoS	Line of Sight
MBB	Mobile Broadband
ML	Machine Learning
mmWave/mmW	Millimeter-wave
MR	Mixed Reality
NCR	Network Controlled Repeater
NCR-Fwd	NCR Forwarding
NCR-MT	NCR Mobile Termination
NG-RAN	Next Generation Radio Access Network
NI	Network Interface
NN	North Node
NR	New Radio
O2I	Outdoor-to-Indoor
O-CU	O-RAN Central Unit
O-DU	O-RAN Distributed Unit
O-RAN	Open Radio Access Network
O-RU	O-RAN Radio Unit
OTT	Over-the-top
PAPR	Peak to Average Power Ratio
PRB	Physical Resource Block
PTP	Precision Time Protocol
QoE	Quality of Experience
QoS	Quality of Service
RAN	Radio Access Network
rAPP	RAN Application
RB	Resource Block
RC	RAN Control
RF	Radio Frequency
RI	Research Infrastructure
RIC	RAN Intelligent Controller
RIS	Reconfigurable Intelligent Surface
RL	Reinforcement Learning

RMSE	Root Mean Squared Error
RRH	Remote Radio Head
RRM	Radio Resource Management
RT	Real Time
RU	Radio Unit
Rx	3GPP Release x
SC-FDE	Single-Carrier Frequency Domain Equalization
SDR	Software-Defined Radio
SINR	Signal-to-Interference plus Noise Ratio
SMO	Service Management and Orchestration
SN	South Node
SNR	Signal-to-Noise Ratio
SW	Software
T	Task
TDD	Time Division Duplexing
THz	Terahertz
TRX	Transmit-Receive
UE	User Equipment
UI	User Interface
UL	Uplink
UMa	Urban Macro
UP	User Plane
UPF	User Plane Function
uRLLC	ultra-Reliable and Low Latency Communications
VR	Virtual Reality
Wi-Fi	Wireless Fidelity
WP	Work Package
xAPP	eXtended application
XR	Extended Reality
XRM	XR and Media Services

1 INTRODUCTION

Extended Reality (XR) is an umbrella term covering Virtual Reality (VR), Augmented Reality (AR) and Mixed Reality (MR), which provides immersive experiences from a blend of the virtual and real worlds and finds applications in several emerging use cases across different domains and sectors. XR requires performance enablers that can support stringent requirements with respect to low latency, high capacity, low power consumption and high reliability, among other KPIs [1].

This deliverable D4.2 introduces the initial design done in the project, and initial evaluation of identified new XR enabler technologies that have been identified in the project and documented in D4.1. Structure follows the categorization of XR enablers to three alternative paths from current commercial 5G technology to 6G - 3GPP based evolution path, OPEN-RAN (O-RAN), and DISRUPTIVE 6G. In addition to XR enablers contributing to three alternative paths, this document describes also the deployment of Trial Controller, which is implemented to ease the automatic deployment of XR-related experimentations in the two test facilities of the project (south node and north node) [2].

1.1 OBJECTIVE OF THE DELIVERABLE

This deliverable has three main objectives for each new XR enabler and for the Trial Controller: (1) Justification of the value, or motivation, of each enabler supporting the respective path towards 6G, (2) Solution design of the implemented enabler giving the reader a sufficient level of details of the structure of each new asset to support the utilization of XR based services in a mobile environment and (3) initial validation results of the deployments if available.

1.2 STRUCTURE OF THE DELIVERABLE

The 6G-XR project aims to demonstrate technological feasibility of innovative radio spectrum technologies of beyond 5G and 6G spectrum and validate an E2E beyond 5G architecture including E2E service provisioning supporting evolution from current architectures with slicing capabilities, and at cloud implementation level (Open RAN).

Therefore, the deliverable D4.2 is covering the state of the art for RAN, beyond 5G RAN, core, and open-source networks, as well as disruptive RAN XR enabling technologies. Those enabler technologies are categorized to support alternative paths from 5G networks towards 6G as described above.

Deliverable D4.2 is structured as follows:

- Chapter 2 details identified five XR enablers following the evolution of 3GPP defined extensions for XR support in each 3GPP release.
- Chapter 3 focuses on introducing three enablers relevant to O-RAN architecture, and utilizing customized xAPPs/rAPPs allowing modifying the RAN behaviour to maximize the operational efficiency based on the service needs.

- Chapter 4 describes two enablers relevant for high-frequency solutions and thus assuming mobile connectivity for tailored network use.
- Chapter 5 describes the trial controller common design components and selected deployments to north and south experimentation sites.
- Chapter 6 concludes the document.

1.3 TARGET AUDIENCE OF THE DELIVERABLE

This deliverable is a public report which targets the project consortium, stakeholders, academic and research organizations, EU commission services, and the public.

2 3GPP XR ENABLERS

2.1 SUMMARY OF PROPOSED 3GPP ENABLERS IN D4.1

After XR was introduced in R15 and then enhanced in R16 with additional features the basis was set for the introduction of XR based services assuming 5G New Radio (NR). It presented the baseline XR use cases and services, core enablers and network interfaces, as well as the description of its media functions, formats, and features, among others. Evolution of XR capabilities through 3GPP releases have been analyzed in the project and documented in D4.1.

To fill some of the non-solved gaps, the project presented five technology enablers studied in 3GPP and supporting and enhancing XR. This chapter describes the interim enabler research results showing the value or motivation of each enabler, explaining the solution design giving the reader a sufficient level of details of the structure and initial validation results of the deployments if available.

Table below summarizes the five technical enablers presented in this section, while highlighting their applicability to the 6G-XR use cases described in deliverable D1.1 [3].

Table 1. Summary of proposed 6G-XR enablers in the 3GPP path

Proposed 3GPP XR Enabler	Target XR gap	Relation to 6GXR use case
Network-controlled repeaters for coverage extension	Coverage enhancements for indoor UEs	Contributes to UC1 – holoportation, by enhancing the UL and DL capacity that is required for capture and transmission of point clouds
Network assisted rate control API for XR services	Enhance performance of rate control mechanisms used by XR services. Focus is on shifting from OTT estimation mechanisms to network assisted mechanisms.	Contributes to UC1 – holoportation, by allowing the application to control the data rate according to network capacity
ATSSS based capacity enhancements	Combines indoor Wi-Fi with public 5G to enhance capacity of indoor XR users	Contributes to UC1 – holoportation, by enhancing the UL and DL capacity that is required for capture and transmission of point clouds
Energy and application aware management of 3GPP infrastructure	Optimize 3GPP configuration (cells, DRX) according to application needs	Contributes to UC4 – Collaborative 3D Digital Twin-like Environment and UC5 – Energy Measurement Framework for Energy

		Sustainability: Enhancing energy efficiency of both UEs and network with slow (non-RT) control when XR applications are used.
Upgrade of experimental facilities	Deployment of local breakout, FR1+FR2 and network exposure capabilities in 6G-XR experimental sites	Transversal – applies to all use cases

2.2 3GPP XR PROPOSED ENABLERS: DESIGN AND INITIAL IMPLEMENTATION RESULTS

2.2.1 Network-Controlled Repeaters in indoor environment

2.2.1.1 Motivation

The deployment of XR applications in indoor environments faces significant challenges related to coverage and signal quality. As highlighted in D4.1, these challenges stem from indoor blockages caused by objects, high Outdoor-to-Indoor (O2I) penetration losses, and increased path losses from the outdoor serving gNB. These issues are exacerbated at higher frequency ranges, particularly Frequency Range 2 (FR2), which is more susceptible to blockage and higher path losses compared to Frequency Range 1 (FR1). The motivation behind the development and implementation of Network-Controlled Repeaters (NCRs) is to address these challenges by enhancing signal quality, extending coverage, and improving the overall user experience (QoE) for indoor XR users. NCRs, with their advanced beamforming capabilities and dynamic control by the gNB, provide a robust solution to mitigate the coverage and blockage issues inherent in indoor XR deployments.

2.2.1.2 Solution design

Figure 1 shows the NCR-assisted building blocks of the architecture for the XR application scenario considered, where the blocks newly introduced/enhanced are coloured in brown. The architecture’s principal modules were considered to design and choose simulation parameters. The approach was aligned with 3GPP specifications, aiming to enhance indoor coverage by facilitating outdoor-to-indoor (O2I) signal propagation using NCR technology. The solution design investigates the NCR setup through system-level simulations in an urban environment, using real-world location data for an area in Barcelona, Spain, which corresponds to the location of the 6G-XR south node site. The focus is on benchmarking NCR against traditional setups to observe enhancements in throughput, signal-to-noise ratio (SNR), and other performance indicators, particularly for XR applications.

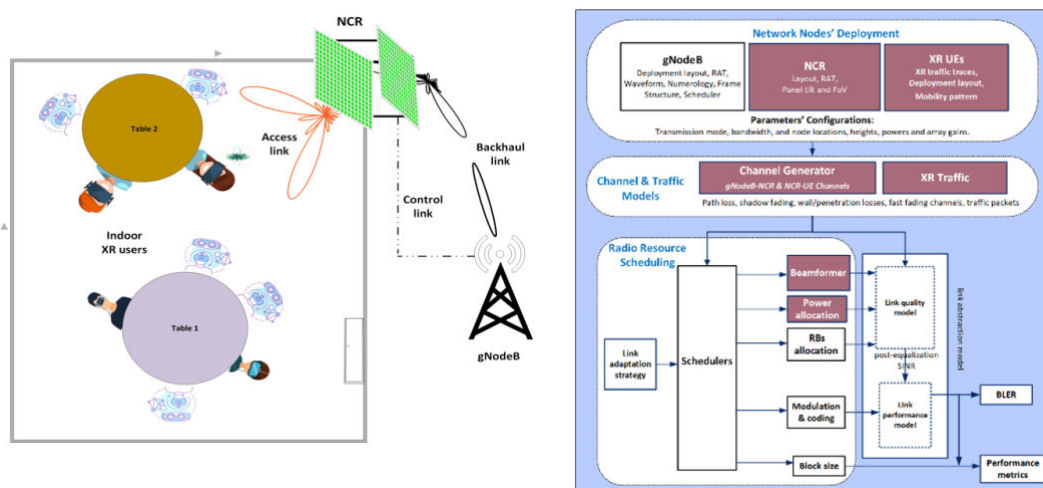


Figure 1. Deployment scenario for indoor XR applications with NCR-assisted network architecture for XR

2.2.1.3 Initial evaluation results

2.2.1.3.1 Evaluation methodology

The Vienna LTE-A (Long-Term Evolution-Advanced) Simulator, also known as the Vienna System Level Simulator, is being explored and studied [4]. It is an open-source tool designed for research and development in the field of mobile communications. Developed by the Institute of Telecommunications at Vienna University of Technology, it provides a detailed and flexible platform to simulate and analyse various aspects of wireless communication systems, including LTE-A and 5G NR (New Radio) networks. The simulator can be adapted for XR applications, focusing on mobility, beam tracking, and optimization algorithms, which are essential for delivering high-performance user experiences.

The simulation was conducted using the **Vienna 5G SLS base simulator** and mapped to a real-world urban scenario. Simulation parameters include a 3.5 GHz frequency, 20 MHz bandwidth to establish a baseline performance for the system. Starting with 20 MHz provides a foundation for model validation, making it easier to scale to wider bandwidths, such as 100 MHz, to evaluate the system's performance under higher throughput and more stringent requirements. Moreover, a 100 MHz bandwidth is more applicable at higher frequency bands, such as 28GHz which is planned to consider for FR2 bands. Various network configurations such as NCR and UE distances (c.f. Table 2 below) and channel models such as Urban Macro and Street Canyon were used to emulate real deployment scenarios.

Mapped Area: The simulation was conducted in the i2CAT area of Barcelona, Spain, chosen for its urban characteristics that closely resemble typical deployment environments where outdoor-to-indoor (O2I) propagation faces challenges, and because it hosts the radio equipment of the 6G-XR south node. The specific area is mapped using OpenStreetMap coordinates, with a latitude of 41.38475 and longitude of 2.10797. This urban setting features densely packed buildings, diverse infrastructure, and environmental factors that simulate real-world complexities for signal propagation, making it an ideal testing ground for evaluating the effectiveness of Network-Controlled Repeaters (NCR) in improving indoor coverage.

Table 2. Main simulation settings for the NCR-based indoor coverage model

Parameter	Details
Mapped Area	i2CAT area, Barcelona, Spain
Frequency (Freq.)	3.5 GHz
Bandwidth (BW)	20 MHz
Base Station (BS)	Power: 48 dBm, Height: 30 m, Tri-sector
Network-Controlled Repeater (NCR)	Height: 10 m, Gain: 35 dB (maximum), Distance: 20 m
User Equipment (UE)	Power: 0 dBi, Height: 1.5 m
Subcarrier Spacing (SCS)	30 kHz
Channel Models	Urban Macro (BS-UE), Street Canyon (NCR-UE)
Scheduling	Full buffer, round robin
Base Simulator	Vienna 5G SLS
Latitude/Longitude	Latitude: 41.38475, Longitude: 2.10797

2.2.1.3.2 Results

Initial results indicate that a system-level simulation of NCR-based setups for both FR1 and full-buffer traffic outperforms traditional non-NCR setups, particularly in overcoming O2I signal loss. Key metrics observed include improvements in throughput and downlink-uplink Signal-to-Noise Ratio (SNR). The visualizations are shown in the Figure 2 below which supports the defined case with parameters for NCR’s potential in improving indoor network coverage and reliability.

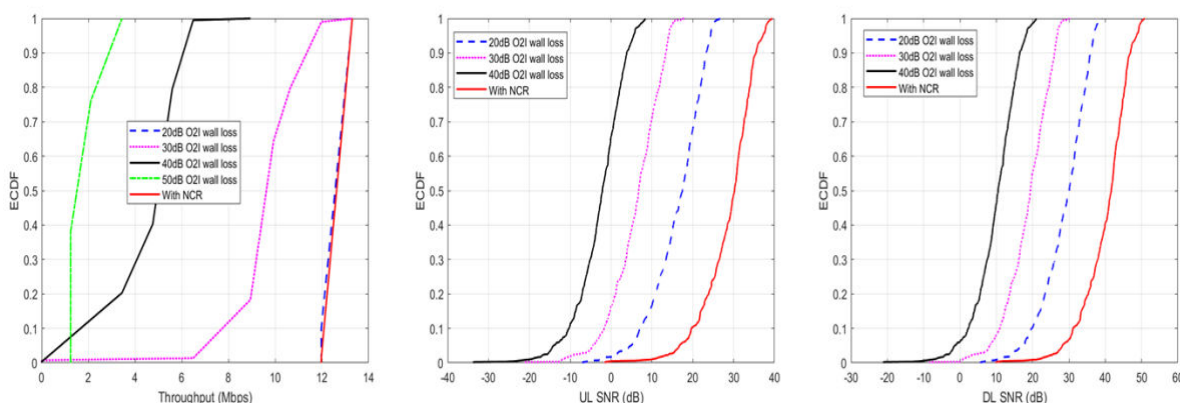


Figure 2. Performance Analysis: ECDF of SNR and Throughput for NCR and non-NCR configurations.

Key Observations:

Throughput Improvement: The NCR-based setup demonstrated a noticeable improvement in throughput over traditional non-NCR setups, even under full-buffer traffic conditions.

Enhanced Downlink-Uplink SNR: NCR implementation showed superior downlink and uplink SNR compared to setups without NCR. This enhancement is particularly beneficial for environments with high interference and signal attenuation, such as indoor spaces.

Benchmarking Against Baseline: The NCR setup was benchmarked against a non-NCR setup under similar conditions. The results consistently indicated that the NCR provides significant gains in both

throughput and SNR, highlighting its potential as an effective solution for delivering consistent indoor coverage.

2.2.1.4 Planned next steps

Next steps involve developing an analytical model for XR traffic by incorporating experimental data to capture XR-specific requirements such as high data rates and low latency. The NCR setup will be extended to operate at FR2 frequencies, providing higher bandwidth for XR demands. Advanced beamforming techniques, like adaptive beam tracking and narrow-beam steering, will be integrated to enhance signal reliability. Additionally, exploring of new XR scenarios are planned to further refine network performance in diverse, high-frequency indoor environments.

2.2.2 Network assisted Rate Control API

2.2.2.1 Motivation

As mentioned in D4.1, XR applications are expected to transmit large amounts of data both in the uplink and downlink directions. Since radio resources are also shared with Internet users, XR users are then pushing the cell to congestion that leads to QoS degradation. XR services use mechanisms that rely on over-the-top (OTT) estimations of available capacity to adapt the data-rate of the media flows, but those mechanisms are not efficient in interactive XR services since the buffering should be kept at the minimum. Therefore, new mechanisms based on the information provided by the network are required to allow the media origins to tune rate for the media flow. The 3GPP envisioned having the network as a platform offering APIs that enhance performance. Motivated by this approach, CAMARA project [5] developed APIs tailored to contribute to services. Among those APIs, CAMARA Quality on Demand (QoD) API [6] is foreseen as an essential enabler for XR services. In 6GXR, one of the useful XR network enablers is the network assisted rate control API that leverages the use of XR client feedback, and the network offered capacity to tune the XR media rate.

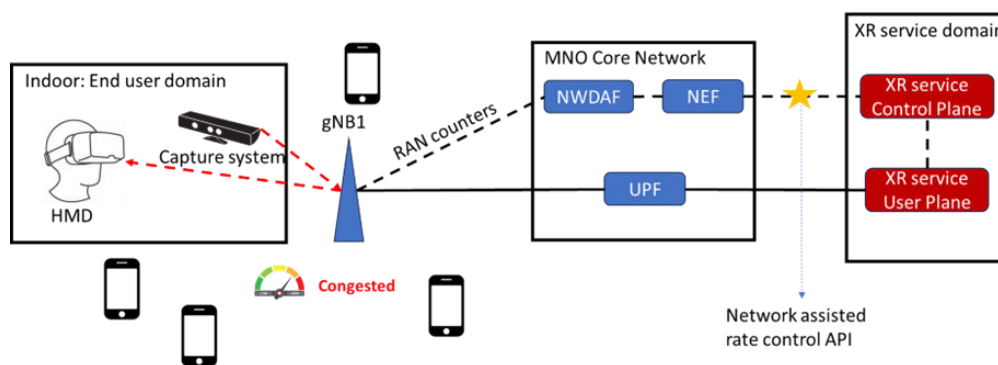


Figure 5. NetXRate components interaction and signalling messages. Usage scenario for XR network assisted rate control API enabler

Figure 3. Network Assisted rate control API architecture (NextXRate) visualized in Figure 5. NetXRate components interaction and signalling messages. depicts the scenario for XR network assisted rate control where the XR user uses the capture system to generate data in uplink, and Head Mounted Display (HMD) to receive data in the downlink. The XR user shares the cell capacity with Internet users that produce a variable load, leading the cell to congestion. The XR service functions are connected to the Core Network of the public network, both in the user and the control planes.

2.2.2.2 Solution design

To address the previous gap, an API called NetXRRate is proposed. The architecture is depicted in Figure 3. The main novelty of NetXRRate is that the rate control function of the XR service can subscribe to explicit rate recommendations from the network. This subscription is available through the Network Exposure Function (NEF) of the 5GCore. The NetXRRate rate recommendations are with configurable interval, and each recommendation should be understood as the maximum capacity for that session available at a given time. Thus, NetXRRate is not meant to replace the OTT rate control algorithm, but to complement it by making the NetXRRate recommendation to be a maximum cap on the data rate recommended by the XR rate control function.

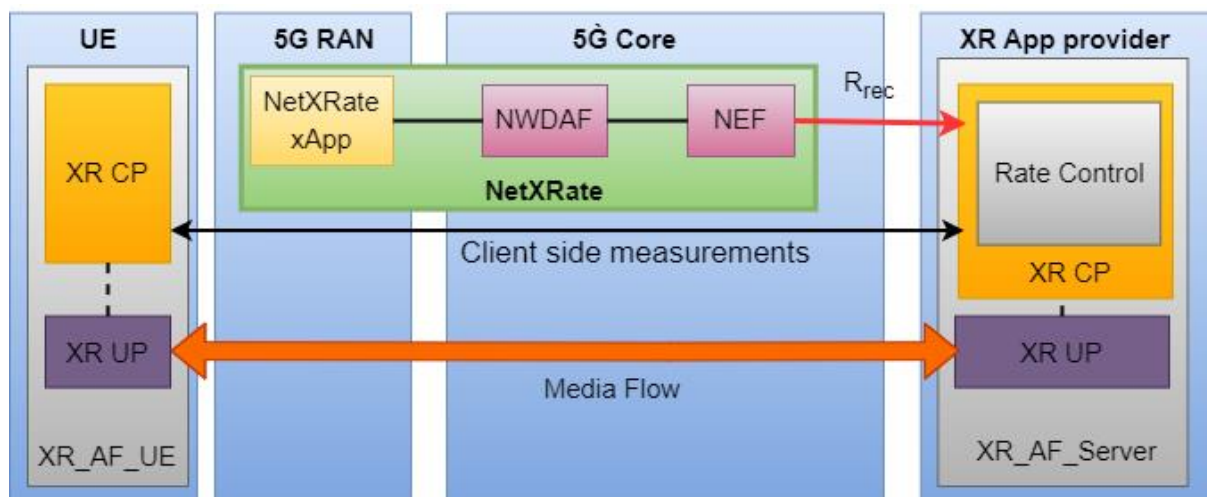


Figure 3. Network Assisted rate control API architecture (NextXRRate) with red arrow indicating the new proposed analytics.

The sequence diagram in Figure 5 details the signalling between the components of NetXRRate and their interaction. The XR rate control function of the XR AF Server requests the required Uplink (UL)/ Downlink (DL) data rates for a given PDU session through the NEF using an IP address. The NEF forwards this request to the NWDAF, which stores the NetXRRate recommendations. The NWDAF module identifies the UE's serving cell using AMF's LocationReporting APIs, then identifies the appropriate NetXRRate xApp instance to handle this UE. Each xApp instance manages a limited number of cells. The NWDAF module maps the IP address to a RAN identifier (RANID) using AMF services, as the NetXRRate xApp understands only RANIDs. The xApp subscribes to the Distributed Unit (DU) handling the target cell, requesting E2 Key Performance Measurement (KPM) counters. These counters are used to derive the recommended rate for each XR UE in the cell. The rate recommendations are then reported back to the XR rate control function, which uses them to limit the maximum rate for the XR user plane function.

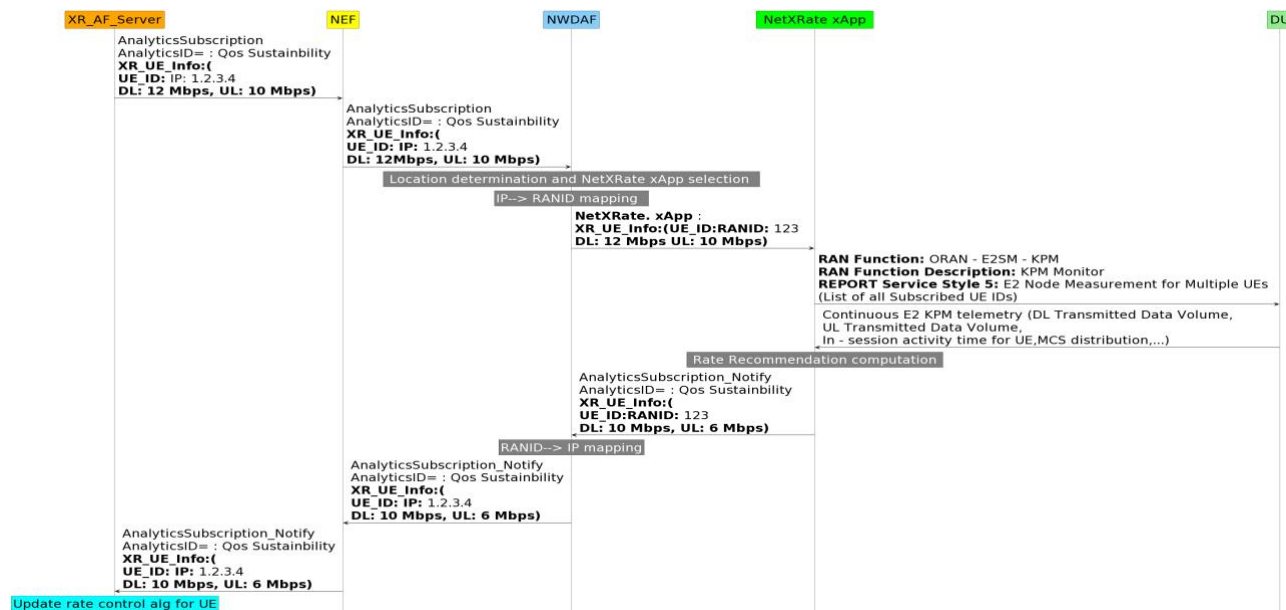


Figure 5. NetXRRate components interaction and signalling messages.

The NetXRRate xApp aims to generate rate recommendations by estimating a fair network capacity that can be allocated to each XR user in the cell. The MAC scheduler in the DU uses a Proportional Fair (PF) scheduling algorithm. This link between the NetXRRate xApp (seated in the nrt-RIC) and the PF scheduler seated in the DU is challenging. However, thanks to the E2-KPM service model that provides the necessary data such as: 1) The Required data rate for i^{th} XR user in the cell at time t is $r_i(t)$, 2) Maximum cell capacity $C_i(t)$ derived from the cell's configuration parameters via the E2 interface, and 3) Effective data rate, $R_i(t)$ received by each user, using the minimum MCS over the last τ seconds to avoid exceeding cell capacity, with MCS statistics obtained through the E2 KPM service model. Using this information, the NetXRRate xApp calculates the recommended capacity for each XR user in the below three steps:

1. The effective data rate share for each user is calculated as the ratio between the $R_i(t)$ and $C_i(t)$. Then the weighted required XR rate per user is the ratio between the required data rate and effective data rate share.
2. The water-filling algorithm is then applied with inputs, the maximum cell capacity and the weighted required XR rate per user to generate initial per-user capacity assignments.
3. Scale each per-user capacity assignments by its associated effective data rate share resulting in the recommended rate per user.

2.2.2.3 Initial evaluation results

2.2.2.3.1 Evaluation methodology

The Network assisted Rate Control API has been evaluated. Using ns3 simulations where it is used to study the maximum gains achievable by this API when a tight integration between the RAN and our analytics module is possible.

2.2.2.3.2 Results

The preliminary results obtained in Figure 5 (a) demonstrate the growth of outage probability across all strategies as the number of clusters increases. However, when NetXRRate is applied, the PacketSize and IPA rate adaptation strategies exhibit significantly lower outage rates. Specifically, under the considered scenario, NetXRRate achieves up to a 60% reduction in outage probability for the PacketSize

strategy and up to a 72% reduction for the IPA strategy. This improvement is attributed to NetXRate’s ability to align the media source rate with the instantaneous channel capacity, thereby avoiding network overload. Such overloads typically arise in over-the-top (OTT) strategies when multiple UEs independently execute their rate control algorithms and simultaneously demand data rates that exceed the network’s available capacity. By implementing NetXRate’s recommendations, the aggregate data requests from XR UEs within the same cell are regulated, ensuring they remain within the cell’s total capacity. However, despite the reduction in overload situations, some may still occur with NetXRate due to inaccuracies in MCS estimation.

In Figure 5 (b), each XR rate adaptation strategy’s throughput is shown over the wireless channel (dashed bars) and as the aggregated throughput after playback buffering at each UE (solid bars). For a given rate adaptation strategy, the disparity between dashed and solid bars reflects wasted throughput—data transmitted over the wireless channel but failing to reach the playback buffer in time. By adapting the media rate to match the estimated wireless capacity, NetXRate improves effective throughput by up to 30% for the PacketSize strategy and up to 25% for the IPA strategy compared to the OTT approach. The results clearly show the enhanced network efficiency achieved by NetXRate’s centralized capacity allocation for each XR session.

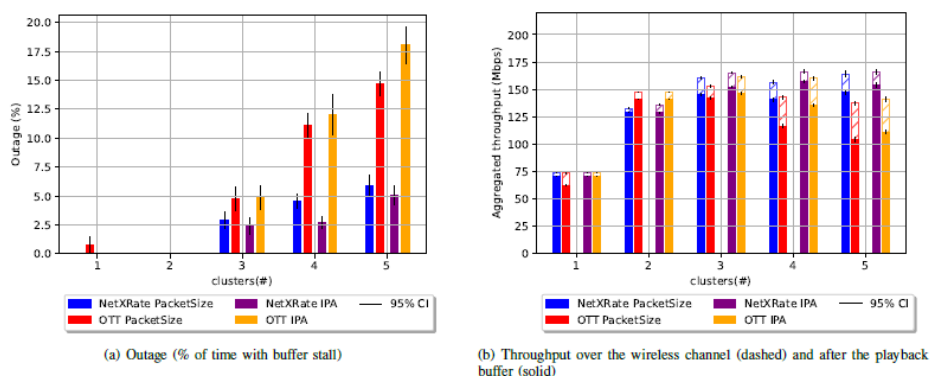


Figure 5. (a) NetXRate outage vs number of clusters (left) and (b) NetXRate aggregated throughput vs number of clusters (right)

The results depicted are summary of what were demonstrated in the accepted paper at Globecomm 2024 [7].

2.2.2.4 Planned next steps

The work presented in this deliverable has focused on scenarios where only XR users are present in the same cell. This work will be evolved towards D4.3 by considering more realistic scenarios where both XR and eMBB users coexist in the same cell, and evaluating the benefits provided by NetXRate when XR users are prioritized by the core network (e.g. through CAMARA QoD). The next is to have a simplified version of our API to be tested in the i2CAT laboratory, using a Amarisoft gNB. This step is essential to define the API communication between the network and the holoportation application developed in WP3. In the final step the API and the holoportation application will be integrated and validated in the south node infrastructure. Results will be shown in D4.3.

2.2.3 ATSSS based capacity enhancement

2.2.3.1 Motivation

As described in D4.1, one of the main gaps that need to be addressed to enable a widespread deployment of holographic communications is to enhance uplink and downlink capacities. The Adaptive Traffic Steering, Switching and Splitting (ATSSS) enabler addresses this gap by allowing end-users of XR devices to aggregate capacity available in their Wi-Fi networks with the capacity made available by a public 5G network.

Figure 6 depicts the high-level architecture envisioned for this enabler, where collocated with the UPF and with the XR devices (HMD and capture system), an ATSSS function that is in charge of controlling the data that flows through Wi-Fi and the public 5G networks is observed, in a way that is transparent for the XR application.

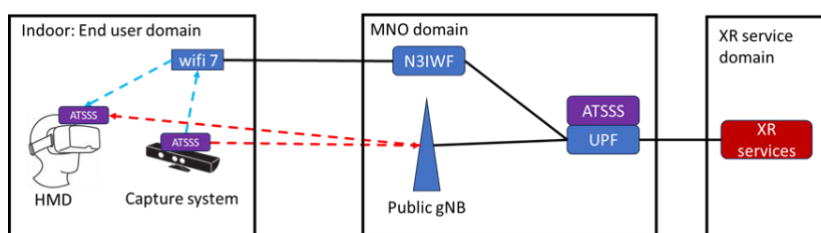


Figure 6. ATSSS enabler to aggregate public 5G with indoor Wi-Fi

2.2.3.2 Solution design

In this section an implementation of the ATSSS enabler is presented, which allows to split multiple holograms transmitted to a given user through the Wi-Fi or the 5G networks. The main underlying idea behind our design is the following. In a holographic communication session including N users, each participant will receive $N-1$ holograms in the downlink and will transmit one hologram (its own) in the uplink. Each hologram can be encoded individually, since the maximum resolution for that hologram depends on the capture system and the uplink bandwidth available for the participant generating the hologram. Therefore, from the service perspective, it is possible to assign a target bitrate to each of the holograms that need to be received or transmitted by each participant. Thus, our main idea is the following: *“If the network is aware of the capacity required by each hologram, and each hologram can be recognized as a single flow, then the network can take optimal decisions as to whether each flow needs to be routed through 5G or Wi-Fi to maximize capacity.”*

To accomplish the previous design goals, the solution design depicted in Figure 6 is proposed, which contains two main modules:

- ATSSS user plane: Implemented with a switching function in a network proxy and the CPE, using `openvswitch`¹. This switching function will be programmed with the flow description (IP address and TCP ports) and the resulting interface (Wi-Fi or 5G) to switch this flow.
- ATSSS control plane: Composed of a 5G/Wi-Fi capacity estimation function (CEF), which estimates the dynamically changing capacity available in each network, and a local controller function, which exposes an API that allows the CEF to program the switching rules for each flow.

¹ <https://www.openvswitch.org/>

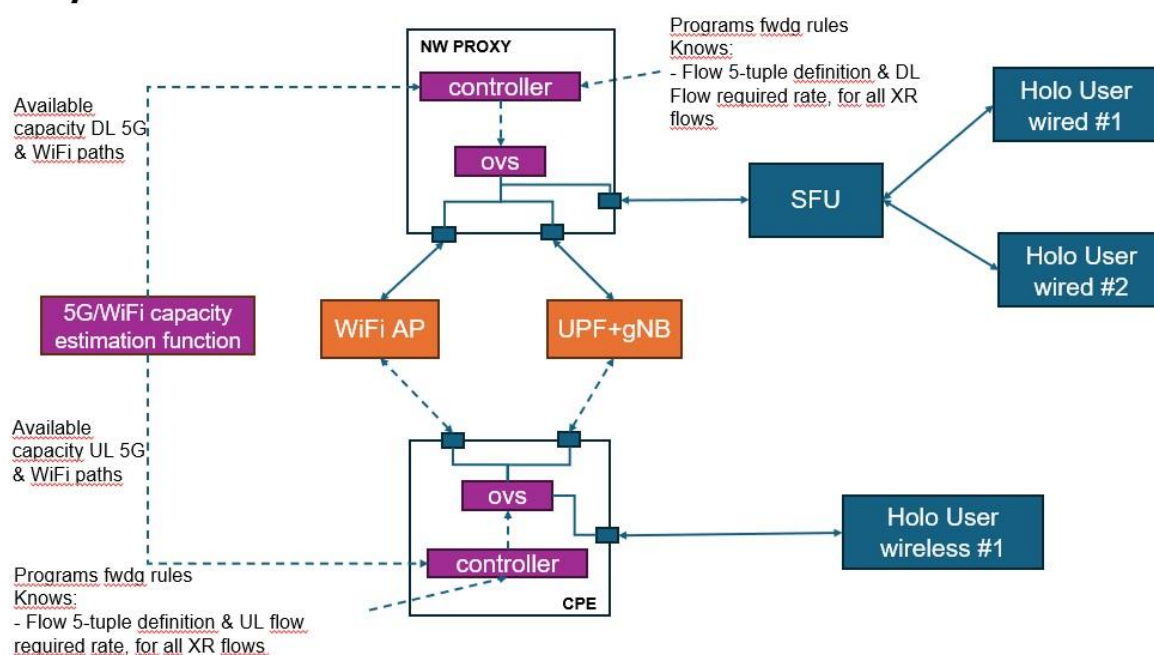


Figure 7. Envisioned ATSSS enabler architecture, featuring openswitch and a 5G/Wi-Fi capacity estimation function

The base design of the 5G/Wi-Fi CEF is presented next, which is currently under development and will be reported in D4.3:

- Information available from each flow: FDataRate
- Information available from each cell:
 - o 5G:
 - Cell level utilization (CellPrb)
 - UE required MCS (UeMcs)
 - PRBs required for a given datarate: $UePrb = EstimateResources(FDataRate, UeMcs)$
 - o Wi-Fi:
 - AP utilization (ApUtil)
 - STA MCS (StaMcs)
 - Utilization required for a given datarate: $StaUtil = EstimateResources(FDataRate, StaMcs)$

Where EstimateResources() is a function that estimates the physical resources required to serve a data rate for a given MCS in each network. Based on this information, the CEF can estimate if a given flow fits in the 5G or Wi-Fi cell, i.e. “CellPrb + UePrb < 1”, or “ApUtil + StaUtil < 1”. A packing algorithm can then be defined to decide where to transmit each flow.

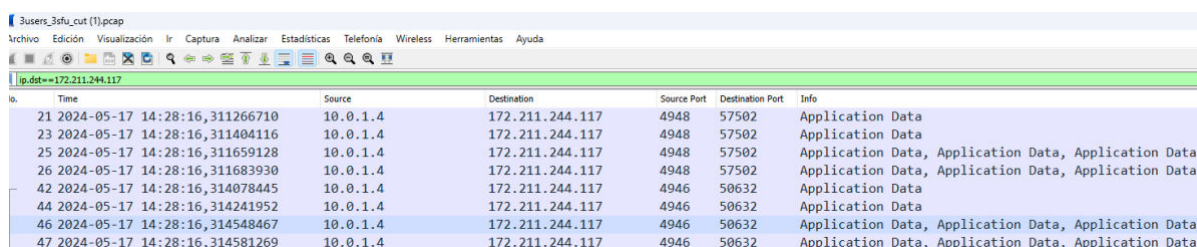
2.2.3.3 Initial evaluation results

2.2.3.3.1 Evaluation methodology

The ATSSS enabler will be evaluated in the i2CAT laboratory using a private 5G network composed of two Amarisoft Cells, an open5gs core and a Wi-Fi 6 Access Point. To emulate terminals capable of connecting both to Wi-Fi and 5G, a custom CPE will be used featuring a Quectel RM500Q 5G module and an Intel Wi-Fi6 M2 module. The Holomit application developed in WP3 will be used as the holographic service to validate the ATSSS enabler.

2.2.3.3.2 Results

This deliverable is focus in the first evaluation on validating our main design assumption that is that individual holograms in the same session can be identified as different flows by the network. To this end, i2CAT's Holomit application developed in WP3 and configure a three-party call is used. In its default configuration Holomit uses the same websocket to transmit all holograms towards a given participant, which makes it impossible to distinguish individual holograms in the network. To address this gap, Holomit has been reconfigured to feature an individual SFU for each participant in the call, which allows then to generate individual flows for each hologram. Figure 8 depicts a Wireshark trace of our experiment, where is possible to see user with IP address 172.211.244.117 receiving from its SFU with IP address 10.0.1.4 two data flows: i) one between ports 4948 and 57502, and ii) one between ports 4946 and 50632. Each of these two flows carries the application data for the holograms of the other 2 participants in the call.



No.	Time	Source	Destination	Source Port	Destination Port	Info
21	2024-05-17 14:28:16,311266710	10.0.1.4	172.211.244.117	4948	57502	Application Data
23	2024-05-17 14:28:16,311404116	10.0.1.4	172.211.244.117	4948	57502	Application Data
25	2024-05-17 14:28:16,311659128	10.0.1.4	172.211.244.117	4948	57502	Application Data, Application Data, Application Data
26	2024-05-17 14:28:16,311683930	10.0.1.4	172.211.244.117	4948	57502	Application Data, Application Data, Application Data
42	2024-05-17 14:28:16,314078445	10.0.1.4	172.211.244.117	4946	50632	Application Data
44	2024-05-17 14:28:16,314241952	10.0.1.4	172.211.244.117	4946	50632	Application Data
46	2024-05-17 14:28:16,314548467	10.0.1.4	172.211.244.117	4946	50632	Application Data, Application Data, Application Data
47	2024-05-17 14:28:16,314581269	10.0.1.4	172.211.244.117	4946	50632	Application Data, Application Data, Application Data

Figure 8. Validation of i2CAT's Holomit application transmitting each hologram in different TCP ports in a 3-party call

2.2.3.4 Planned next steps

After validating in this deliverable that individual holograms can be identified at the network level, our next steps towards D4.3 will be to setup in the lab the scenario described in Figure 7 in order to: i) first, validate the ability of the ATSSS user plane to steer holograms through the 5G or the Wi-Fi access networks, and ii) second, prototyping an ATSSS control plane based on a capacity estimation function that tracks radio KPIs at the 5G and Wi-Fi networks to estimate capacity, driving accordingly the allocation of holograms towards the 5G and Wi-Fi networks.

2.2.4 Energy and Application aware management of 3GPP infrastructure

2.2.4.1 Motivation

As discussed in 6G-XR deliverable D4.1, traditional techniques used in 3GPP networks, such as cell/gNB sleep modes, transmission power/bandwidth adjustments, and Discontinuous Transmission (DTX) are very generic and application agnostic in their approach to the energy consumption minimization. However, in the most recent releases, 3GPP has also investigated more XR specific energy efficiency enablers. These newer approaches are based on application awareness in the scheduling process and require more dynamic behaviour from the gNBs when carrying out the reconfiguration of the RAN. Before purpose-built support for such dynamic changes is available at scale, the activation time of the required energy conserving changes in the current SoTA 3GPP-compliant RAN systems (usually tens of seconds or minutes) as well as the effects of the changes to the connected UEs (potentially lower QoS or even interruptions in the service) can become a bottleneck in real-life deployments.

To familiarize ourselves with the limitations of the current SoTA 3GPP RAN equipment, a series of network configuration changes related to potential energy saving methods for XR data traffic will be tested. A predetermined application specific configuration change (App1 and App2 in Figure 9) is triggered from the network management plane (slow control) when an application change is detected

in the aggregated KPI monitoring data collected from the UE, gNB and 5GC. The time for the changes to take effect in the RAN and their impact on the connected UEs and RAN energy consumption will be recorded.

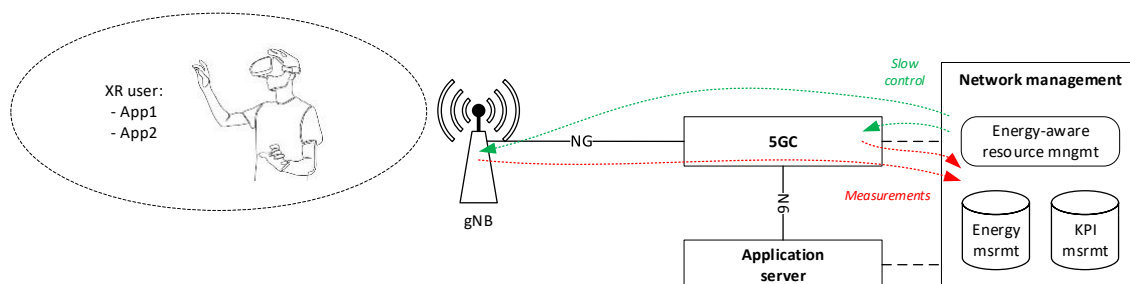


Figure 9. Usage and test scenario for energy efficient XR services in 3GPP infrastructure.

2.2.4.2 Solution design

Figure 10 depicts the RAN setup in the VTT 5GTN test facility utilised for the tests with the 3GPP infrastructure. The test setup is configured around a 5G SA architecture where a macro radio provides a 5G coverage cell for a larger area and pico radios provide 5G capacity booster cells for both the outdoor and indoor environments. This setup provides possibilities to test the suitability of multiple generic high-level RAN energy saving methods with XR application traffic, including at least the following:

1. Putting a capacity cell to deep sleep mode
2. Putting a capacity cell to light sleep mode (cell blocking)
3. Shutting down active transmitters
4. Decreasing the number of antenna beams
5. Decreasing downlink transmission power
6. Decreasing channel bandwidth
7. Discontinuous Transmission (DTX)

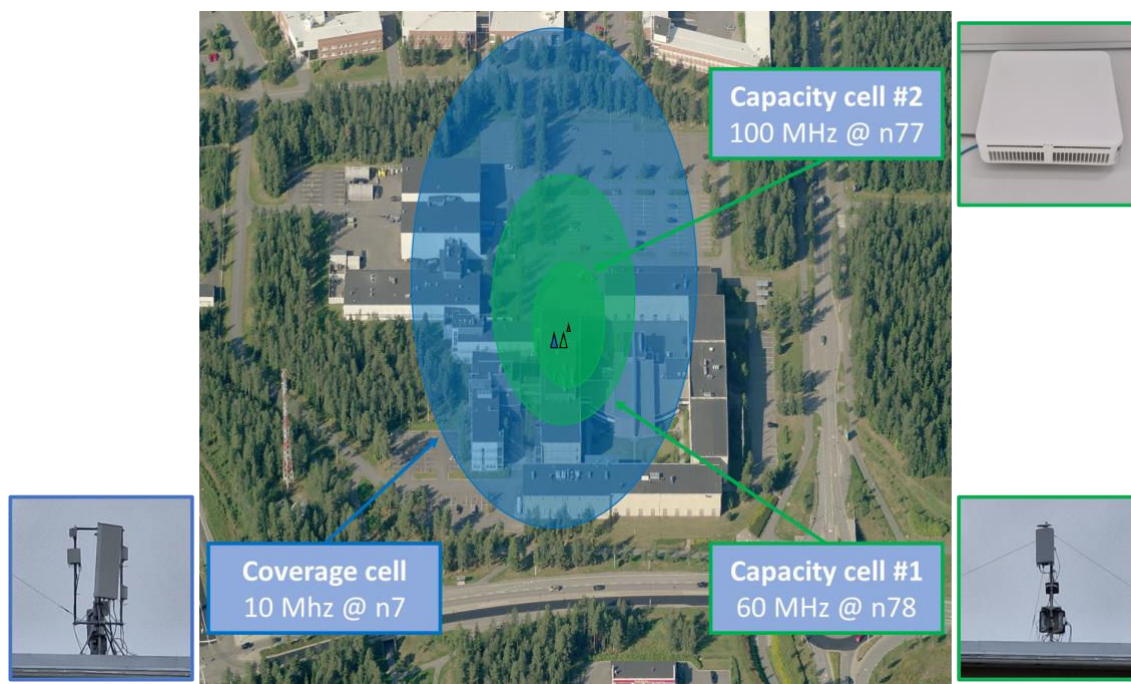


Figure 10. 3GPP RAN infrastructure setup utilised in the VTT 5GTN test facility.

The energy consumption of both the 5G baseband and radio units can be measured with the energy measurement framework described in 6G-XR deliverable D5.1 [8]. In addition to RAN infrastructure components, energy consumption of the UE utilised in the tests can also be measured. The network KPIs (throughput, latency, etc.) are measured mainly by using external KPI measurement tools, i.e., Qosium [9]. Inclusion of the core network and application server components as well as the analysis of the usage scenario with multiple simultaneous users is planned to be brought into the measurement setup towards the end of the experimentation process.

2.2.4.3 Initial evaluation results

2.2.4.3.1 Evaluation methodology

The initial tests to be performed in the measurement setup presented in Figure 10 contain several steps aiming to clarify the potential of the state-of-the-art 3GPP infrastructures in simultaneously supporting energy efficiency optimisation at the architecture level and XR applications with acceptable QoE. The XR applications to be tested are streaming video and VR. These applications were selected for the test as they have very different QoS requirements towards the network. With this aim, the following experimentation steps are performed:

1. Define the data traffic characteristics of the XR application utilised in the test at a level that allows accurate XR application traffic emulation. In the later experimentation phases, the emulated XR application traffic can be used for longer automated measurement campaigns as well as for the emulation of multiple simultaneous users with UeSIM [10].
 - Streaming video requires continuous high data rates per user but is less susceptible to latency and jitter variations.
 - Interactive VR scenarios generate low amounts of data per user but require low latencies and jitter to support user interactions without visible lag.

- In addition to the traffic logs recorded in the VTT 5GTN test facility, utilisation of existing open datasets for test traffic generation will be considered especially for the VR scenario.
2. Use the selected XR applications (and maximum cell loads as reference) to test the potential energy saving methods that can be utilised in the current 3GPP infrastructure without gNB reboots. Relying on synced KPI and energy efficiency measurement data, the test results are analysed so that the trade-offs between the XR application performance and UE/network energy efficiency can be assessed and feasible as well as unfeasible energy saving methods for XR applications can be identified.
 3. Assess the current capabilities (measurement results) and expected future capabilities (3GPP study items) of 3GPP infrastructures in the energy efficient handling of XR application traffic to identify feature gaps and layout the plans for the required future work.

2.2.4.3.2 Results

The deployed test facility updates to be utilised in the tests have been verified to work as expected and initial tests have been performed to find out the most efficient ways to preserve energy in the 3GPP RAN infrastructure. As the aim of these initial tests was to clarify the best-case energy saving potential of the different methods listed in subsection 2.2.4.2, generic test traffic was used to load the network instead of XR applications.

Based on the initial tests, the most suitable and effective energy saving methods in the 3GPP RAN infrastructure (including the coverage cell and two capacity cells) are listed in Table 3. Based on the initial tests, the baseline setup to be used in the further measurements using XR applications will have DTX turned on permanently as it causes no capacity degradation in the RAN. Compared to this baseline setup, the power consumption reductions achievable in best case scenario were -20 % for halving the number of active transmitters which is done autonomously by the base station according to traffic load, -30 % for putting capacity cells to light sleep mode which stops transmission of all signals and allows turning off Power Amplifiers (PA) longer periods of time than in DTX, and -50 % for putting capacity cells to deep sleep mode which allows most of the radio module components to be turned off. Depending on which energy saving method is used, the state changes at the gNB can take from few second up to several minutes which must be taken into consideration when assessing the suitability of these methods for different usage scenarios involving XR applications.

Table 3. Measured maximum power consumption reductions at 3GPP RAN infrastructure level with different energy saving methods

Energy saving method	RAN-level power consumption compared to baseline	Remarks
DTX	Baseline setup	Always on
Shutting down active transmitters	Approx. 20 % reduction	Base station state transition time > 10 seconds (no service break)
Putting a capacity cell to light sleep mode (cell blocking)	Approx. 30 % reduction	Base station wakeup time is few seconds
Putting a capacity cell to deep sleep mode	Approx. 50 % reduction	Base station wakeup time is few minutes

In addition to the energy saving methods deemed to be suitable for the further testing and listed in the above table, some of the methods listed in subsection 2.2.4.2 were verified to be unsuitable or of

low value in the network configuration used for the tests. These included the Tx power and channel bandwidth reductions, both of which could not be configured to be used without full gNB reset leading to long service interruption as well as the reducing the number of antenna beams, which was seen as not applicable for the planned tests due to mixed energy saving results in the utilised test setup. Hence, all further tests will be performed with the subset of energy saving methods listed in the table above.

2.2.4.4 Planned next steps

The deployment of the required infrastructure updates, initial tests, and finalisation of the methodology for the full assessment of this 3GPP RAN enabler have been performed as described above. The next step will be to perform the final measurements using the selected XR applications and analyse the results. This includes the synchronisation of the measurement data from the network KPI and energy measurement frameworks as well as the analysis of the results from the XR applications' QoS requirement perspective to find the best methods to use for networks that are serving varying amounts of XR users. This means that in addition to the system level KPIs on KPI monitoring granularity and RAN re-configuration related service interruptions listed in D4.1 and assessed during the initial tests, new network KPIs will be included into the final measurement campaigns, e.g., in the form of user experienced throughputs for streaming video and content delivery latencies for VR. Based on the findings done during the experiments and review of the ongoing standardisation activities, conclusions on potential technology gaps regarding energy and application aware management of 3GPP infrastructures will be provided in D4.3.

2.2.5 Upgrade and evaluation of experimental RAN infrastructure in SN and NN

2.2.5.1 Motivation

The RAN deployment for experimentation of the UCs in this project aims to tackle the challenges for offering XR services already exposed in D4.1. It enables the local breakout of application traffic by having a User Plane Function (UPF) close to the RAN equipment. It uses the FR2 band to boost capacity both in UL and DL traffic. And it provides features for slicing, QoS profiling and partitioning to be able to guarantee a QoS to the XR services.

2.2.5.2 Deployed network architecture

In this section, the experimental network infrastructure that has been deployed in the South Node and North Node test sites is described. This experimental network will be integrated with the Trial Engine developed in Task 4.4 and will be open to OC3 experimenters.

2.2.5.2.1 3GPP SN deployment

Slight modifications had to be made to the RAN solution from the proposed one in D4.1. The final solution deployed at 5Tonic lab for preliminary testing is the one depicted in Figure 11 (left) and described next. The Ericsson's AIR 4435 is the selected antenna for mid-band. It operates in B77D band (3700-3980 MHz). Two Ericsson's AIR 5322 are used for millimetre wave (mmW) band. They work in B258 band (24.25-27.5 GHz). Two Baseband 6648 are needed to be able to aggregate the mid-band and mmW carriers. An Ericsson's Router 6675 provides components to all components within the solution and to the outside world. There is also a GPS antenna, which allows the router to get the clock reference from GPS and distribute it to the Basebands and Radios via Precision Time Protocol (PTP) for synchronization in phase and time. All this equipment has been installed in a flight rack, cabled and configured. Figure 11 (right) shows the actual appearance of the equipment ready for testing at 5Tonic lab.

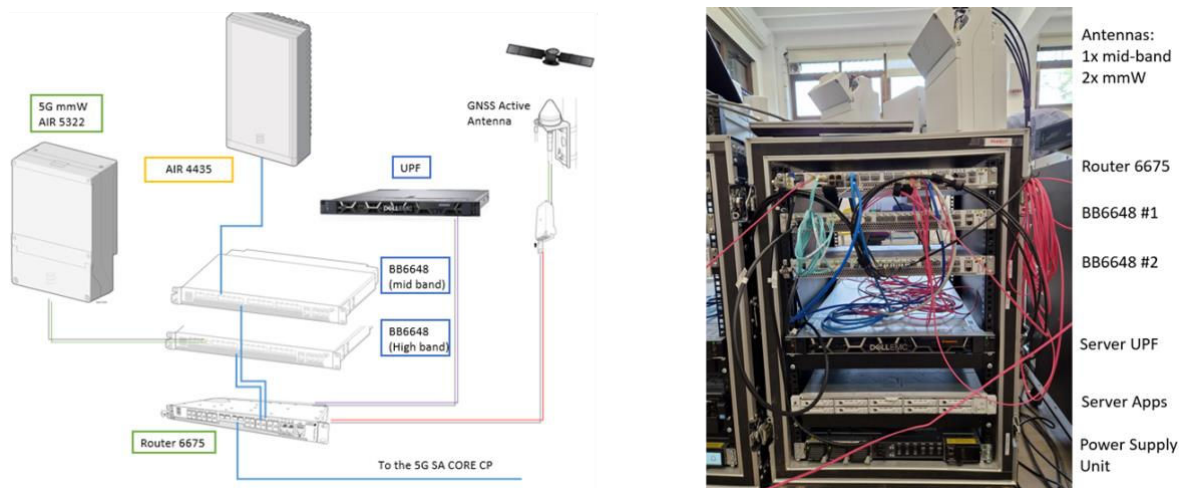


Figure 11: Solution design including FR1+FR2 radios and UPF for local breakout (left) and rack deployed in 5TONIC during the preparation phase (right)

There is one difference between the deployment at 5TONIC and the final deployment at i2CAT campus. At the lab, direct optical fibers are used to connect the mmW antennas with the Baseband, while at i2CAT a Dense Wavelength Division Multiplexing (DWDM) fiber solution is used.

At the moment of writing this deliverable, the flight rack has already been deployed at i2CAT premises. Figure 12 demonstrates that the equipment is powered and cabled at its final location.

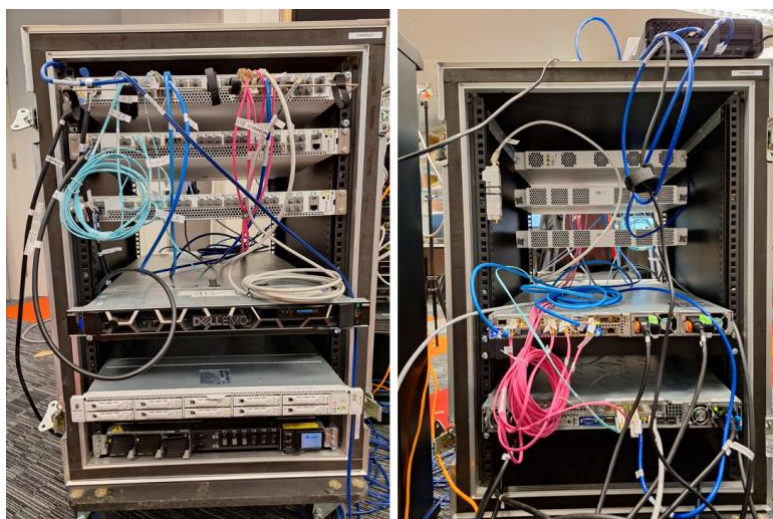


Figure 12: Rack deployed in i2CAT

2.2.5.2.2 3GPP NN deployment

6G-XR NN consists of two different but interconnected test networks and architectures: 5GTN of VTT Oulu and 5GTN of the University of Oulu. In this chapter the architecture with upgrades since D4.1 are described. 5GTN of the University of Oulu is described first and secondly that the 5GTN VTT Oulu.

University of Oulu 5GTN is one of the first private 5G Test Networks that were deployed in the world. Outdoor FR1 5G radios (n78) were recently modernized and n77 also introduced for better radio cell coverage for the whole University of Oulu campus area. Also, some new BaseBand units as well as

indoor radio units have been introduced. The amount of FR2 radios in the network will also increase over time. Outdoor network is shown in Figure 13.

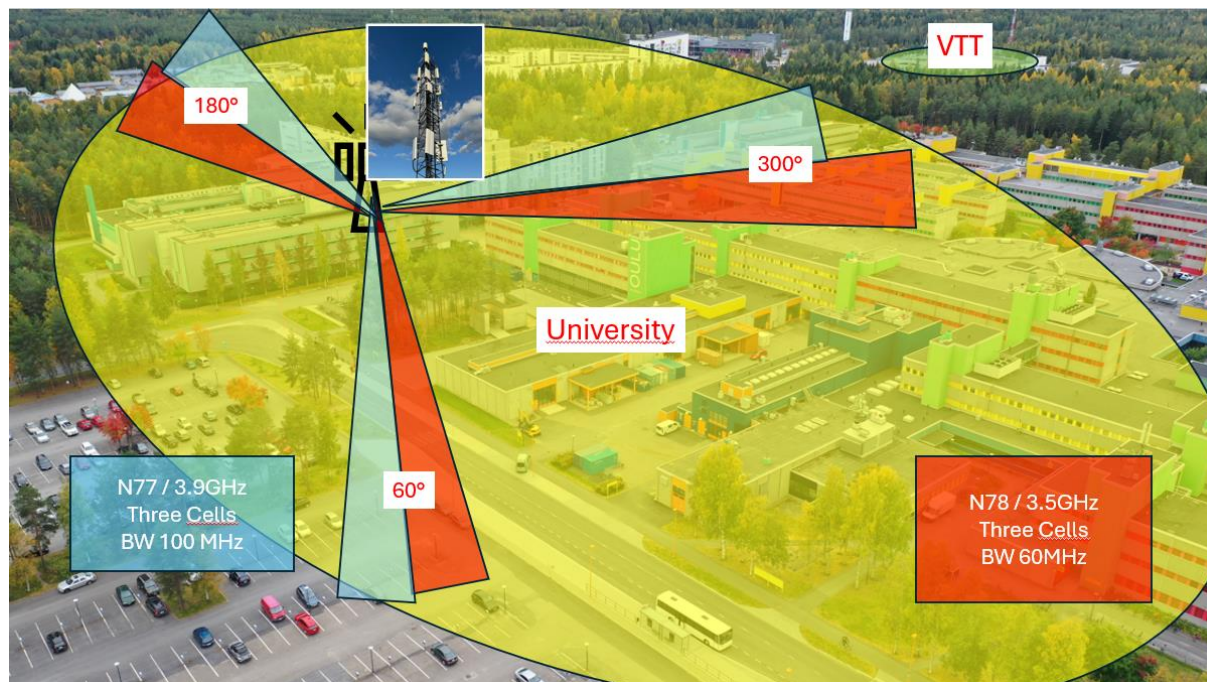


Figure 13: Outdoor 5G at UOulu 5GTN

New network components include also new option for the core (Cumucore) with dynamic 5G slicing. Also new edge servers are introduced for running AI for dynamic slice management and other local processing needs. Integration of Qosium measurement system is proceeding to assume automated QoS measurement.

VTT 5GTN is deployed in parallel with the University of Oulu infrastructure. The upgrade process for the RAN equipment providing FR1 outdoor radio coverage at the test facility has been performed (see Figure 14), including new coverage at the n77 frequency band (with 100 MHz bandwidth), which now offers more FR1 capacity alongside the previously deployed n78 frequency band (with 60 MHz bandwidth). In addition, new core and edge instances have been added to the test facility. The upgrade process for the FR2 outdoor radio coverage at the n258 frequency band (with 400 MHz UL and 800 MHz DL bandwidth) has also been finalized with two outdoor cells deployed at the VTT 5GTN test facility. The RAN setup shown in Figure 14 provides new wireless access options for even more demanding XR use cases and experiments.

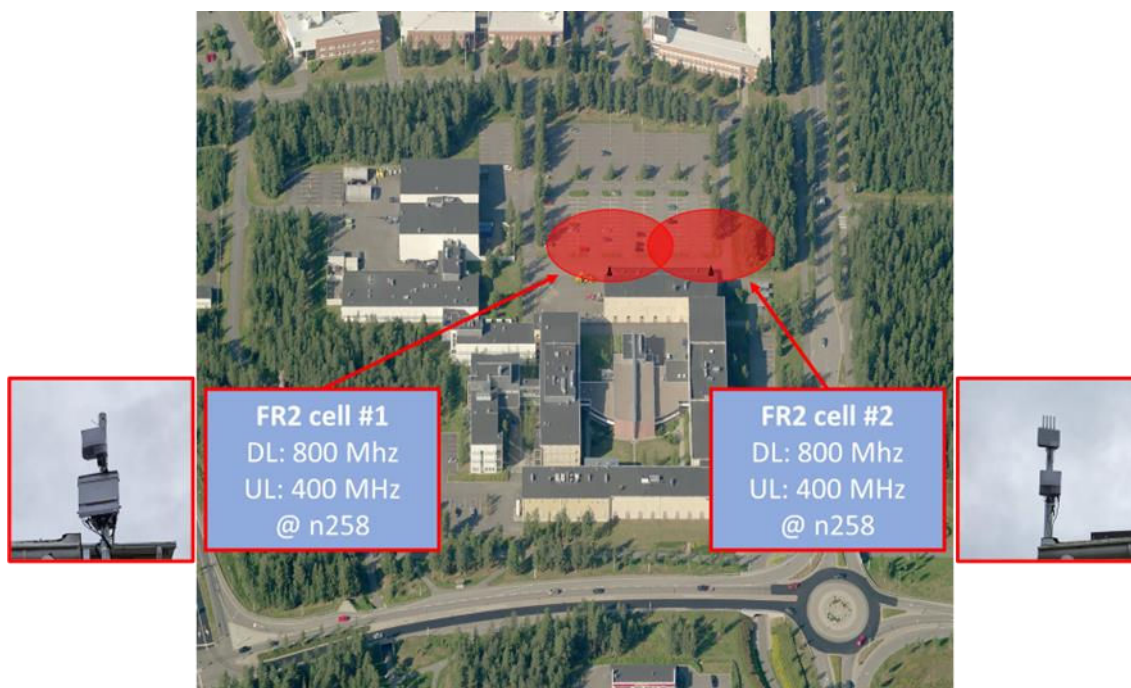


Figure 14. Upgraded FR2 capabilities deployed at the VTT 5GTN test facility.

The summary of the upgrades performed at the VTT 5GTN test facility:

- 5GC: Updated Open5GS with enhanced slice configurations.
- Edge: Enhanced GPU support for multimedia and AI applications.
- 5G NR BB: New baseband units with enhanced radio support and energy efficiency optimizations.
- 5G NR radio FR1: Enhanced network capacity on non-overlapping frequency bands.
- 5G NR radio FR2: Totally new network capacity for XR applications and use cases.

The upgrades still ongoing at the VTT 5GTN test facility:

- Trial engine and North Node adapter API: Connection of VTT 5GTN resources to the framework.

2.2.5.3 Initial network evaluation

An initial performance evaluation of the deployed networks in the South Node and in the North Node is presented next.

2.2.5.3.1 SN performance evaluation

The performance of the South Node network in the laboratory has been evaluated. In D4.3, the same evaluation will be repeated in the campus deployment.

2.2.5.3.1.1 Evaluation in 5TONIC lab

Basic performance tests were done in the lab to ensure the proper behaviour of the solution. The obtained results are dependent on the radio parametrization used. These tests were performed with the parameters shown in Table 4, such as 40 MHz bandwidth plus a 4:1 (DDDSU) TDD pattern on mid-band; and 4x100 MHz bandwidth with several different TDD patterns that will be detailed later in the results table on mmW band. Note that there was no inter-band carrier aggregation, the traffic was using only the high band.

Table 4: Parameters configured in 5TONIC testing

Band	Bandwidth	TDD patt	Power	Modulation DL/UL	DL Layers	UL Layers	DL carriers	UL carriers
Mid	40 MHz	4:1	1W	256/64 QAM	4	1	-	-
High	4x100 MHz	variable	4x2.5W	256/64 QAM	2	2	4	2

Pings and iperfs are run from a 5G terminal to a server that is located at 5Tonic data center. The results obtained for three different TDD patterns: (i) a regular 4:1 which assigns more time for Downlink than for Uplink (DDDSU), (ii) a balanced pattern with same time for Downlink and Uplink (DDSUU), and (iii) a pattern that favours Uplink (DSUUU), are gathered in Table 5. Note that these results have been obtained in the lab under almost ideal conditions.

Table 5: Performance results obtained at 5TONIC lab

TDD pattern	Per-cell FR2 DL Throughput	Per-cell FR2 UL Throughput	User plane round-trip time latency
Regular 4:1 - DDDSU	2.08 Gbps	404 Mbps	5.20 ms
Balanced - DDSUU	1.60 Gbps	902 Mbps	5.47 ms
UL Heavy - DSUUU	951 Mbps	1.63 Gbps	6.85 ms

2.2.5.3.2 NN performance evaluation

Following the deployment of the main capacity enhancing upgrade, i.e., FR2 outdoor radios, at the VTT 5GTN test facility, a series of installation verification measurements were performed against an unoptimized site configuration using a handheld UE (Asus Smartphone for Snapdragon Insiders). The E2E measurements were performed over-the-air in the coverage area of the two FR2 radios in front of the VTT Oulu premises, highlighted with red circles in Figure 14.

The preliminary KPIs reported in Table 6 were achieved by downloading and uploading data to a self-hosted OpenSpeedTest [11] server residing in the VTT 5GTN test facility infrastructure. OpenSpeedTest is an open-source HTML5 network performance estimation tool that enables us to easily verify the outdoor installations, although only at the application level and with lower measurement accuracy than with an E2E synchronised Qosium setup. Consequently, the performed preliminary measurements only indicate to us at this point that the installed hardware is working, and it will be used as the baseline and starting point for the optimisation of the deployed sites and full KPI measurement setup during the coming months.

Table 6: Preliminary application-level KPI results measured with the FR2 outdoor radios at the VTT 5GTN test facility

Band	DL BW	UL BW	DL:UL ratio	MIMO	DL tput	UL tput	RTT latency
n258	8x100 MHz	4x100 MHz	4:1	2x2	3.5 Gbps	250 Mbps	13 ms

n77	100 MHz	100 MHz	4:1	8x4	724 Mbps	133 Mbps	14 ms
N78	60 MHz	60 MHz	4:1	8x4	589 Mbps	87 Mbps	14 ms

2.2.5.4 Planned next steps

In the SN infrastructure, the next steps will consist in deploying the FR1 and FR2 antennas in the target outdoor locations in the i2CAT campus, a process that is currently underway. Once the RAN is setup, a field campaign will be carried out to benchmark the radio and E2E performance of the network throughout the campus. These results will be provided to OC3 projects, such that integration can be properly planned.

In the NN infrastructure, the next steps will focus on the installation of the still pending enablers such as the FR2 radios at the UOULU 5GTN test facility site. After all installations are done, configuration and performance optimisation of the new deployed FR1 and FR2 upgrades will be performed. Building on top of the initial KPI results presented above, the aim is to first integrate the newly installed gNBs better into the existing multi-RAT environment at the NN and then find optimum parameterisations for different use cases emphasizing either DL capacity, UL capacity, or low communication latencies. More comprehensive KPI measurement are planned to be performed with the optimised configurations and the final results will be analysed against target values defined for the enablers in the upcoming 6G-XR deliverable D4.3.

3 O-RAN XR ENABLERS

3.1 SUMMARY OF ORAN ENABLERS IN D4.1

Unlike 3GPP, the working group structure in O-RAN alliance is not focusing on specific service enablers like XR. Instead, O-RAN focuses on transversal RAN optimization topics that can be applied to different verticals. To align with this kind of RAN optimization aim, the 6GXR project is investigating and designing three technology enablers, implemented as rApps and xApps that can be used to enhance performance of XR applications. Analysis and selection of the enabler research was documented in D4.1. Similarly, as with 3GPP enablers, the motivation for each enabler followed by solution description is documented. If available, initial evaluation results are described.

Table 7 summarizes the three technical enablers presented in the O-RAN path, while highlighting their applicability to the 6G-XR use cases described in deliverable D1.1.

Table 7. Summary of proposed 6G-XR enablers in the O-RAN path.

Proposed O-RAN XR Enabler	Target XR gap	Relation to 6GXR use case
Network controlled load balancing triggered by XR application	Ensure available of enough radio resources for holoportation services delivered over public networks, where radio resources are shared with Internet users	Contributes to UC1: XR Congestion detection described in D1.1, by providing a new mechanism (load balancing) to react to congestion
XR application-aware joint optimization of QoS and energy efficiency.	Dynamic runtime adjustment of RAN resources based on the changing XR service usage patterns.	Contributes to UC4 – Collaborative 3D Digital Twin-like Environment and UC5 – Energy Measurement Framework for Energy Sustainability: Enhancing energy efficiency of both UEs and network with fast (near-RT) control when XR applications are used.
O-RAN enabled slicing to support XR services	Dynamic adjustment and allocation of RAN resources specifically, PRBs to the slices according to the slice demand	Related to UC4 described in D1.1.

3.2 O-RAN XR PROPOSED ENABLERS

3.2.1 Congestion aware load balancing

3.2.1.1 Motivation

As was indicated in the preceding section, there are substantial capacity needs for the XR service considered in 6GXR, both in the uplink and downlink directions. It is envisioned that O-RAN techniques can help maintain the quality required by the XR user in an O-RAN enabled public network, using the 6GXR congestion aware load balancing enabler. The O-RAN-enabled gNBs and a near-real-time RIC can serve both XR indoor users and Internet users. Figure 15 depicts the target usage scenario, where a XR user is connected to a congested cell in the presence of other terminals performing Internet traffic, while in the neighbour cell, the XR user could connect to experience a lower congestion.

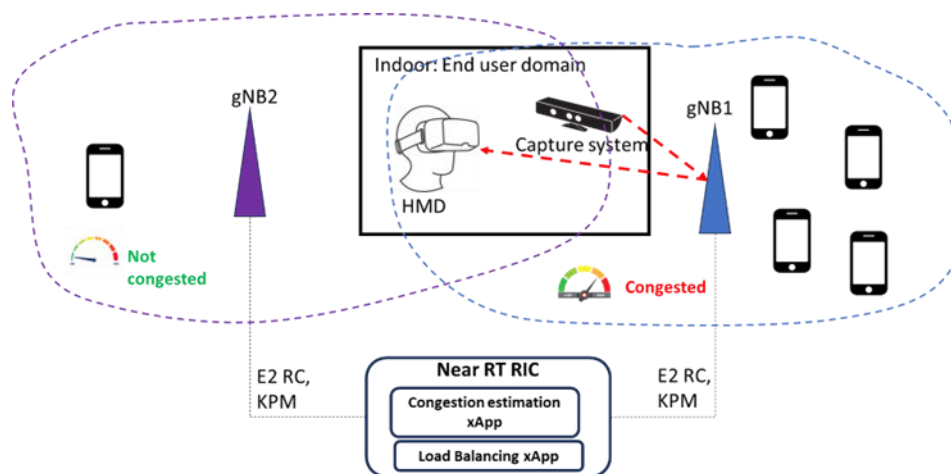


Figure 15. Usage scenario for O-RAN congestion aware load balancing enabler.

3.2.1.2 Solution design

Figure 16 describes our software architecture to implement the ORAN congestion aware load balancing enabler. The proposed system has the following components:

- A *UE location rApp*, based on E2 service models, discovers the UEs that are in RRC_CONNECTED state in each cell. This rApp receives as input a UE_ID provided by the near-real time RIC and can return the cell the UE is currently connected to, as well as a list of neighbouring cells. This rApp offers a REST API to external rApps.
- A *Congestion reporting rApp*, which using E2 KPM service model subscribes to cell-level PRB utilization counters and determines if a given cell, provided as input, is congested. This rApp offers a REST API to external rApps.
- An *Amarisoft HO xApp*, which using the E2 RAN control service model, can force a network handover between two cells for a given UE_ID. This xApp offers a REST API to external rApps.
- A *Congestion Detection Function (CDF) rApp*, which implements the E2E business logic by interacting with the XR application function (XR AF), and with each of the three previous x/rApps. The CDF rApp implements the following workflow:

- It receives a subscription from the XR AF indicating an IP address of a UE currently consuming the XR service, which requires assistance of the CDF rApp to avoid congestion. The CDF rApp then resolved the UE IP address into an internal UE_ID that can be understood by the x/rApps deployed in the non/near-real time RICs.
- The CDF rApp subscribes to location updates for that UE_ID with the UE location rApp, where the provided updates contain both the current serving cell and the list of neighbour cells.
- Armed with the cell identifiers, the CDF rApp subscribes to congestion information on those cells provided by the Congestion reporting rApp.
- Upon congestion reported on the current UE cell by the Congestion reporting rApp, and after determining a non-congested neighbouring cell, the CDF rApp invokes the network-controlled handover xApp to move the XR UE towards a non-congested neighbour cell. Before executing the handover, the xApp requests the UE for a measurement of the neighbour cell to verify that the handover is indeed feasible.

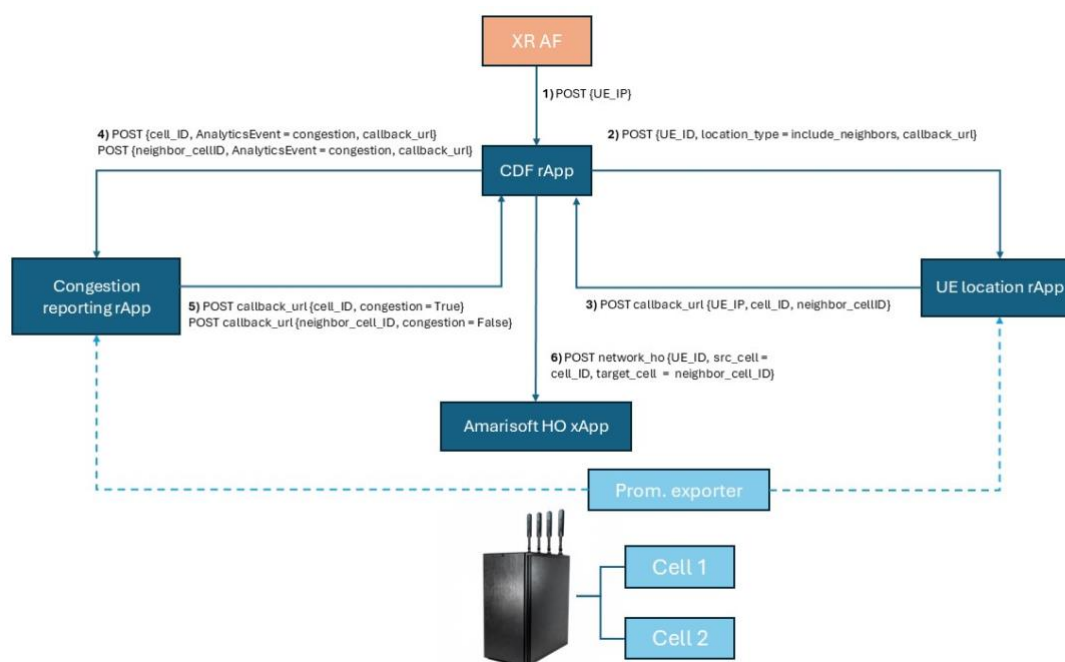


Figure 16. Design of ORAN CDF function to enforce HO upon congestion

3.2.1.3 Initial evaluation results

3.2.1.3.1 Evaluation methodology

To evaluate the congestion aware load balancing enabler, the xApps and rApps have been implemented and are described in Figure 16 in a laboratory testbed composed of an Amarisoft call-box Pro, 1 COMM365 modem as XR user and one Quectel RM500Q modem doing iperfs to congest the 5G cell.

Note that Amarisoft does not implement E2 service models, thus is not possible to connect an O-RAN compliant near-real time RIC to the Amarisoft box to deploy the required xApps. To address this gap, a custom-made Prometheus exporter for Amarisoft has been developed, which exposes the information required by the UE location and the Congestion reporting xApps. To implement the

network-controlled HO xApp it's possible to leverage an API for network-controlled handovers natively supported by Amarisoft, which delivers the functionality that is required from an ORAN compliant gNB. There is a different implementation between xApps and rApps as individual APIs implemented using FastAPI [12]. The developed xApps can be easily ported to an ORAN near-real time RIC in a testbed where E2 compliant RAN nodes were available.

3.2.1.3.2 Results

In this section, the initial results obtained in the development of this enabler are reported. At the time of writing D4.2 an initial prototype of the three-component x/rApps described above is available. The development of the CDF rApp orchestrating the three xApps will be demonstrated in D4.3.

3.2.1.3.2.1 Validating the UE Location rApp

The preliminary results for the UE location reporting rApp were obtained through simulations, as illustrated in Figure 17. The results indicate that the XR AF (e.g. holo orchestrator from UC1) successfully established a session with the CDF. Following session creation, the UE location reporting rApp utilized the provided UE ID to identify the serving cell. This process is crucial for optimizing network queries by preventing the need to monitor and query the entire network.

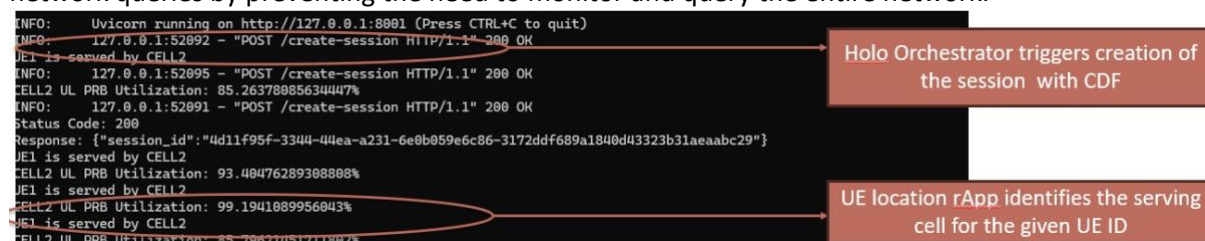


Figure 17. UE reporting rApp signalling messages

3.2.1.3.2.2 Validating the Congestion reporting rApp

Figure 18 shows the evaluation results obtained for the Congestion reporting rApp obtained through simulations. It clearly shows that the Congestion reporting rApp received the cell ID from the UE location reporting rApp then it starts querying the RAN metrics database to monitor the cell performance in real time. In addition, it was able to trigger an alarm that the cell is congested and notified the XR AF about the cell status.

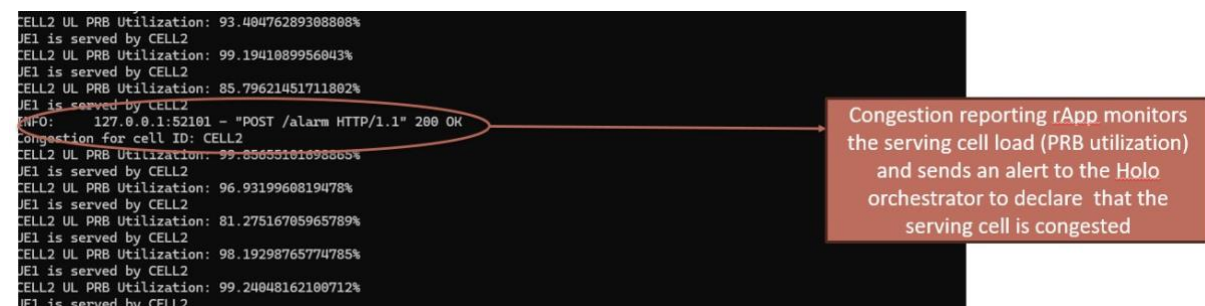


Figure 18. Congestion reporting rApp signalling messages

3.2.1.3.2.3 Validating the Amarisoft HO xApp

Figure 19 demonstrates the functionality of the Amarisoft HO xApp, showcasing a gNB with two cells, i.e. cell 0x002 and cell 0x00c, where a network-controlled handover is executed to force the movement of the UE from cell 0x002 to cell 0x00c, while the UE is performing a constant download using iperf.

The left-hand side of Figure 19 depicts the configuration of the two cells in the Amarisoft box, illustrating: i) the two cells, each configured at a different frequency (top left figure), ii) the neighbor configuration of cell 0x002 containing the parameters of cell 0x00c, and iii) a call issued by the xApp to the Amarisoft API to trigger the handover from 0x002 to 0x00c. The right-hand side of Figure 19 depicts the DL throughput experienced by the UE during the handover using iperf TCP, where it's possible to just see a small glitch when the handover is executed, but otherwise the application session continues uninterrupted.

This experiment validates the feasibility of applying network-controlled handovers to address congestion situations during XR sessions.

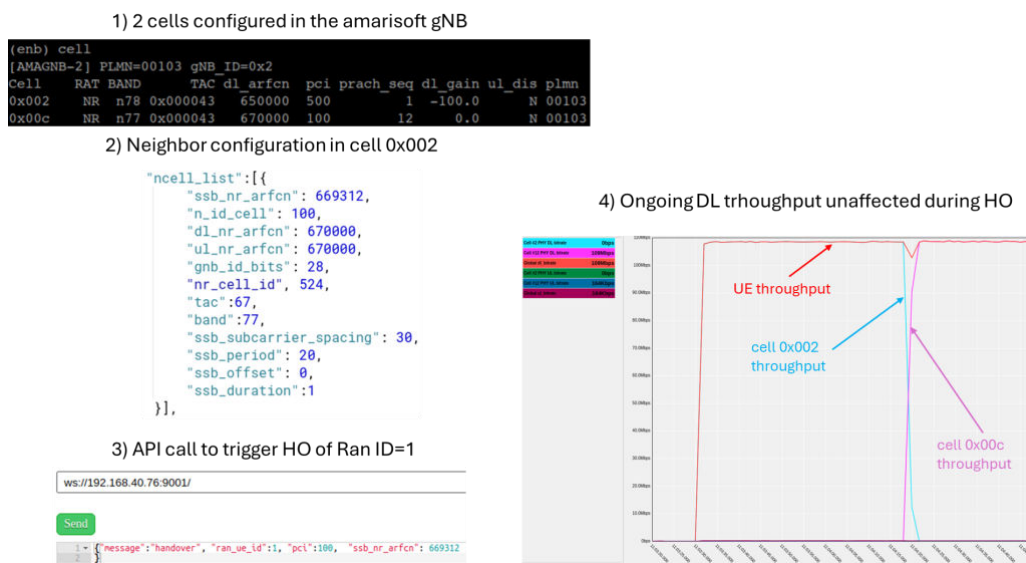


Figure 19. Validating Amarisoft HO xApp

3.2.1.4 Planned next steps

The next steps for this enabler towards D4.3 consist in demonstrating the closed-loop control, whereby upon congestion detected by the congestion reporting rApp, the rApp issues a policy towards the Amarisoft HO xApp, forcing the XR UE to move towards a less congested cell.

3.2.2 Energy-aware E2E resource management

3.2.2.1 Motivation

As discussed in 6G-XR deliverable D4.1, the disaggregated O-RAN architecture and open interfaces are able to provide control loops operating in different time windows at different levels of the architecture hierarchy. The non-RT control loops (slow control) have a typical time range of >1 s and are running at the non-RT RIC or at the Service Management and Orchestration (SMO) framework. The near-RT control loops (fast control) run at the near-RT RIC and have a typical time range of less than 1 s, whereas the RT control loops run directly at the E2 Nodes and have a typical time range of less than 10 ms. In the O-RAN architecture, these different control loops can be utilised to perform RAN resource management with varying granularity, also providing the required enablers for dynamic resource management targeting for energy efficiency in the RAN part of the E2E communication path.

Extending the experimentation of RAN energy efficiency optimization methods executed at the network and gNB/cell level in 3GPP networks (see Section 2.2.4), KPI monitoring and dynamic UE specific radio resource management functionality running at the near-RT RIC will be tested for different

types of XR services. Based on the change between two different XR applications (App1 and App2 in Figure 20) detected from the near-RT KPI measurement data collected from the gNB, the energy-aware resource management xApp running in the near-RT RIC will adjust the RAN configuration to better serve the specific needs of the utilised application in an energy efficient manner. Similarly to the experiments performed in the 3GPP network infrastructure, the XR applications used in the O-RAN tests will stream video and VR.

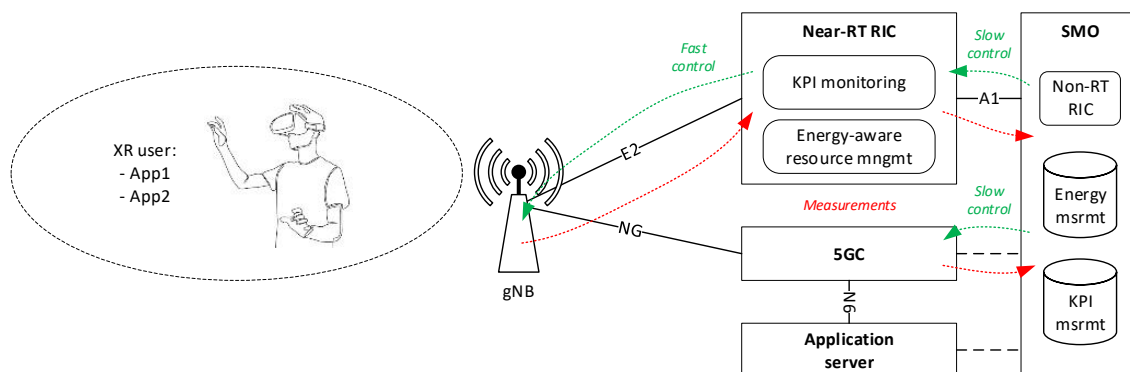


Figure 20. Usage and test scenario for energy efficient XR services in O-RAN infrastructure.

3.2.2.2 Solution design

Figure 21 depicts the O-RAN platform deployed at the VTT 5GTN test facility for the initial tests on this enabler. Compared to the initial plans laid out in 6G-XR deliverable D4.1, the test setup has been migrated from the SDR-based lab deployment into an E2E O-RAN environment provided by Accelleran [13]. From the point of view of the planned measurements, the E2E disaggregated O-RAN environment running on COTS server hardware and RUs supporting the 7.2x split results into more realistic energy consumption data that can be more convincingly compared to the results achieved in the 3GPP infrastructure. In the O-RAN measurements, the focus is on the performance and energy consumption of the new platform components, i.e., the near-RT RIC and the E2 Node (gNB in the O-RAN architecture terminology) comprised of a O-CU, O-DU, and O-RU.

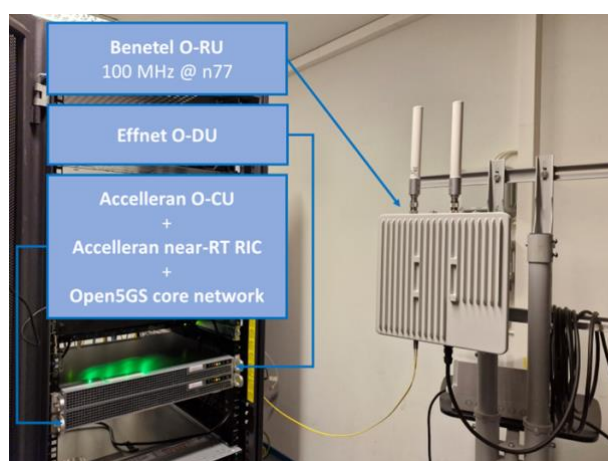


Figure 21. O-RAN infrastructure deployed at the VTT 5GTN test facility.

The network KPIs in the O-RAN infrastructure are measured mainly by using a monitoring xApp running on top of the near-RT RIC platform. At least the following parameters available through the KPI monitoring xApp are of interest to the targeted usage scenario with XR applications:

1. Downlink and uplink throughputs for the E2 Node at the O-CU level.
2. Average downlink data packet delay for a Packet Data Convergence Protocol (PDCP) session at the O-CU level.
3. Downlink data packet delay distribution for a PDCP session at the O-CU level.

The data available through the monitoring xApp is compared to the KPI measurement data collected with the external KPI measurement tools, i.e., Qosium. Combination of the O-RAN measurement data (collected either through the monitoring xApp or external monitoring tools) with the data collected from the UE, core network and application server components is done in a common measurement database in the VTT 5GTN test facility. Feasibility of running the usage scenario with multiple simultaneous users is evaluated separately.

3.2.2.3 Initial evaluation results

3.2.2.3.1 Evaluation methodology

The tests to be performed in the measurement setup presented in Figure 21 aim to clarify two main points:

1. Test the capabilities of the KPI monitoring xApp on top of the O-RAN platform and clarify if it is enough to collect the RAN performance KPIs only through the O-RAN interfaces. This is done by first relying only on xApp-based KPI monitoring and comparing the measurement data (available parameters, results accuracy, results granularity, etc.) to the data collected through the external KPI monitoring framework available at the test site. The feasibility of syncing the xApp-based KPI monitoring data with the energy measurement data is also assessed.
2. When the best KPI measurement methodology for the O-RAN infrastructure has been verified, identify the most suitable dynamic energy saving methods extending and complementing the results and conclusions achieved with the 3GPP infrastructure in the evaluations described in Section 2.2.4. The implementation of the dynamic energy saving methods in the O-RAN infrastructure is done through RAN resource control xApp(s). At least the following RAN control methods will be investigated from E2E energy efficiency perspective:
 - UE-specific resource allocation by adjusting the minimum and/or maximum amount of resources allowed for a single user/application.
 - UE-specific admission control for cells experiencing high temporal traffic loads.
 - Load balancing/traffic steering between cells to even out resource and power consumption or aiding higher level energy saving mechanisms, such as cell switching and sleep mode adjustments.
 - Adaptive energy-aware transmission scheduling (feasibility on top of the current test setup to be clarified).

3.2.2.3.2 Results

The test facility updates related to the O-RAN capabilities were deployed during the summer 2024 in the form of the Accelleran O-RAN platform. As first preparatory steps towards the planned tests described above, the O-RAN system configurations have been finalised and its basic functionality verified. The basic setup to be utilised in the experiments comprises of a single indoor E2 Node show with an attached commercial UE in Figure 22 as seen through the Accelleran dRAX dashboard. The

radio parameters for the connected UE are extracted from the *RRC Measurement Report* messages, periodically sent to the E2 Node by the UE, and visualised through a Grafana dashboard.

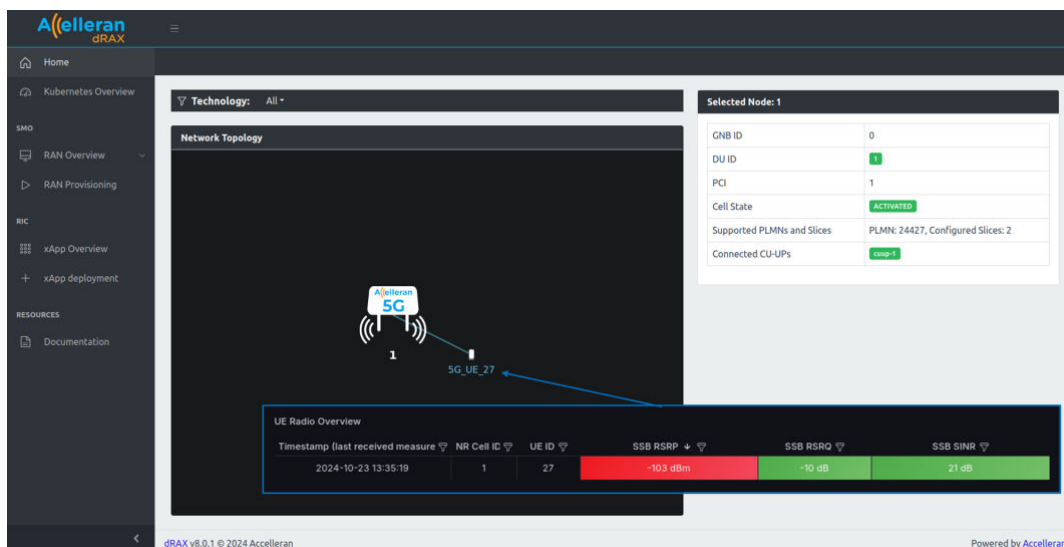


Figure 22. O-RAN test setup overview shown through the Accelleran dRAX dashboard.

The individual components of the disaggregated indoor E2 Node are shown in Figure 23 and highlighted inside the blue rectangle. These components include the Accelleran CU Control Plane (cu-cp) and User Plane (cu-up) instances listed in separate tables in the dashboard view and running on one physical server machine together with the Accelleran’s near-RT RIC and Open5GS 5GC (see Figure 21). The remaining components are the Effnet [14] DU (du-1) and Benetel [15] RAN650 RU (ru-1) shown at the top of the DU/RU List table. The disabled DU and RU instances shown in the table are part of the outdoor E2 Nodes, which are not used for the planned energy consumption measurement and optimisation experiments.

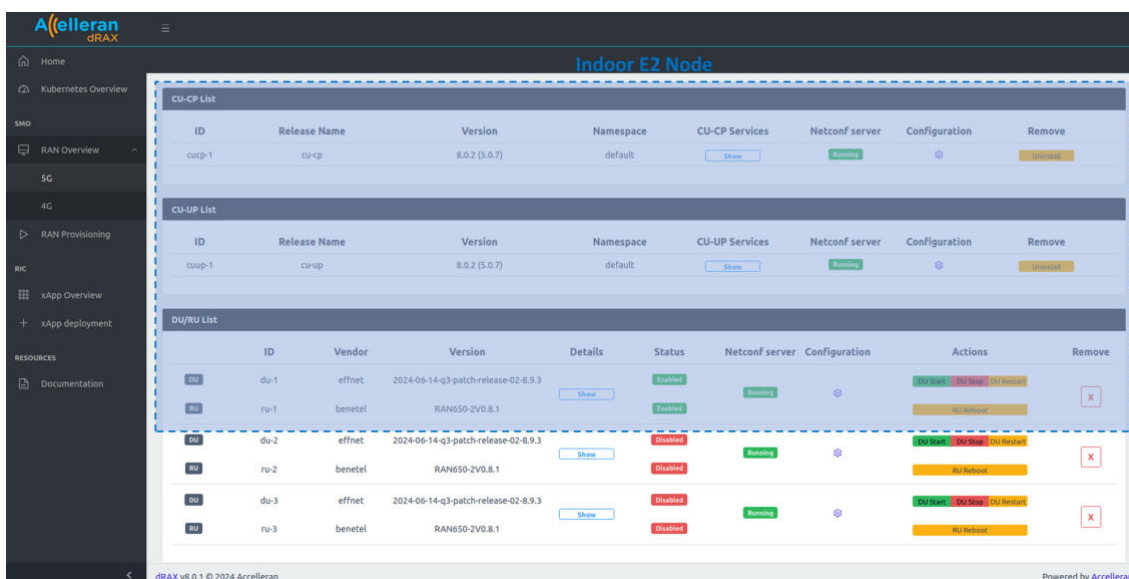


Figure 23. E2 Node components shown through the Accelleran dRAX dashboard.

The near-real-time KPI monitoring and radio control capabilities supported by the deployed O-RAN platform’s latest release version are currently under investigation. Based on the conclusions, the final

selection of the most feasible options to be implement from the radio control feature list presented in subsection 3.2.2.3.1 will be made.

3.2.2.4 Planned next steps

As the deployment of the required infrastructure updates and finalisation of the methodology for the assessment of this O-RAN enabler have been performed as described above, the next steps will be to clarify the most efficient O-RAN KPI measurement approach, implement the radio control functionality to be tested as xApp(s) on top of the near-RT RIC platform, perform the final measurements, and analyse the results. Synergies with the results achieved using the energy conservation methods suitable for 3GPP infrastructures are also studied when providing final conclusions in D4.3 Slice-aware resource allocation.

3.2.3 O-RAN enabled slicing to support XR services

3.2.3.1 Motivation

With this enabler an O-RAN based sliced 5G network with Split-8, where resources are allocated per slice, was created. The intention was to allocate resources independently to each of the slices so that the slice resources are not impacted by the other slice(s) and their load. The system also introduces a near-RT RIC for xApps so that a specifically created xApp will do the dynamic resource allocation between the separate slices. With this architecture each slice can be given a guaranteed service level independent of the load to the rest of the network or other slices. This gives reliability to slice users and assurance that critical services will not lose connectivity even in high network load situations.

3.2.3.2 Solution design

The system and related new technologies in question were developed in conjunction with three 6G-XR Open Call 1 projects for the 6G-XR North Node: 6G-SLICE by Allbesmart, Faladin by Finwe and BANQ by Kaitotek. University of Oulu created the topics for the Open Calls, mentored all three projects, integrated all the project deliverables to form a real functioning system and demoed it together with all three Open Call projects. The result was the “Co-Creative Cyber-Studio in a Sliced 5G ORAN Network” demo that was presented at the EuCNC & 6G-Summit conference in Antwerp in June 2024 [16].

6G-SLICE project by Allbesmart Ltd. was responsible for the creation of the Sliced O-RAN network, Near-RT RIC and the xApp. The system solution was based on two Allbesmart OAIBOXes that were converted into O-CU and O-DU [17]. Ettus USRP X410 was used as the O-RU radio unit in the system with Split-8 functional split between the O-DU and O-RU. The purpose was to create independent E2E slices that have their own independent resource allocation of the 5G Network resources. The project focused on creating slicing also in the RAN and, dynamically and efficiently, sharing the RAN resources between the slices. A near-RT RIC (FlexRIC) was also integrated into the system to run the xApp that can automatically adjust the slice configuration and also monitor the network performance of the system. The O-RAN setup was built on two OAIBOX PCs so that one included the O-DU and the other one had O-CU, 5G Core, FlexRIC, and the WebUI in it. The system block diagram is shown in Figure 24.

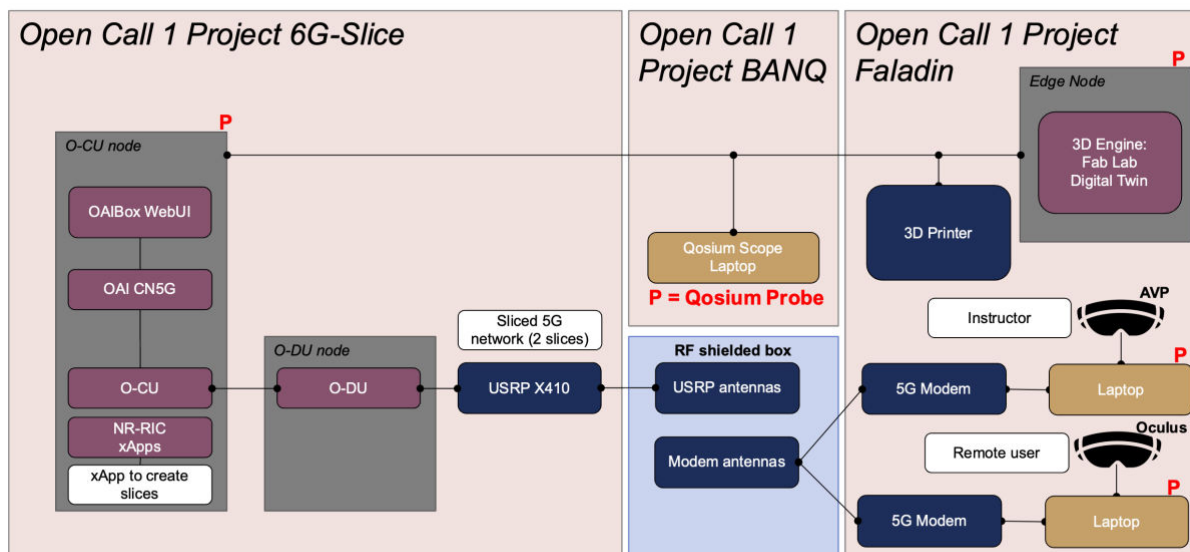


Figure 24. O-RAN disaggregated network architecture brought by the OC1 6G-SLICE project to 5GTN facility.

The Faladin project by Finwe Ltd. implemented the 3D digital twin of the UOULU Fab Lab and the required SW to run the VR environment. The implementation was based on available open-source technologies like Node.js for web services, React.js for frontend, and SQLite for backend. The 3D engine was created using Babylon.js and the XR environment with WebXR and the real time video and audio communication was created using OpenVidu. All the SW was run in one Edge server connected to the IP network that was installed for the system. Apple Vision Pro and Meta Quest 3 glasses were used for the VR part. 5G connectivity for the VR glass sub-system was implemented utilizing Quectel RM520Q-GL modems attached to the laptop PCs that served the VR glasses. Cables were used to connect the USRP and the modems instead of radio antennas. This 3D digital twin environment and the SW was then used to run the 6G-XR Use Case 4 “3D Digital Twin”. This use case was then run during the demo and during the measurements that were done to verify the performance of the system created.

The third Open Call project BANQ by Kaitotek Ltd. created the automated Quality of Service (QoS) test system for the setup. Kaitotek implemented the required automated test system additions to Qosium Storage part of the real time Qosium QoS test SW. Qosium Scope was used to control the measurement system and to visualise the measurement results on a real-time basis. Using the created measurement system, it was possible to measure up to 60 different QoS parameters. This system can measure the parameters separately for uplink and downlink and thus it was utilised to implement E2E QoS measurement for the setup.

In the integration phase all three sub-systems were first built to the UOULU laboratory. First every one of the three systems was brought to the same maturity level they were in the project laboratories. Next the systems were connected to the IP network that was planned for the system by UOULU and all components were configured accordingly. Components were then integrated together and tested that the module interfaces worked as planned. After the integration the whole system was tested. As usual some functionality errors were found during all phases of the process and they were reported, fixed, re-released, integrated and tested again until targeted maturity level was reached. 3D Digital Twin use case was used in the testing of the modules and the system. Altogether this phase lasted for 1.5 weeks. Several people from UOULU and the OC1 projects participated in the system level

operations. After the system was ready it was transported to Antwerp for the demo. After the initial Antwerp demo the system has been presented in three additional demos in Finland, like in the 6G Test Network Finland conference in Espoo 26th of September 2024. See TRAFICOM (Finnish Transport and Communications Agency) Momentum News Letter (in Finnish): <https://uutiskirjeet.traficom.fi/a/s/168638389-1da9dd1db6e7931c7f3b5a5e9fc1aa5e/5884932>.

3.2.3.3 Initial evaluation results

3.2.3.3.1 Evaluation methodology

The O-RAN system that was presented at the EuCNC & 6G Summit was then re-built to the University of Oulu laboratory for performance evaluation with wireless and wired cable connectivity. 6G-XR Use Case 4 “3D Digital Twin” was used in the evaluation to create the environment and required data traffic so that the performance evaluation could be done. Following test cases were implemented:

1. Network with two slices created
 - a. Two UEs connected to the system. Apple Vision Pro VR glasses connected to URLLC slice and Oculus Quest 3 VR glasses to eMBB slice
 - b. Data bandwidth and latency recorded for downlink and uplink
2. Network with two slices created
 - a. Three UEs connected to the system
 - i. Apple Vision Pro VR glasses used in the URLLC slice
 - ii. Oculus Quest 3 VR glasses used in the eMBB slice
 - iii. Mobile phone connected also to the eMBB slice.
 - b. Mobile phone in the eMBB slice used to overload the eMBB slice with UDP data traffic
 - c. Data bandwidth and latency recorded for downlink and uplink

In both test cases, Qosium was used to perform measurements for both uplink and downlink latency and data bandwidth. O-RAN test setup was presented in the Figure 25 and the implementation of it at the University laboratory can be seen in Figure 25.



Figure 25. Test setup in the University of Oulu laboratory

As stated before, the 6G-XR Use Case 4 “3D Digital Twin” was used when doing the measurements. In the use case a remote user wishes to print an object using Fab Lab 3D printer. The user enters the Fab Lab 3D digital Twin environment using VR glasses. Fab Lab instructor enters the 3D environment also wearing VR glasses. Both persons have their own avatars in the 3D world. Persons can communicate using real time audio and the avatars are visible for the users. The instructor evaluates the object the remote user wishes to print and if it is not directly printable it can be modified in real time to reach a state where the object can be printed. When the instructor gives permission to start the printing process, the remote user puts the object inside the digital twin of the real-world Fab Lab 3D printer

and starts the printing process by pressing a button in the digital printer. When done, the real-world 3D printer in the Fab Lab starts to print the object. The Fab Lab printer has two cameras taking videos of the printing process: one on top of the printer and another at front of the printer. These videos are streamed to the 3D environment and attached to the top and front of the digital printer so that the real-world printing process can be followed on the real time in the 3D Digital Twin environment. The printed object can be sent to the remote user when the printing process has been completed.

3.2.3.3.2 Results

In this chapter measurement results for the two test cases defined in the previous chapter are presented.

Test case 1:

- Two slices: URLLC and eMBB.
- Apple Vision Pro VR glasses connected to the URLLC slice.
- Meta Quest 3 VR glasses connected to the eMBB slice.
- 3D Digital Twin use case active.
- Normal load that is below the slice data throughput capacity is in use.
- One way latency and data bandwidth for uplink and downlink measured.
- Purpose of this test case is to measure the parameters in a normal load situation when the slices are not in an overload situation.

Figure 26 below shows the data throughput and latencies for only the Apple Vision Pro glasses in the URLLC slice and only Meta Quest 3 glasses in the eMBB slice. URLLC slice is shown on the left picture and eMBB on the right one. Downlink is presented with blue colour and the uplink direction with green colour. X-axis in both graphs represents time. Y-axis in left side of both pictures is latency in milliseconds and in right side of both pictures y-axis is data throughput in Mbits/s.

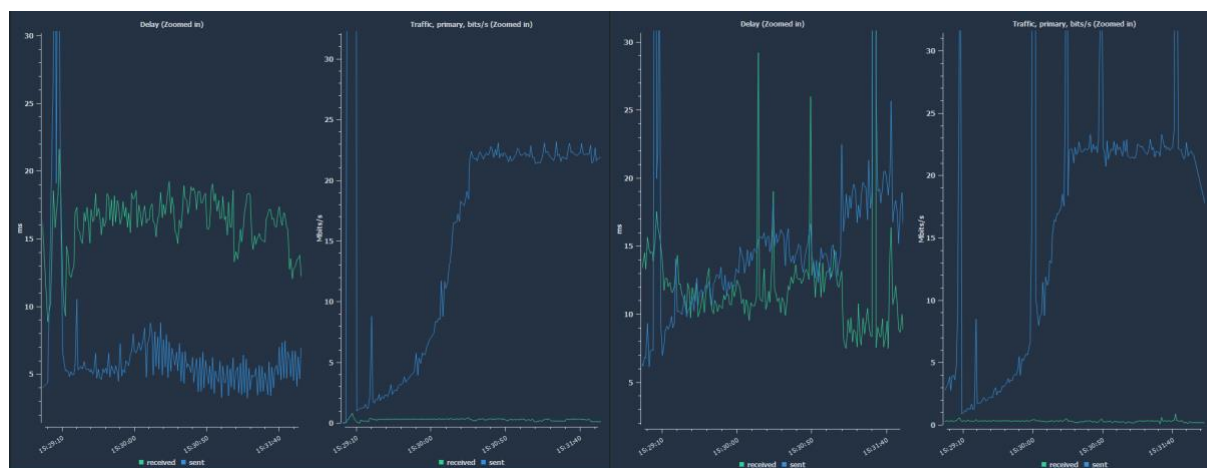


Figure 26. URLLC and eMBB slice data load and latencies in normal load

Measured average data load and the latencies for both slices during the active period:

URLLC		eMBB	
Downlink latency:	6.43 ms	Downlink latency:	16.62 ms
Downlink data load:	19.03 Mbits/s	Downlink data load:	21.35 Mbits/s
Uplink latency:	16.27 ms	Uplink latency:	13.58 ms
Uplink data load:	0.260 Mbits/s	Uplink data load:	0.260 Mbits/s

Test case 2:

- Two slices: URLLC and eMBB.
- Apple Vision Pro VR glasses connected to the URLLC slice.
- Meta Quest 3 VR glasses connected to the eMBB slice.
- Third UE, Quectel modem, is connected to the eMBB slice. 350 Mbit/s UDP traffic is generated for this modem in download direction to overload the eMBB slice.
- 3D Digital Twin use case active.
- One way latency and data bandwidth for uplink and downlink measured.
- Purpose of this test case is to verify if the overloaded eMBB slice has an impact on the URLLC slice resources or not.

Figure 27 below shows the data throughput and latencies for the URLLC slice and the eMBB slice when eMBB is overloaded. URLLC slice is shown on the left picture and eMBB on the right one. Downlink is presented with blue colour and the uplink direction with green colour. X-axis in both graphs represents time. Y-axis in left side of both pictures is latency in milliseconds and in right side of both pictures y-axis is data throughput in Mbits/s.

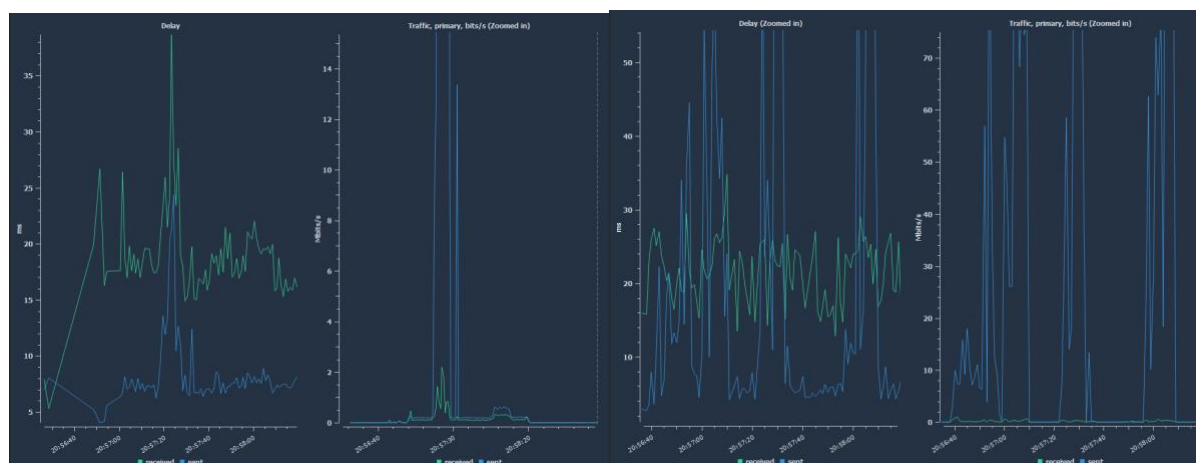


Figure 27. URLLC and eMBB slice data load and latencies when eMBB is overloaded with data

It is clearly visible in the Figure 27 that when eMBB slice is overloaded with data in downlink direction, the downlink latency increases, and it has many latency spikes visible when the slice is overloaded with data. These spikes impact the Quality of Experience for the Meta quest 3 user noticeably. When inspecting the URLLC slice, it can be seen that the overloaded eMBB slice is not impacting the URLLC and the downlink latency is in the same range as in the test case 1 without extra latency spikes as in eMBB. So, the slice isolation in the test platform is working as expected.

Measured average data load and the latencies for both slices during the active period:

URLLC		eMBB	
Downlink latency:	8.36 ms	Downlink latency:	23.85 ms
Downlink data load:	9.95 Mbits/s	Downlink data load:	25.56 Mbits/s
Uplink latency:	19.03 ms	Uplink latency:	21.73 ms
Uplink data load:	0.25Mbits/s	Uplink data load:	0.12 Mbits/s

3.2.3.4 Planned next steps

During the development and test case execution some stability issues were faced in the O-RAN system. First item is then to improve the stability of the system into adequate level. Then FR2 mmW radio is to be integrated into to the system and the slice performance is to be measured and compared to FR1 results that are presented in this document.

After the O-RAN environment the UC4 3D Digital Twin will be integrated to work on top of the target architecture that is based on the CumuCore 5G Core and the Nokia Outdoor macro environment.

4 6G DISRUPTIVE XR ENABLERS

4.1 SUMMARY OF DISRUPTIVE ENABLERS PROPOSED IN D4.1

While 3GPP and O-RAN paths are already introducing tangible results assuming 6G appearance, there is room also for disruptive technologies, like combine communication and sensing networks, extending the coverage and performance by reflective intelligent surfaces and THz level frequency-bands. In this chapter new disruptive technology enablers are considered in the area of RIS, THz and Sub-THz frequency bands, and ISAC.

Table 8 summarizes the enablers presented highlighting their applicability to the 6G-XR use cases described in deliverable D1.1 [5].

Table 8. Summary of proposed 6G-XR enablers in the disruptive path.

Proposed disruptive XR Enabler	Target XR gap	Relation to 6GXR use case
D/H-band transceivers for RIS and ISAC	Ensure enough radio capacity is available for holoportation and 3D Digital Twin-like services enriched with ISAC	Contributes to UC1 – holoportation, by enhancing the UL and DL capacity that is required for capture and transmission of point clouds; and UC4 – Collaborative 3D Digital Twin-like Environment, by incorporating ISAC enablers that complement cameras for 3D modelling of real-world representations
Baseband implementation for the THz-RIS and ISAC based on SC-FDE (used to drive D-band transceivers)	Ensure enough radio capacity is available for holoportation and 3D Digital Twin-like services enriched with ISAC	Contributes to UC1 – holoportation, by enhancing the UL and DL capacity that is required for capture and transmission of point clouds; and UC4 – Collaborative 3D Digital Twin-like Environment, by incorporating ISAC enablers that complement cameras for 3D modelling of real-world representations
DRL-based optimization of THz-RIS network	Reliability and Capacity enhancement support for XR	Indoor XR meeting sessions – aligned with 6G-XR holoportation use case. RIS will

		enhance coverage and capacity in indoor environments
--	--	--

4.2 6G DISRUPTIVE XR PROPOSED ENABLERS

4.2.1 High-Frequency Transceivers for THz-RIS and ISAC

4.2.1.1 Motivation

To stimulate the adoption and further development of XR applications, XR technologies should support wireless connectivity with extremely high data rates and ISAC capabilities for sensing. Mobile communications (both cellular and Wi-Fi systems) have evolved to support higher data throughput. However, to support the high throughput requirements as well as the highly accurate sensing requirements of XR use cases, these enhancements are highly insufficient. The most effective solution to support high throughput and accurate sensing uses wide band spectrum, as currently available in the mm-wave and sub-THz spectrum. The so-called sub-THz regime involves frequencies between 100 GHz and 300 GHz and is considered the most promising range for ultra-high frequencies, where some regulation already exists for communications and active/passive sensing services. Above it, the THz frequency range further extends from 300 GHz up to 10 THz but is less explored due to limited availability of efficient transceiver components. The D-band (110-170 GHz), the G-band (140-220 GHz) and the H-band (220-330 GHz) are considered as the frequency bands where sufficient spectrum can be allocated for wireless communication with data rates of 100 Gbit/s and beyond. Utilizing these frequency bands comes with substantial challenges, requiring disruptive research.

4.2.1.2 140GHz Transceiver design

4.2.1.2.1 Solution design

The 6G-XR 140 GHz transceiver consists of a transmitter and a receiver part. As the receiver has not yet been evaluated fully, the main focus is on the remainder of the section on the transmitter. Its schematic is depicted in Figure 28. It consists of 4 identical transmitter front-ends that are feeding 4 antennas in a uniform linear array. In the front-ends, a complex, differential baseband signal, common to all front-ends is upconverted to the D-band.

The front-ends use a common local oscillator input that is distributed over the front-ends. This local oscillator input is expected to have a frequency of about 15 GHz. Every front-end generates from this input a carrier frequency of about 135 GHz that is used for the two mixers of the complex front-end. It uses 3 factor 3 frequency multipliers: 1 for a first multiplication to 45 GHz that is common for real and imaginary mixer inputs, 2 for the second multiplication to 135 GHz, after the separation of the real and imaginary mixer inputs (the I/Q block).

Programmable phase shifters in the local oscillator frequency domain can be used to control the phase of the RF signal of each front-end individually, to direct the beam in the desired direction. With the antenna lay-out being an array, this beamsteering is one-dimensional: only it's possible to control the direction in a single plane, typically the azimuth plane.

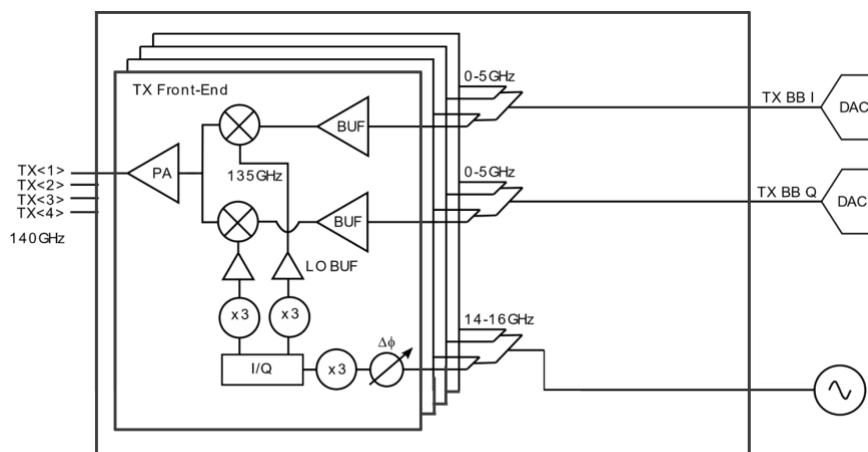


Figure 28. 140 GHz beamsteering transmitter schematic.

4.2.1.2.2 Initial evaluation results

4.2.1.2.2.1 Evaluation methodology

For the evaluation of the 140GHz Transceivers, a set-up based on test and measurement equipment has been used. The evaluation hardware set-up is depicted in Figure 29. As the currently focus is on evaluating the transmitter, the Device-Under-Test (DUT) in this set-up is the 140 GHz beamsteering transmitter. It is powered by a lab power supply providing 3 voltage sources and 1 current source to the transmitter. The baseband input signal of the transmitter is a complex, differential signal that is generated by an Arbitrary Waveform Generator (AWG). The arbitrary waveform generator output is attenuated and biased before it is connected to the input of the DUT. The DUT also requires a local oscillator input that the DUT uses to create the carrier at 9 times the local oscillator input frequency. With a 15 GHz LO input, all baseband input waveforms are modulated at a carrier frequency of 135 GHz.

To evaluate the signal transmitted by the DUT, the signal is received by a reference receiver consisting of off-the-shelf waveguide components: a horn antenna, a waveguide amplifier and a harmonic mixer. The harmonic mixer also needs a local oscillator input, of which the frequency is multiplied by a factor 6 for the down-conversion operation. The mixer output signal at an intermediate frequency of 9 GHz is recorded with a high-speed digitizing oscilloscope.

The metric used to quantify the signal quality is the error vector magnitude (EVM) of the waveform transmitted. The waveform used is a standardised waveform: a 5G-NR Uplink waveform for FR1. To increase the bandwidth of the waveform, the AWG plays it at increased speed. On the oscilloscope, it is demodulated considering this timescale factor. Both the signal generation as the demodulation and EVM measurement are performed with commercial software from the test and measurement equipment vendor (KeySight) comparing the EVM with standard EVM requirements

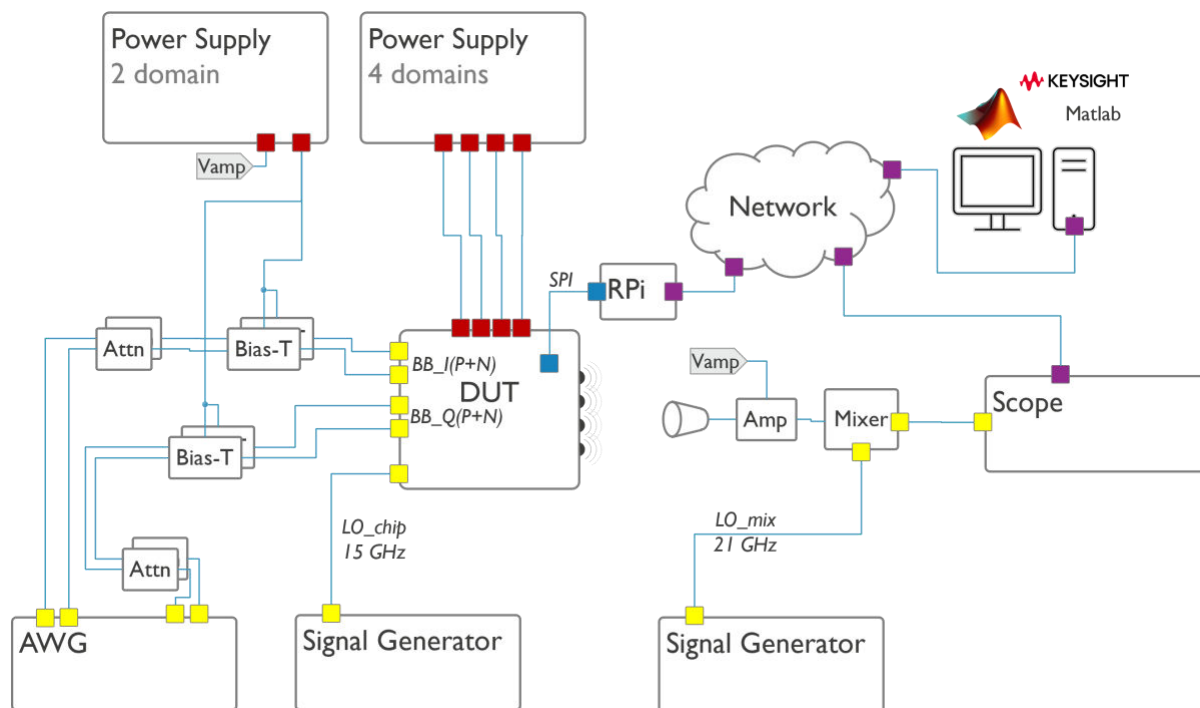


Figure 29. 140 GHz TX evaluation set-up.

4.2.1.2.2 Results

With the measurement set-up described above, EVM measurements for signal bandwidths ranging from 500 MHz to 4 GHz have been performed.

A comparison between the obtained EVM with the EVM specifications for the uplink constellations (for the PUSCH channel) as specified by ETSI has been done. They are shown in Table 9. this works to estimate the raw link capacity: a symbol rate of 1 baud per Hz multiplied with the used bandwidth and the bits per symbol. Even if this is a simplification of the real situation, it is a good first order estimate of the link capacity.

Table 9: 5G NR PUSCH EVM conformance specifications

Constellation	EVM (%)	EVM (dB)
pi/2 BSPK	30.0	-10.5
QPSK	17.5	-15.1
16QAM	12.5	-18.1
64QAM	8.0	-21.9
256QAM	3.5	-29.1

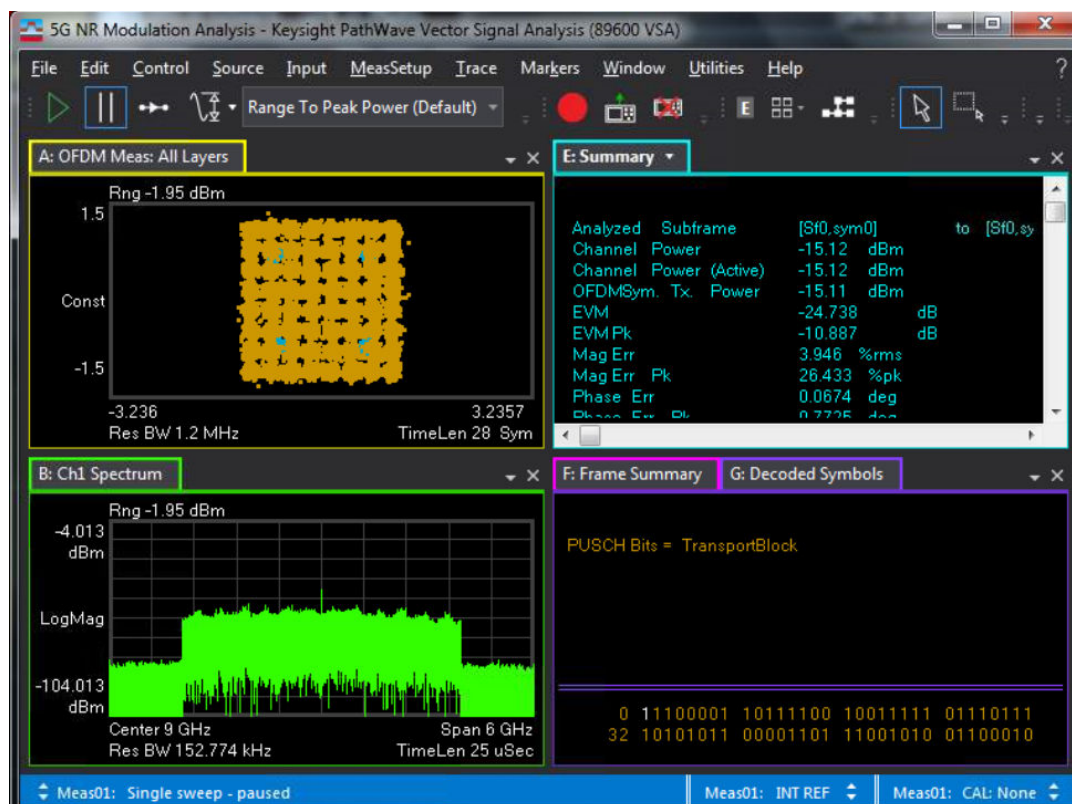


Figure 30 Screenshot of 5G-NR modulation analysis

Figure 30 shows an example of such an EVM measurement. For this measurement, a 64 QAM modulation scheme was used over a bandwidth of 4 GHz. The measured EVM was at -24.7 dB, exceeding the conformance specification of -21.9 dB for 64 QAM.

Table 10 summarizes the results obtained from these EVM measurements. The bandwidth and the modulation scheme used are specified in the first two columns. The estimated raw datarate is obtained from multiplying the bandwidth with the bits per symbol from the modulation scheme. Practical implementations will reduce this raw datarate as channel coding is required to reduce the Bit Error rate and protocol overhead is incurred. Bandwidth and raw datarate of these modes do however provide sufficient margin for the targets set forward in D4.1 (400 MHz and 1-2 Gbps respectively). The last 2 columns show the observed EVM in dB and % respectively. Also there, there is sufficient headroom, as the EVM is not very modulation dependent, it even seems feasible to upgrade the modulation to 256 QAM if the bandwidth is limited to 500 MHz.

Table 10. EVM Measurements results summary

Bandwidth (MHz)	Modulation	Raw datarate (Gbps)	EVM (dB)	EVM (%)
500	QPSK	1	-30	3.2%
500	64 QAM	3	-29.8	3.2%
2000	64 QAM	12	-27.5	4.2%
4000	64 QAM	24	-24.7	5.8%

4.2.1.2.3 Planned next steps

After the evaluation of the transmitter, the main point is to replace the reference receiver with the designed CMOS beamsteering receiver to complete the 140 GHz wireless link.

In parallel, a replacement of the lab equipment with more compact, cheaper development boards to enable a more compact, transportable system with more stations to serve as a test platform for baseband waveforms is being done. This includes off-the-shelf FPGA boards for waveform generation and demodulation, custom build PCBs to supply power to the transceivers and for signal conditioning and compact frequency synthesizers to replace the lab signal generators.

4.2.1.3 300GHz Transceiver design

4.2.1.3.1 Solution design

The 6G-XR 300 GHz Transceiver design is an ongoing activity during the project duration. The 300 GHz transceiver includes both receiver and transmitter functionalities and the receiver part has been now implemented and verified with the measurements.

The implemented RF architecture of the 300 GHz sliding intermediate frequency (IF) receiver chip and a photograph of the RF chip are shown in Figure 31.

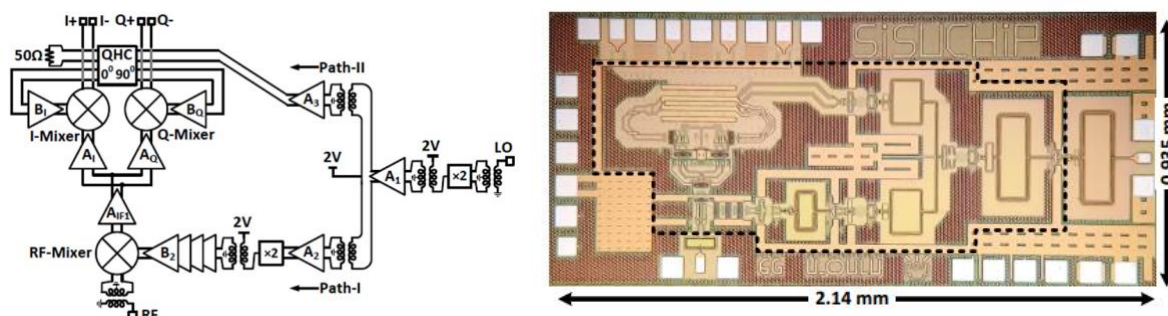


Figure 31. RF architecture of the designed 300 GHz sliding IF receiver and photograph of the manufactured RFIC [18]

The sliding-IF receiver is based on a double downconversion of the RF signal, first by two-thirds and then by one-third of carrier frequency, respectively. The selection of RF, LO and IF frequencies causes image frequencies to fall at one-third of carrier frequency which is very far from the passband of the first mixing stage. This eases the implementation of the image frequency filtering inside of the receiver. The receiver has been designed to be fully differential.

The local oscillator (LO) signal uses doubling frequency stages where a low-frequency reference signal, in this case 50 GHz, is raised to the required mixing frequency inside the chip. The LO signal at two-thirds and one-third of the carrier frequency is generated by the multiplication of the external LO signal of 50 GHz. First, the external LO input signal frequency is multiplied by 2 by a frequency doubler that generates the LO signal at 100 GHz. This signal is amplified and then divided into two paths. Path-I of the LO chain generates the LO signal for the RF mixer using one additional frequency doubler and LO signal amplifiers. Path-II generates quadrature LO signal for I/Q mixer stages by using signal amplifiers and a quadrature hybrid coupler (QHC) for 90-degree phase shift.

4.2.1.3.2 Initial evaluation results

4.2.1.3.2.1 Evaluation methodology

The operation of the implemented 300 GHz receiver has been verified with single-tone sinewave (CW) measurements and with modulated signal measurements. First, the CW and S-parameter measurements of the receiver have been measured. The measurement setup and the gain curve of the receiver are shown in Figure 32. The measured 3-dB and 6-dB RF bandwidths of the receiver are 26 GHz and 36 GHz, respectively when keeping fixed baseband frequency at 2 GHz.

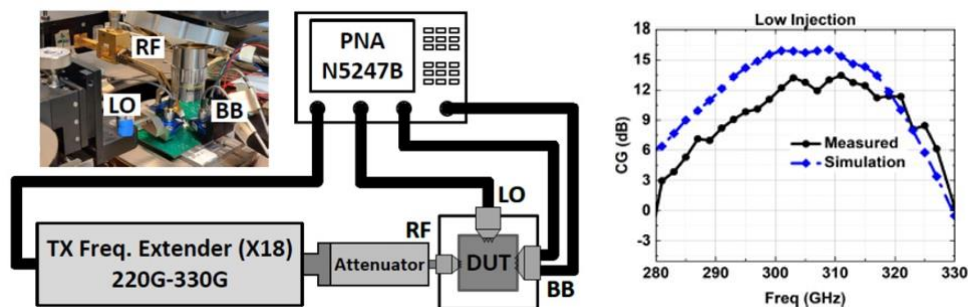


Figure 32. Sinewave signal measurement setup and 300 GHz receiver's gain curve

Modulated signal measurements have been done with the following measurement equipment setup with the developed 300 GHz receiver in below Fig.

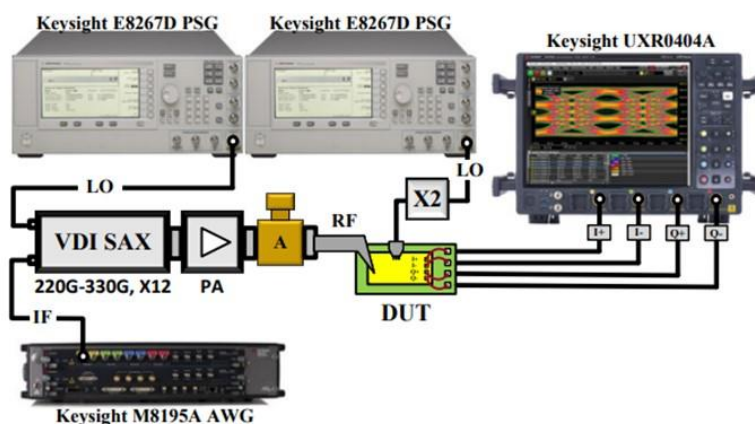


Figure 33. Modulated signal measurement setup for 300 GHz receiver testing [19]

A modulated signal is generated from the Keysight M8195A arbitrary waveform generator (AWG). Using VDI's WR3.4 modulated frequency extender (mFEx) SAX module, the modulated signal is upconverted to sub-THz/THz frequencies. A VDI's power amplifier is used to boost the low output power of the mFEX. PA is followed by a mechanical waveguide attenuator to control the overall RF power going to the DUT. Two separate Keysight's E8267D PSG are used to provide the LO signal to both mFEX and DUT. The input LO signal at 50 GHz is provided with the help of PSG and an external Marki Markowave MMD-2060LU frequency doubler. The downconverted low-IF I/Q modulated signal is demodulated and analyzed with the help of Keysight's UXR 0404A oscilloscope and PathWave Vector Signal Analysis (VSA) 89600 software, respectively.

4.2.1.3.2 Results

Figure 34 depicts the measured constellation, EVM, and SNR of the demodulated signal. It is important to note that the measured EVM includes the EVM of the measurement system as well. The constellations and corresponding EVMs are depicted with a 16/64/256-QAM signal with maximum possible bandwidths of 4 GHz, 2 GHz and 500 MHz, respectively. The modulated constellation and EVMs are measured for an input RF power of -22 dBm to the DUT.

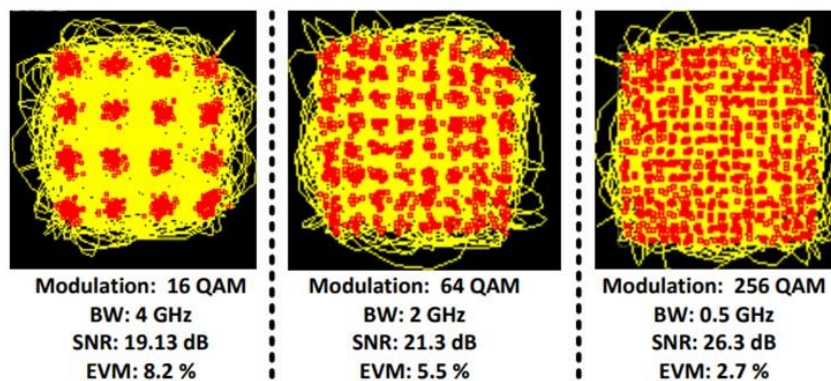


Figure 34. Measurement setup for 300 GHz receiver testing

4.2.1.3.3 Planned next steps

The design of the 300 GHz transceiver work continues to implement a receiver array based on the 300 GHz receiver results. After this design effort, the transmitter functionality will be added to the RFIC so that the full functionality of the transceiver is achieved.

4.2.2 Baseband implementation for THz-RIS and ISAC based on SC-FDE

4.2.2.1 Motivation

XR Metaverse use cases like remote control, remote maintenance, enterprise metaverse, real-time holographic communications, and collaborative 3D digital twin-like environment demand ultra-high bandwidths and sensing capabilities. To enable this, ISAC-capable technologies with very wide bandwidths are required, as currently available in the sub-THz spectrum. Some of the challenges experienced at sub-THz and THz frequencies include limited propagation distances; HW complexity and inefficiencies; need to overcome blockage and obstruction impairments; and channel sparsity as described in D4.1.

Due to the above-described challenges, most of the current approaches at very high frequencies exhibit very limited communication capabilities and generally lack ISAC capabilities. 6G-XR will bridge that gap by developing an ISAC-capable baseband design for Sub-THz communications that will be integrated with the High-Frequency Transceivers for THz-RIS and ISAC.

4.2.2.2 Solution design

Baseband implementation on the THz experimental platform will be based on SC-FDE waveform. Some useful properties of SC-FDE for higher frequencies can be summarized below:

- Better power efficiency than OFDM waveform and its variants thanks to the constant-envelope property (0 dB Peak to Average Power Ratio (PAPR) in the complex baseband domain), although PAPR can be degraded by the prototype filter. SC-FDE is thus susceptible to operating in the non-linear region of the power amplifiers enabling a higher power efficiency.
- Support of 1-tap frequency-domain equalization based on FFTs.

- Challenging to multiplex data/control signals in the frequency domain without degrading PAPR.

A single SC-FDE waveform will be used in the solution for both communication and sensing following a unified ISAC approach. Sensing will entail the transmission of an a-priori known pilot sequence, such as a reference signal (RS) for sensing, that the receive side will exploit to perform sensing measurements aimed to determine the location, speed, and characteristics of a target being sensed.

The main building blocks of the experimental platform connecting the baseband implementation with the high-frequency transceivers are illustrated in below Figure 35. A hardware-in-the-loop setup will comprise a Matlab implementation of the main software blocks running the physical-layer processing steps, a couple of USRPs aimed to upconvert/downconvert the IQ samples to a sub-6 GHz intermediate frequency, a couple of Tx-Rx frontends at 140 GHz and 300 GHz, and a time source to synchronize all Tx-Rx blocks. The aimed frontends are the high-frequency transceivers described in section 4.2.1.

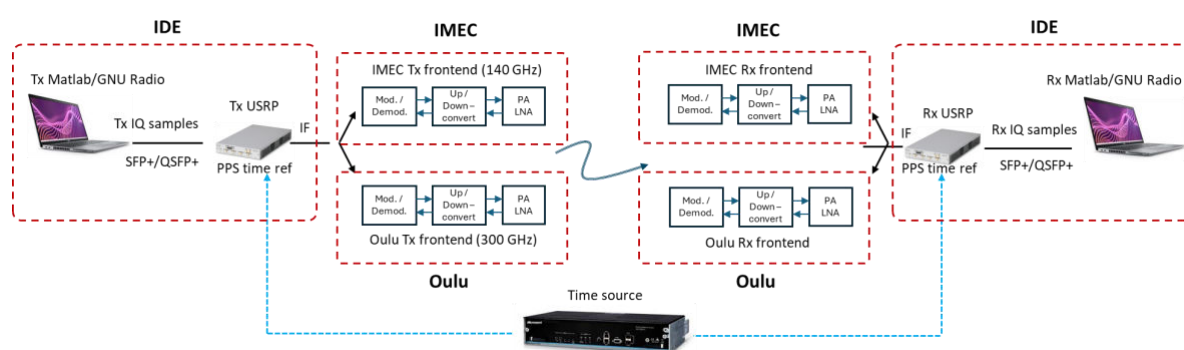


Figure 35: building blocks of the experimental platform comprising the baseband and high-frequency transceiver implementation.

The principles followed in the solution design for the baseband implementation blocks are the following ones:

- Waveform transmission will be based on generation of time-domain sampled versions of, e.g., a QPSK modulation with root-raised cosine (RRC) prototype filter.
- A cyclic prefix (CP) will be added to the beginning of a group of symbols for DFT-based detection and equalization in frequency selective channels. This is more convenient than time-domain equalization schemes because of the already high maturity of FFT-based receiver implementations. Whereas the CP ensures frequency-domain equalization and inter-symbol interference avoidance, the RRC filter can shape the frequency response of the transmit symbols to, e.g., improve on the spectral confinement of the signal for better coexistence with other signals and/or services in the same band, or an adjacent one.
- FFT receiver processing will rely on some design parameters like, e.g., FFT size (number of samples prepended by the CP and processed upon detection), subcarrier spacing (equal to the inverse of the duration of a block of symbols following the CP), sampling rate, and number of subcarriers allocated to a user or set of users.
- Sensing will be performed by the receiver based on a set of measurements, e.g., the Time of Arrival (ToA) and Angle of Arrival (AoA) of the signal, as required by the sensing algorithms in use. A basic sensing algorithm will be incorporated to the design based on ToA and AoA for the determination of the location, and eventually also the speed, of the target.
- Evaluations of the testbed performance will be first realized with a link-level Matlab simulator based on the Communications Toolbox. Link-level performance figures of BER (bit error rate),

BLER (block error rate), throughput, PAPR (peak to average power ratio), and PSD (power spectral density) will be further compared with those measured in the lab testbed, and differences in the channel characteristics will be accounted for in the evaluations.

4.2.2.3 Initial evaluation results

4.2.2.3.1 Evaluation methodology

The evaluation methodology comprises two stages. A first stage, purely SW-oriented, comprises a link-level Matlab simulator specifically developed to implement the baseband processing blocks that illustrate the bit error rate performance and PAPR of SC-FDE waveform under high-frequency impairments. A second stage involves the development of the baseband processing blocks into the HW-in-the-loop platform of above Figure 35 after proper integration with the high-frequency transceivers described in section 4.2.1.

Ideally, simulations should be conducted at sub-THz bands (above 100 GHz). However, no channel model has been yet standardized at higher frequencies and some companies have their own implementations, sometimes based on Open Source, which makes comparisons biased by the type of effects that they incorporate. Moreover, the 3GPP channel model described in [20] is only applicable up to 100 GHz, but the main propagation effects usually considered by stochastic channel models are already well captured in it, only disregarding specialized phenomena like surface roughness effects, atmospheric attenuation, or pathloss modelling, which can be negligible in a lab environment. In consequence, evaluations were performed with TR 38.901 at a frequency range of 71 – 100 GHz, which can capture most of the effects expected at sub-THz.

The simulation assumptions are given in Table 11.

Table 11 : Simulation assumptions for evaluation of the SW-based link level simulator of the baseband processing blocks.

Parameter	Value
Waveform	CP-OFDM and SC-FDE
Channel estimation	Ideal
Carrier frequency	75 GHz
Subcarrier spacing, SCS	240 kHz, 480 kHz and 960 kHz
User bandwidth	100 RB (288 MHz, 576 MHz, 1.152 GHz)
Channel model	3GPP Indoor CDL-E (26 ns), CDL-B (26 ns), and CDL-C (5 ns), 3 km/h,
CP size	Normal length (293 ns at 240 kHz SCS)
Modulation	64QAM
SC-FDE RRC filter	Not present
DM-RS	Type A, single symbol (position = 2), additional position: 3, configuration type A
Phase Noise	No phase noise modelled, no PT-RS
FEC	LDPC 0.65 coding rate
LDPC decoding	Belief Propagation/Normalized min-sum

The KPIs obtained are the uncoded BER, coded BLER, and PAPR. In this section, an initial evaluation results of the uncoded BER and coded BLER performance was captured.

Rice (CDL-E) channel, 240 kHz SCS

Figure 36 depicts the BER and BLER performance for both waveforms. At low SNR, both have the same performance given the strong LOS component and negligible Doppler impact. There is an apparent advantage in SC-FDE at high SNR; however, this is attributed to spreading the bits over the user bandwidth in a frequency-selective channel. When FEC is applied (which already spreads the information in frequency), this advantage disappears in the coded BLER (Figure 39). Therefore, both waveforms are equivalent in performance in a Rician channel at low Doppler.

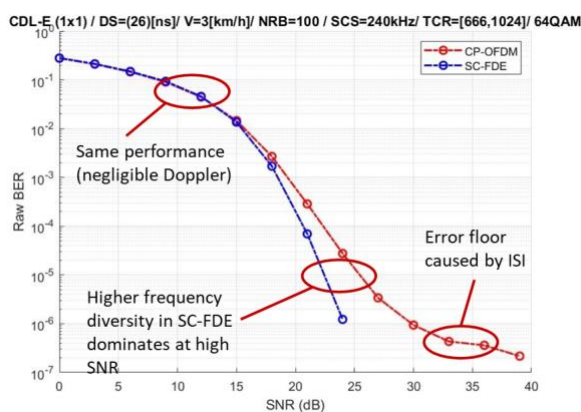


Figure 36: Uncoded BER comparison between SC-FDE and CP-OFDM for CDL-E channel.

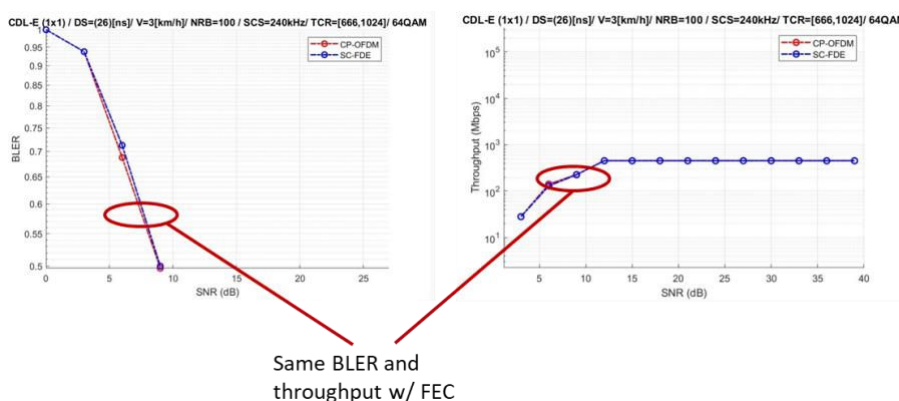


Figure 37: Coded BLER comparison between SC-FDE and CP-OFDM for CDL-E channel.

This is the most likely channel condition encountered in practice for sub-THz links, especially in indoor lab environments.

NLOS (CDL-B) channel, 240 kHz SCS

In NLOS, Doppler is more noticeable, and waveforms exhibit different performance per the differences in their support. At low SNR, SC-FDE exhibits slightly poorer performance per the spread operation that worsens the inter-carrier interference caused by Doppler, which is visible in the BLER. However, at high SNR, SC-FDE shows again a higher frequency diversity that vanishes when FEC is applied. The result is a better BLER performance of CP-OFDM. Notice that NLOS channels are in practice unlikely for sub-THz links, unless an obstructed path finds its way to the receiver through a reflection. Results are shown in Figure 40.

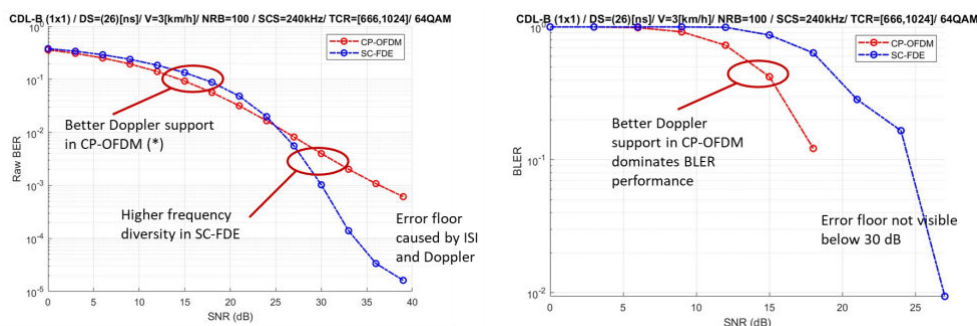


Figure 38. Coded BLER comparison between SC-FDE and CP-OFDM for CDL-B channel.

4.2.2.4 Planned next steps

The next steps will consider the following tasks:

- Obtain simulation results of PAPR and spectral density with and without RRC filter.
- Incorporate phase noise and a PT-RS-like signal to compensate it and compare the results at different carrier frequencies.
- Develop the FPGA blocks in the HW platform and integrate it with the high-frequency transceivers to perform the first lab tests.

4.2.3 Deep Reinforcement Learning for THz-RIS

4.2.3.1 Motivation

To motivate the use of RIS for XR applications, has been considered that the XR meeting use case in Figure 41 aligned with the 6G-XR holoportation scenario. This involves a mix of physical and virtual participants interacting in a 3D-rendered virtual space. The THz spectrum offers the necessary bandwidth for this demanding use case but faces challenges with sparse channels and LOS blockages. RIS can transform sparse channels into rich scattering ones, enabling 3D beamforming. Intelligent beamforming and resource allocation, facilitated by DRL (Deep Reinforcement Learning) frameworks, ensure reliable communication by adapting to dynamic environments and user mobility.

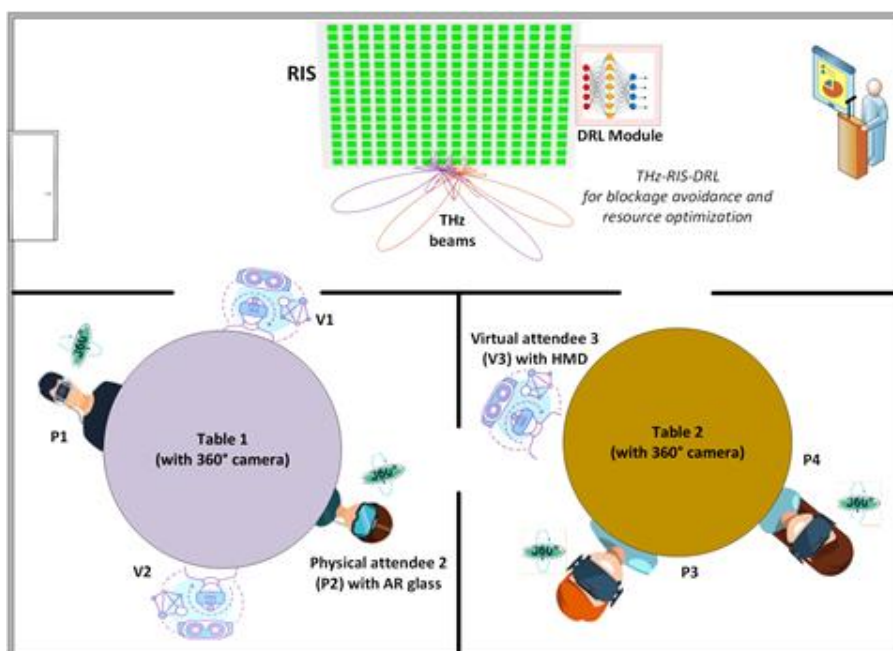


Figure 39. Indoor XR meeting enabled by DRL-aided THz-RIS

4.2.3.2 Solution design

The THz-RIS environment is meticulously modelled to represent a scenario involving various critical metrics, such as user mobility, channel conditions, and RIS configurations, operating at THz frequencies (specifically at 140 GHz). Given that XR scenarios typically involve Multi-User Multiple-Input Single-Output (MU-MISO) or Multiple-Input Multiple-Output (MU-MIMO) configurations, the THz-RIS system's performance is simulated, and rigorously evaluated within these contexts to ensure its applicability and effectiveness in real-world XR use cases.

A key aspect of this environment is the optimization of phase shifts, which are modelled to enhance both network performance and user experience. This factor is critical in ensuring that the RIS-based system can effectively adapt to the dynamic conditions characteristic of XR applications.

To enhance the accuracy and reliability of the simulation results, authentic channel data for the THz frequency band (140 GHz) is incorporated. This data is meticulously gathered through an extensive review of existing THz channel models documented in the literature, providing a robust foundation for the simulation, in contrast to less reliable synthetic data methods [21] [22] [23]. This approach ensures that the simulation results are not only precise but also closely aligned with real-world conditions, thereby strengthening the validation of the THz-RIS system for XR applications.

The system set up consists of modelling the channel paths between the Transmitter and RIS panel with N elements and then channel paths between the RIS and the XR users. The performance of THz RIS is evaluated by calculating the average SE (spectral efficiency) for all the users. The THz RIS environment is thus set up and validated. Graphs simulated are shown below in the following sections. A key part of the solution design includes the DRL framework. In the context of optimizing phase shift configurations within a THz-RIS environment for enhanced user applications, various techniques have been explored to achieve this objective. One of the most recent approaches involves leveraging Machine Learning (ML) to optimize these phase shifts, thereby improving both throughput and user experience. In this regard, a Machine Learning methodology known as Deep Reinforcement Learning (DRL) should be adopted, which integrates the principles of reinforcement learning with deep learning.

4.2.3.3 Initial Evaluation Result

4.2.3.3.1 Evaluation methodology

The simulation environment, as previously described, was established and rigorously tested. The performance of the THz-RIS system was initially evaluated using MATLAB. The data generated from these MATLAB simulations were subsequently integrated into a Python-based DRL framework, executed on Google Colab. Within this framework, a DRL agent is implemented using a specialized algorithm, selected for its robustness and effectiveness in optimizing the THz-RIS system. The agent learns optimal behaviours by interacting with its environment through a process of trial and error, continually refining its decisions to achieve the desired outcomes. A series of comprehensive simulations were conducted, employing a minimal number of episodes to facilitate the execution of the reinforcement learning algorithm.

However, due to current computational constraints, it was not feasible to conduct extensive training of the algorithm. Despite these limitations, the preliminary results obtained from the simulations are promising, indicating the potential effectiveness of the proposed approach. The DRL agent is integrated with a system-level simulator that models the THz-RIS network. This allows for continuous feedback and adjustment based on real-time system performance.

4.2.3.3.2 Results

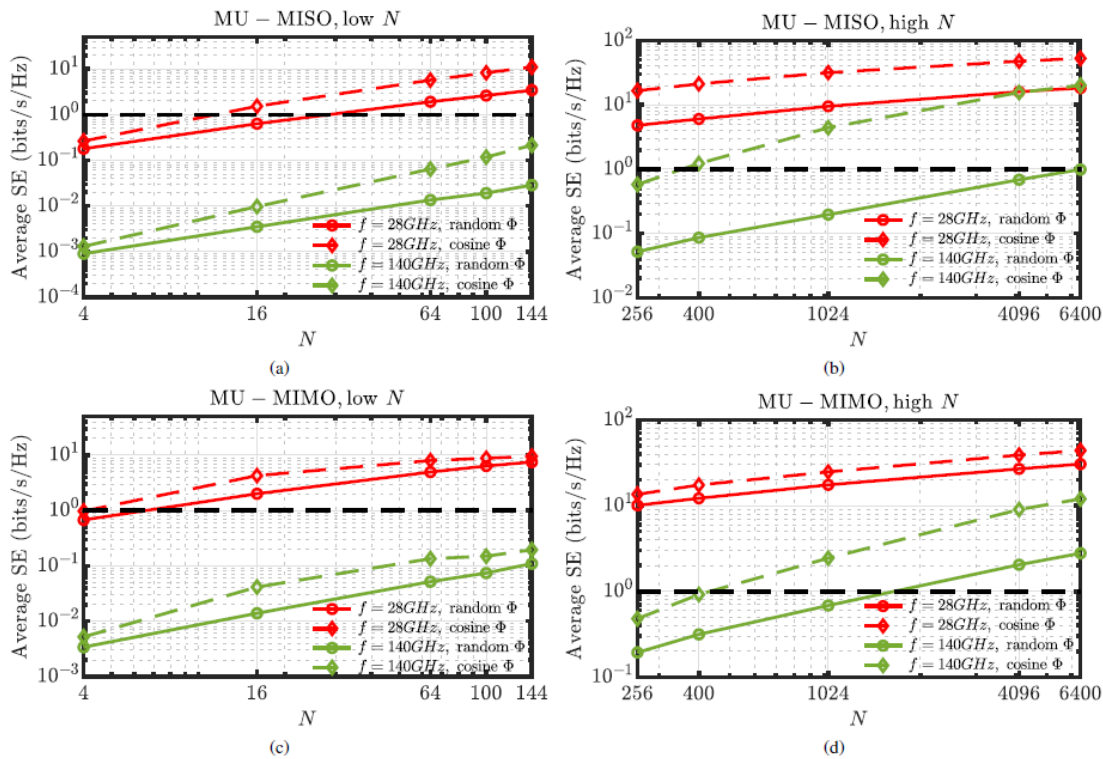


Figure 40. Comparison of average spectral efficiency (SE) with number of RIS elements for in multi-user XR scenarios typically using 28GHz and 140GHz.

The analysis in Figure 42 demonstrates the impact of the number of RIS elements on network performance, highlighting the effectiveness of different optimization methods in enhancing spectral efficiency in multi-user RIS scenarios at mmWave and THz frequencies in XR application scenarios.

DRL simulation: The training process of the algorithm was closely monitored, and it was observed that the agent demonstrated a learning trajectory towards achieving the maximum designed reward. To evaluate its efficacy, the algorithm was tested at 28 GHz, confirming its potential effectiveness.

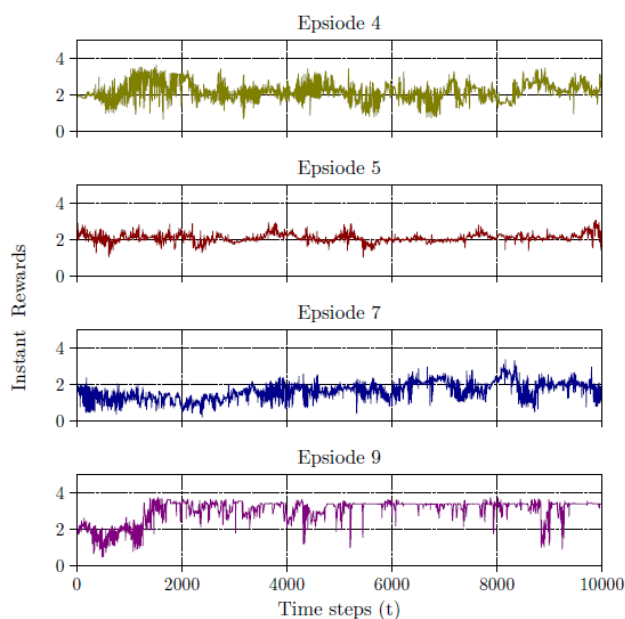


Figure 41. DRL algorithm curve for different time steps.

Figure 41 highlights how the DRL algorithm effectively learns to optimize the RIS phase shifts over time. While there is fluctuation in rewards during exploration, the overall trend indicates improvement, showing that the algorithm adapts well to the dynamic environment of the system. This is crucial in XR environments, which are highly dynamic—with users frequently moving, interacting with objects, or changing their positions relative to the network infrastructure. A more complete description of the results is mentioned in the publication [24].

4.2.3.4 Planned next steps

It's planned to extend the training duration across a greater number of episodes and introduce a broader variety of channel realizations to enhance the learning effectiveness of the DRL framework. Building on the initial simulations conducted at 28 GHz, which yielded promising results, it's intended to extend this simulation framework to Terahertz frequencies. This extension is designed to optimize the simulation environment for XR applications, leveraging the benefits of higher frequency bands.

5 6G-XR TRIAL CONTROLLER

5.1 UPDATE TRIAL CONTROLLER ARCHITECTURE

The initial architecture design of the 6G-XR Trial Controller was described in Deliverable D4.1 and it is reprinted here on Figure 42.

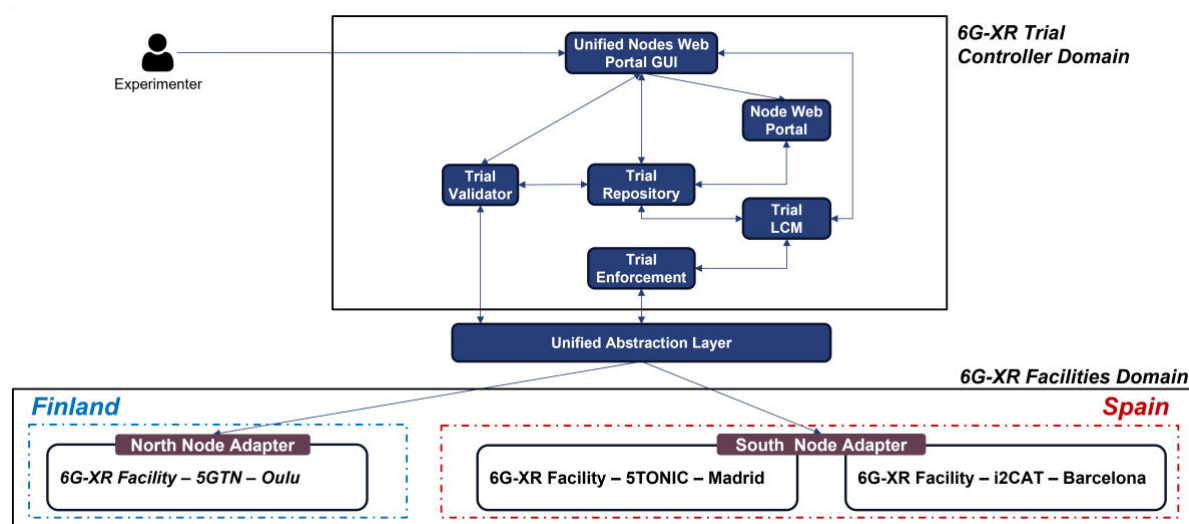


Figure 42. Initial Architecture Design of 6G-XR Trial Controller.

After the publication of the deliverable D4.1 the analysis of the 5G!Drones based trial controller has continued and it has been identified to require revision. Firstly, the efficient management and orchestration of the trials requires to be pushed closer to the facilities so to avoid unnecessary latencies of e.g., VPN tunnelling while the trial is running. Hence, the Node Adapters are seen as excellent candidates for management and orchestration of the trials. Secondly, the initial Trial Controller is unnecessarily complex for the purposes of providing the experimenter the ability to define and execute trials as there is no external collaborative entity, like the unmanned traffic management for uncrewed aerial systems. As a result, the architecture of the trial controller has been revised to better suit the purposes of the project. Finally, the services provided for the trial experimenter remain the same and there is no perceived difference in the ability to execute trials with the two approaches. The approach described in the following is better suited for the 6G-XR project purposes than the original 5G!Drones approach described in D4.1. In addition, there exists added functionality to the initial architecture, including components such as real-time KPI presentation using Grafana at the Facility Web Portal, ability to adjust resource balance between slices through introduction of AI algorithms, and extended network slice template.

The architecture of the trial controller is designed with two distinct north and south portals, as well as a unified portal. This design ensures efficient control and coordination across different access points, while also incorporating key features that enhance overall system performance and user experience. The updated architecture is depicted in Figure 43.

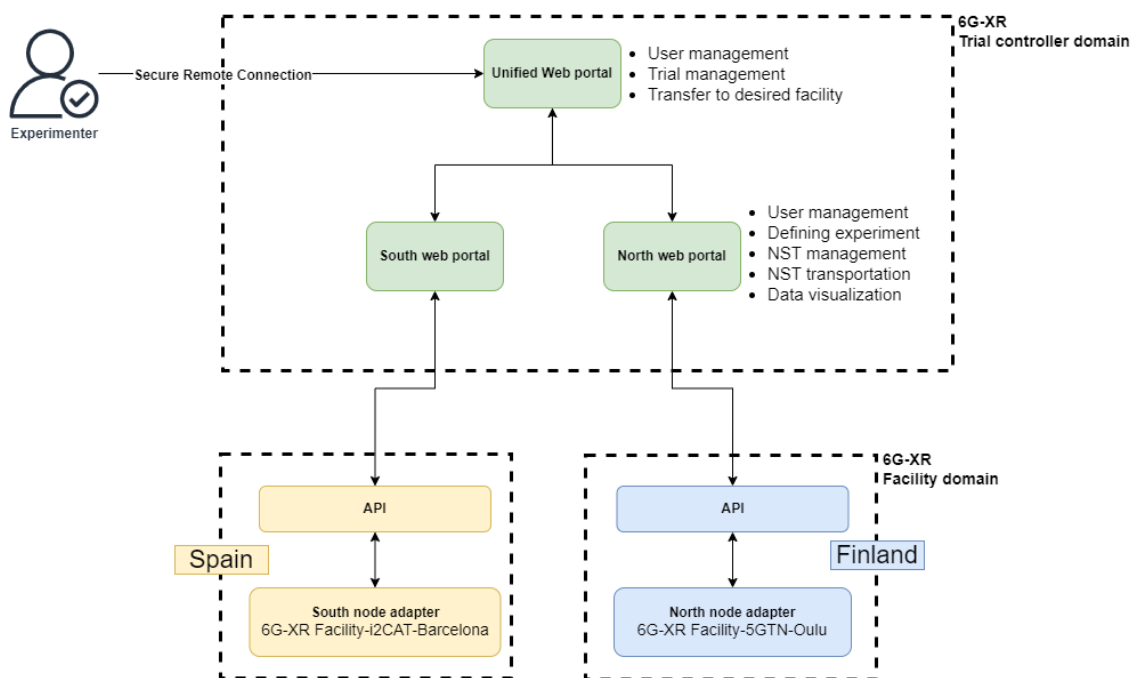


Figure 43. Trial Controller Architecture

5.2 INITIAL TRIAL CONTROLLER IMPLEMENTATION

The trial controller is presented to launch trials based on resource allocation feedback in this section. By accessing the provided portals, users have the possibility to launch and manage various trials according to their needs. In the following, a first explanation of the components of the trial controller that are common to all nodes are explained and then, a description of the node specific components.

5.2.1 Common Trial Engine components

The trial engine has three main components. The unified web portal, the north web portal and the south web portal are shown in above Figure 43. By authenticating and entering the unified web portal, the user can define the trial and be transferred to the desired portal.

Then, in the north and south web portals, the user defines the Network Slice Template (NST), creates an experiment, send NST to the node adapters (NNA/SNA) and finally controls the experiments, including edit, start, stop, delete and status of the experiments.

5.2.1.1 Unified Web Portal

The unified web portal is designed with the aim of managing the trial on both the north and south web portals. The unified web portal is implemented using the Django framework, including two applications to handle user and trial management and Django REST framework to handle trial ID. By logging into this system, the user can create a trial and then according to the user's needs, user is directed to desired portal (north or south). The main key of communication between the unified web portal and the north and south portal is the trial id. By creating a trial, a unique number and trial facility is assigned to it. The north and south web portals are only able to view and select trials that the facility considered during trial generation at the unified web portal is the same as those facility.

Figure 44 is a view of the unified web portal services. Some features of the main portal include:

- User management: including registration, logging in and out, forgetting password and editing user information.
- Trial management: create and edit the trial.
- Transfer to facility: by clicking on the facility, the user will redirect to desired web portal.

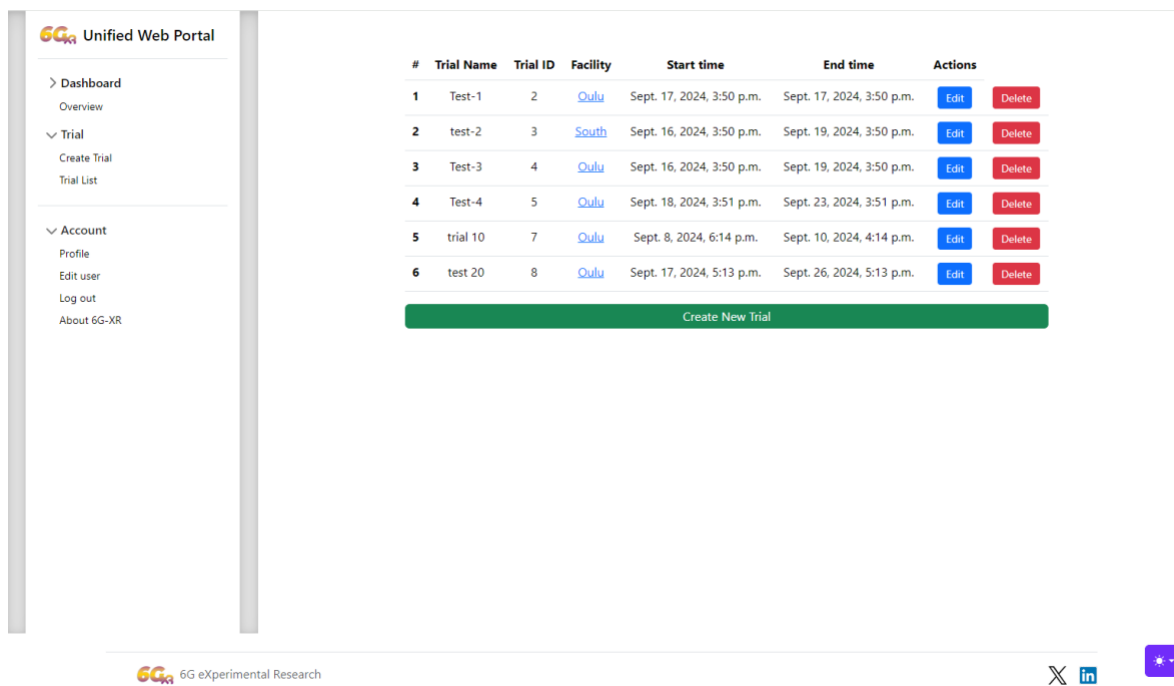


Figure 44. Unified web portal.

5.2.1.2 KPI collection engine

Trial controller uses Qosium for measuring QoS KPIs such as latency, throughput, jitter, packet loss, etc. Qosium is a software-based solution that allows measuring QoS in a network technology agnostic way. The relevant Qosium components for our trial controller solution are as follows:

- **Qosium Probe:** Software agent that performs the actual QoS measurements. Probes are installed on measurement points such as UE and an end-point server.
- **Qosium Scope:** The main controller software for manual measurements, which commands and controls Qosium Probes. Scope also visualizes received results in a browser-based UI.
- **Qosium Scopemon:** An automated measurement controller that monitors a specific type of data transmission and starts measurements with probes.
- **Qosium Storage:** Server and database software used for collecting measurement results. Results can be accessed through a web browser and a REST API. Qosium Storage can control individual measurements by Qosium Scopemon instances under-the-hood; in this case Qosium Scope is not needed.

The design principle of Qosium is that probes perform the actual measurements, but they are controlled by a measurement controller (Qosium Scope, Qosium Scopemon, or Qosium Storage). Then trial controller solution at south and north node commands measurements to start and stop, and

fetches measurement results through REST APIs, which the Qosium controllers provide. Details of how south node and north node trial engine solution uses Qosium KPI collection engine are given in sections 5.2.2 and 5.2.3, respectively.

5.2.1.3 Network Slice Template (NST)

The 6G-XR Network Slice Template (NST) is a collection of configuration parameters for experiments run in the south and north node adapters. NST is created by the unified web portal which is then forwarded to south and north node adapters including south/north node specific additional fields. Node specific additional fields are needed as the implementations of south and north node adapters are based on different set of technologies. The common fields of the 6G-XR NST are as follows. South node and north node specific fields are described in their respective sections below.

- **"trialId"**: Id forwarded from the Experimenter Webpage
- **"experimentName"**: Name of the experiment to be launched
- **"startTime"**: Time when the experiment began
- **"stopTime"**: Time of the experiment's end
- **"targetNode"**: Node location where the experiment will take place
- **"targetFacility"**: Infrastructure location where the experiment will take place

5.2.2 South Node Trial Engine Components

The South Node Trial Engine components and interfaces are represented in Figure 45. Once SOUTH is selected as the experiment target (see "targetNode" field in section 5.2.1.3), the Unified Web Portal redirects to the South Node Web Portal, which will use the South Node Adapter for storage, management and launch of the experiment on to the south node infrastructure (information on the MEC and NEF components at the south node can be found in D2.2 deliverable). The South Node Web Portal will login with users registered in the South Node Adapter database.

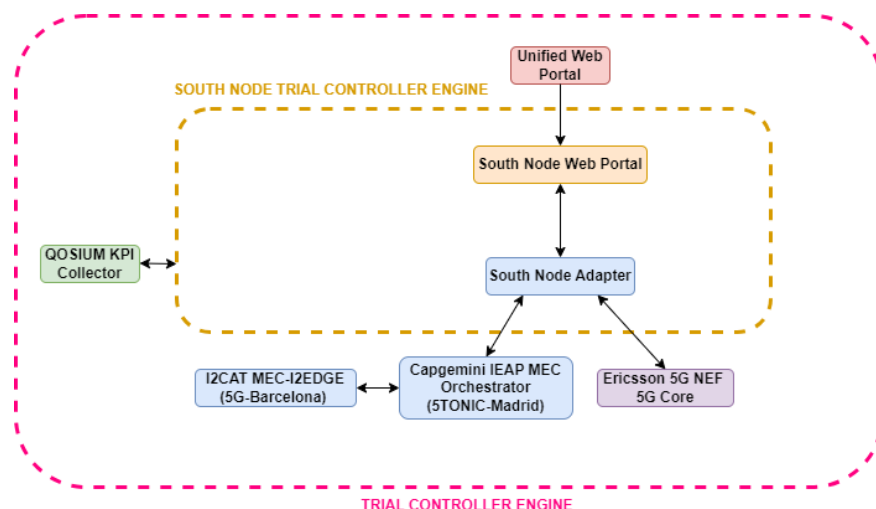


Figure 45. South Node Trial Controller Components

5.2.2.1 South Node Web Portal

The South Node Web Portal is implemented in JavaScript with React framework. Its aim is to handle user authentication, NST management and experiments for the South Node test facilities, including 5Tonic in Madrid and i2CAT in Barcelona.

By logging into this system, the experimenter can manage the creation and modification of the NST, as well as the instantiation of the experiment resulting from the NST definition. The NST creation relies on the communication with the Unified Web Portal, which must provide the initial information required to generate the NST, including the trial identifier (trial Id), start and end time of the experiment. Moreover, the communication with the South Node Adapter (SNA) provides insight into the resources available at the South Node test facilities.

Figure 46 shows the form employed by the experimenter to create the NST. By selecting the trial Id among the available ones, the information configured previously through the Unified Web Portal is shown. Then, the selection of the South Node resources differentiates two main categories:

- Applications: the form shows a list of the applications available at the edge nodes of the South Node test facilities. The experimenter can select the applications required for the experiment and attach them to the specific slice.
- User Equipments (UEs): the form shows a list of the UEs available at the test facilities. Each UE is identified by its Generic Public Subscription Identifier (GPSI). The experimenter can select the UEs/GPSIs required for the experiment and attach them to the specific slice.

Create NST

Fill in the details to create a new NST.

NST Name	Trial ID
<input type="text" value="Experiment-1"/>	<input type="text" value="Trial-1777"/>
Start Date	End Date
<input type="text" value="07/11/2024 08:04 AM"/>	<input type="text" value="08/11/2024 08:04 AM"/>

Select Application & Slice

1.	<input type="text" value="App 1"/>	-	<input type="text" value="BCN-HIGH"/>	<input type="button" value="-"/>
2.	<input type="text" value="App 2"/>	-	<input type="text" value="BCN-LOW"/>	<input type="button" value="-"/>

Select GPSI & Slice

1.	<input type="text" value="GPSI 1"/>	-	<input type="text" value="MDR-HIGH"/>	<input type="button" value="-"/>
2.	<input type="text" value="GPSI 2"/>	-	<input type="text" value="MDR-LOW"/>	<input type="button" value="-"/>

Figure 46. Creation of a NST in the South Node Web Portal

Once the NST is created, it is presented in the web portal among the “Draft NSTs” section, as shown in Figure 47. This section allows the experimenter to visualize the selected configuration, as well as to provide the following actions:

- Edit: the experimenter can update the draft NST previously created.
- Delete: the experimenter can delete the draft NST.
- Send to the SNA: the experimenter validates the draft NST and sent it to the SNA to deploy the experiment.

After sending the NST to the SNA, the NST is moved from the “Draft NSTs” section to the “Deployed NST (experiment)” section. This section allows the experimenter to visualize the configuration and the status of the experiment (“Ok” or “Error”), as well as to provide the possibility to cancel the experiment.

6G-XR									
Deployed NSTs									
#	NST Name	Trial ID	Node	Application & Slice	GPSI & Slice	Start Time	End Time	Status	Actions
1	Experiment Alpha	Trial-1001	South	●	●	01/11/2024 09:00 AM	02/11/2024 09:00 AM	OK	ⓘ
2	Experiment Gamma	Trial-1003	South	●	●	05/11/2024 11:00 AM	06/11/2024 11:00 AM	OK	ⓘ
3	Experiment Delta	Trial-1004	South	●	●	07/11/2024 10:00 AM	08/11/2024 10:00 AM	OK	ⓘ
4	Experiment Epsilon	Trial-1005	South	●	●	09/11/2024 01:00 PM	10/11/2024 01:00 PM	OK	ⓘ
5	Experiment Zeta	Trial-1006	South	●	●	11/11/2024 10:00 AM	12/11/2024 10:00 AM	Error	ⓘ
6	Experiment Theta	Trial-1008	South	●	●	15/11/2024 11:00 AM	16/11/2024 11:00 AM	OK	ⓘ
7	Experiment Iota	Trial-1009	South	●	●	17/11/2024 08:00 AM	18/11/2024 08:00 AM	OK	ⓘ
8	Experiment Kappa	Trial-1010	South	●	●	19/11/2024 09:00 AM	20/11/2024 09:00 AM	OK	ⓘ

Draft NSTs									
#	NST Name	Trial ID	Node	Application & Slice	GPSI & Slice	Status	Actions		
1	Experiment Eta	Trial-1007	South	●	●	In draft	✎	✖	▶
2	likkeerr	Trial-6930	South	●	●	In draft	✎	✖	▶

[Create new NST](#)

Figure 47. List of NSTs in the South Node Web Portal

Finally, the “Dashboard” section of the web portal will later include a dashboard developed with Grafana to visualize the data collected by Qosium during the execution of the experiment.

5.2.2.2 South Node Adapter

The South Node Adapter (SNA) is the component in charge of storage, management and launch of the experiment onto the actual south node infrastructure, this is interacting with MEC orchestrator and 5G Core components. The SNA receives the experiment NST from the SN Web Portal, which will save in the database (even if the launch fails), and then the involved apps will be launched to begin the experiment. Figure 48 describes the workflow between the SNA and the rest of components in the trial engine and the South Node Infrastructure.

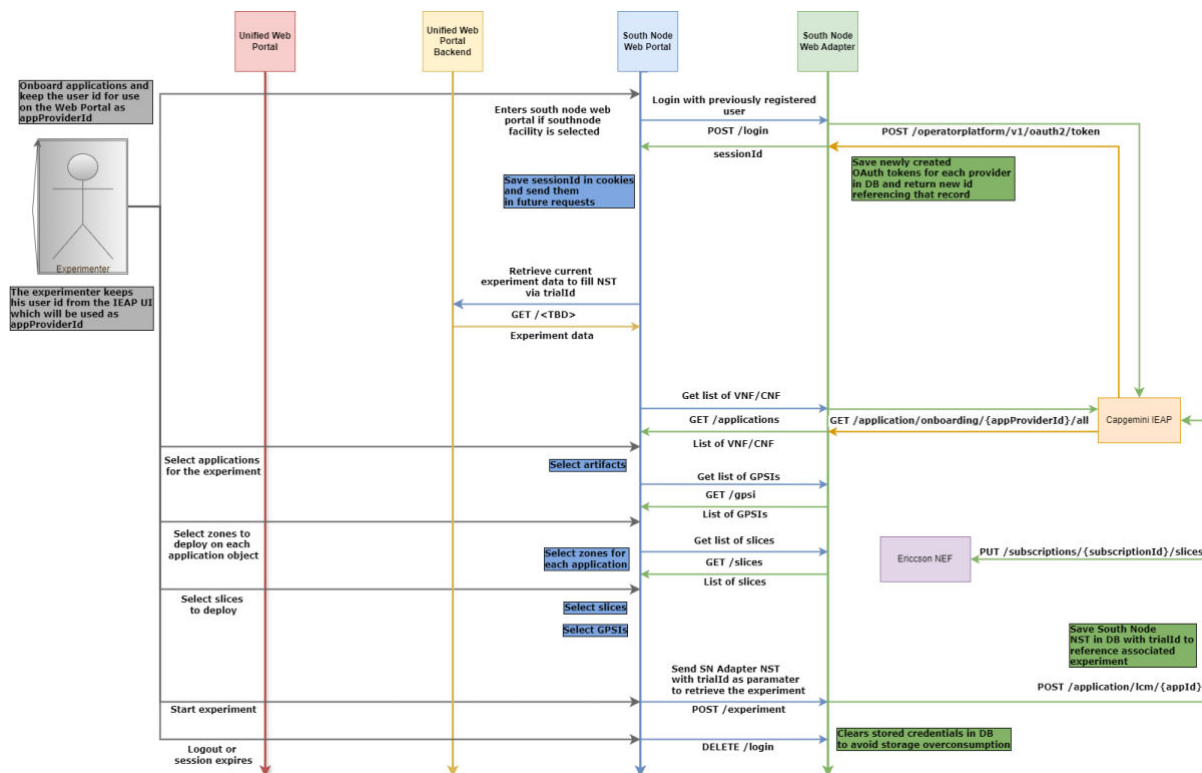


Figure 48. Workflow among South Node Trial Controller Components

1. The flow in above figure represents the process of running an experiment based on already onboarded applications. The onboarding of applications and artifacts previous to this flow will be managed by CGE internally and will not be exposed as an API to third parties. The components represented in Figure 48 and its main functionality is the following: The Unified Web Portal will expose to the end user (the experimenter) the experiment options and based of the location it will be to north or south node web portal. For the sake of simplicity, is assumed that in this case the South Portal is selected.
2. The South Node Web Portal is frontend component which will hold in the browser's session cookies that will be retrieved from the SN Adapter by the /login endpoint using previously registered user/password credentials, and will create an JSON experiment template that will be filled with getter endpoints that will provide the necessary info to later send it to the POST /experiment endpoint of the SN Adapter to save the experiment data and launch it.
3. The South Node Adapter is the backend component with will act as a middleman to hide implementation details of the background process of the experiment, making the above frontend component mostly agnostic of the providers behind. It will be also the main trigger of all the background processes of the experiment, making it a suitable target for monitoring resource and network consumption.
4. The Capgemini IEAP is the Multi Access Edge (MEC) Orchestrator at the South Node that will implement all functionality required for the management of edge cloud computing resources, exposing the CAMARA North Bound Interface standard. Its usage requires an OAuth flow that is described on the picture above.
5. The Ericsson Network Exposure Function (NEF) provides the details on the network infrastructure data and exposes it to third party components that can improve business performance based on taking decisions over the data provided. In this flow they expose a subscription interface to expose network slicing data and update subscriptions to such data.

5.2.2.3 South Node Network Slice Template

The structure of the South Node NST is the following:

- **"southNodeAdapterNetworkServiceTemplate"**: NSD template for the South Node virtualization process. Only fill when targetNode field is SOUTH.
 - **"ieapNetworkServiceDescriptor"**: IEAP LCM request array to launch listed apps
 - **"appId"**: Identifier used to refer to an application. This Identifier is globally unique so that application can be identified uniquely across different OPs.
 - **"appVersion"**: Versioning info in the format major.minor.patch
 - **"appProviderId"**: UserId of the app provider. Identifier is relevant only in context of this federation.
 - **"zoneInfo"**: Object containing the details of the zone it will be deployed to
 - **"zoneId"**: Human readable name of the zone.
 - **"flavourId"**: Flavour identifier. Should corresponds to flavours by the OP for the corresponding zone.
 - **"resourceConsumption"**: Specifies if application can be instantiated using pre-reserved resource or not. App provider can pre-reserve a pool of compute resources on each zone. 'RESERVED_RES_SHALL' instructs OP to use only the pre-reserved resources. 'RESERVED_RES_PREFER' instructs to first try using pre-reserved resource, if none available go for non-reserved resources. 'RESERVED_RES_AVOID' instructs OP not to use pre-reserved resource if possible, it is a choice depending upon the circumstances 'RESERVED_RES_FORBID' instructs OP not to use pre-reserved resources.
 - **"resPool"**: Resource pool to be used for application instantiation on this zone. Valid only if IE 'resourceConsumption' is set to 'RESERVED_RES_SHALL' or 'RESERVED_RES_PREFER'
 - **"operator"**: String identifier of the operator owning the MEC platform.
 - **"opCountry"**: ISO 3166-1 Alpha-2 code for the country of OP
 - **"deploymentSitePreference"**: Specify the value if you want to deploy the instance on all or one edge site
- **"nefNetworkSlicingDescriptor"**: Ericsson NEF Service Parameter Request Object
 - **"sliceId"**: Id of the network slice the UE is currently connected to.
 - **"gpsi"**: Array of UEs that will be attached to the slice

5.2.3 North Node Trial Engine Components

5.2.3.1 North Node Web Portal

The north web portal is designed with the aim of managing the experiments and NST templates. The north web portal is implemented using the Django framework, including two applications to handle user, experiments and NST management. It handles experiment actions and fetches KPIs from Qosium to visualize data in north web portal dashboard. By logging into this system, the user can create an experiment including trial name, target facility, start and end time and selecting slice type.

By creating an experiment by the user, a NST is created, and the user can send this NST to NNA through API. After that, the user will be able to have the control over the experiment like edit, start, stop, delete and status of the experiment. Also, the north portal has a dashboard to visualize the data taken from Qosium. To get data from Qosium and displays these data, it uses API and Grafana plugin.

Figure 49 and Figure 50 provide a view of the north web portal services. Some features of the main portal include:

- User management: including registration, logging in and out, forgetting password and editing user information.
- Defining experiment: including slice type selection.
- NST management: create, edit, start, stop, delete and status of the experiment.
- NST transportation: send NST to NNA by using API.
- Data visualization

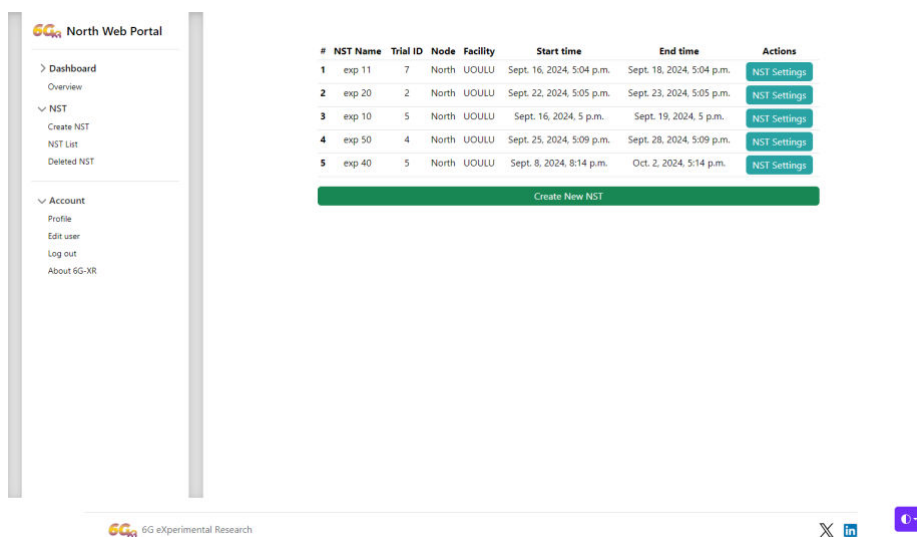


Figure 49. North web portal.

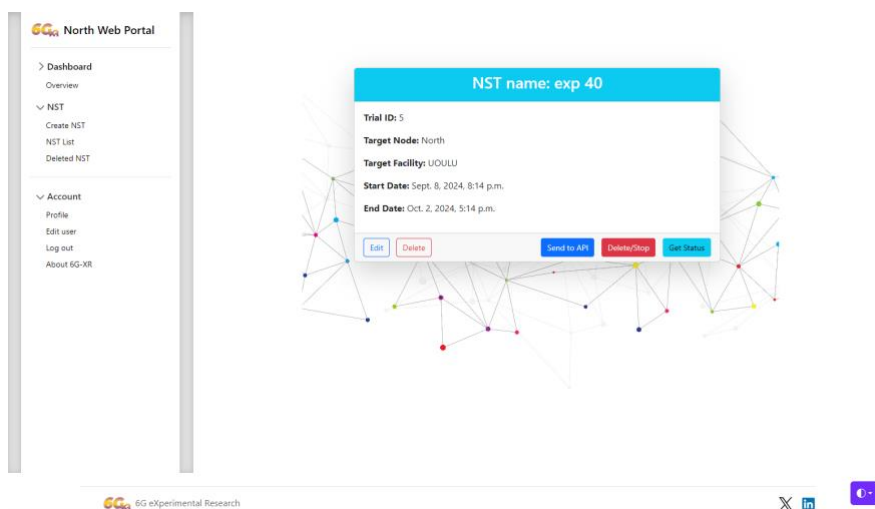


Figure 50. North web portal (NST Management)

5.2.3.2 North Node Adapter

North node adapter (NNA) facilitates the setup and management of network slices and KPIs collection in north node facility, communicating with the underlying resources and orchestration technologies. NNA is a backend component, which acts as a middleware to hide the implementation details of the background process of the experiments human user can manage via north node web portal.

North Node adapter is thus responsible for configuring the north node facility components according to the NST and starting/stopping the experiment. During the experiment NNA transfers measurement parameters from Cumucore and Qosium measurement engine to AI and reconfigures Cumucore based on the network optimization values from the AI component. NNA also keeps a log file of all network parameter changes in Cumucore. The NNA integration with underlying north node facility components is illustrated in Figure 51.

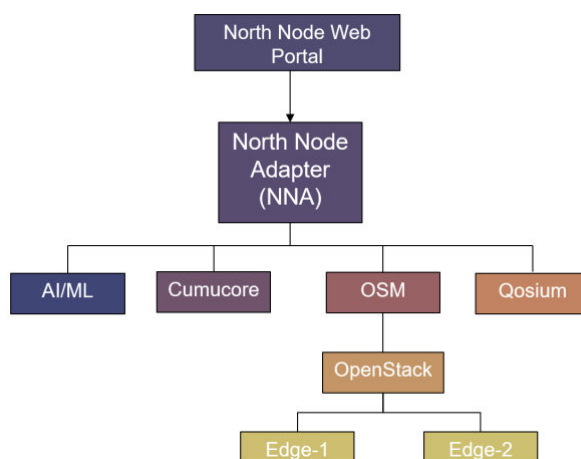


Figure 51. Architecture of NNA.

The role of underlying components are as follows:

- Cumucore:** Cumucore component is a core network, which takes care of the network slicing. By using a REST API provided by Cumucore, NNA creates desired slices defined in the NST of an experiment. During the experiment, NNA reconfigures Cumucore network parameters (latency, max. UL throughput per slice, UL threshold per slice, max. DL throughput per slice, and DL threshold per slice) based on the optimization parameters from AI/ML component.
- AI/ML:** During the experiment, NNA sends network QoS measurement results (latency, jitter, throughput, and packet loss ration) to the AI/ML component. The AI/ML component analyses the values and returns optimised network parameters per used slice which NNA then utilizes to reconfigure Cumucore on-the-fly. The interface between NNA and AI/ML is a REST API.
- Qosium:** This is a Qosium Storage software component, which the NNA uses to start and stop measurements and retrieve QoS parameters (latency, jitter, throughput, and packet loss ration) from during experiment. Qosium provides a REST API to control measurements and get QoS data.
- OSM:** Upon the initialization of an experiment NNA communicates with this component, which is requested to create virtual machines and applications according to the received NST from

the north node portal. OSM translates the request and communicates with OpenStack (through OpenStack VIM API), which provisions desired resources (VMs and networks) to the edge network.

NNA provides a REST API towards the north node web portal. By using the REST API, the portal can create and start experiments for NNA to orchestrate. Through the API the web portal can also stop and delete existing experiments. When the web portal deletes an experiment, a detailed log file is returned. The log file contains details on how NNA has reconfigured slice parameters at CumuCore based on the optimization parameters from AI/ML component during the experiment. The north node web portal can check the status of experiments in NNA by sending a status request to NNA. NNA replies back with the state the NNA is at (“initialized”, “executing”, “terminating”, “done”) or with an error if something has gone wrong with the experiment.

QoS measurements in the experiments are done by Qosium, a measurement system developed in the Open Call 1 project BANQ by Kaitotek. The Qosium measurement software used in north node is called Qosium Storage. The interaction between NNA and Qosium Storage is illustrated in Figure 52.

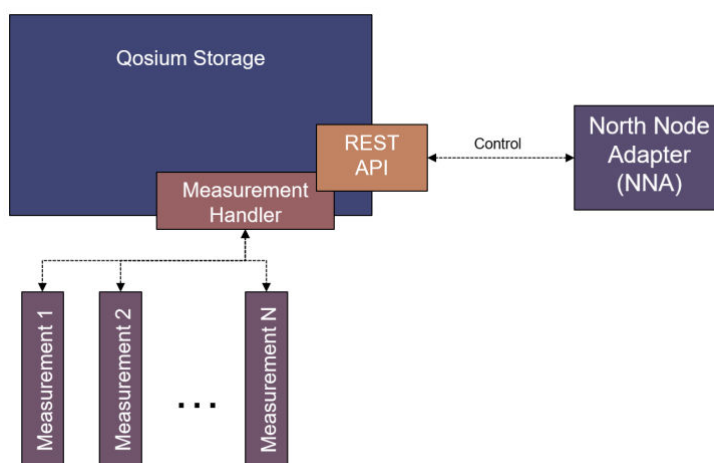


Figure 52. Interaction between NNA and Qosium.

Qosium Storage provides a REST API through which NNA controls the measurement parameters, starts and stops measurements, and retrieves recorded QoS data for sending it to the AI/ML component. In an experiment, NNA creates one Qosium measurement per network slice. The Qosium measurements are identified by slice IDs (unique UUIDs) created by NNA at the beginning of the experiment. When NNA changes CumuCore slice parameters according to the optimization parameters from the AI/ML component, existing Qosium measurement is terminated, and a new measurement is started through Qosium Storage REST API.

Orchestration of an experiment in NNA can be divided into three phases: initialization, execution, and termination. The phases are depicted in Figure 53, Figure 54 and Figure 55.

The initialization phase (Figure 53) starts with north node web portal sending NST to the NNA. This starts an experiment. The NNA checks the received NST and replies back with an ACK response. After that, NNA initializes all the underlying components starting with CumuCore. NNA creates needed slice IDs and requests CumuCore to create network slices according to the NST. After this, slice information is sent to the AI/ML component, which initializes itself accordingly. Next, NNA commands OSM to create all required VMs and applications. The initialization phase finishes with NNA starting

measurements with Qosium. NNA commands Qosium to use desired probes and start collecting and storing KPI information to Qosium Storage instance. There is one measurement in Qosium per slice.

In the execution phase (Figure 54), NNA loops for the duration of experiment (as specified in the received NST) and executes the following operations:

1. Retrieve QoS measurement values from the Qosium component.
2. Send the QoS measurement values to the AI/ML component and receive network optimization parameters back.
3. Change the CumuCore network slice parameters according to the optimization parameters received from the AI/ML component. Store updated slice parameters to a log file.
4. Stop the current measurement and start a new measurement in Qosium

Termination phase (Figure 55) begins when the duration of an experiment is reached. NNA commands Qosium Storage to stop ongoing measurements and requests the AI/ML component to deactivate the AI/ML algorithm. After that NNA tears down all the VMs and applications by sending a command to the OSM component and releases the slices in CumuCore. Finally, the north node web portal deletes the experiment by sending a request to NNA and receives back a log file containing the network adjustments done during the experiment.

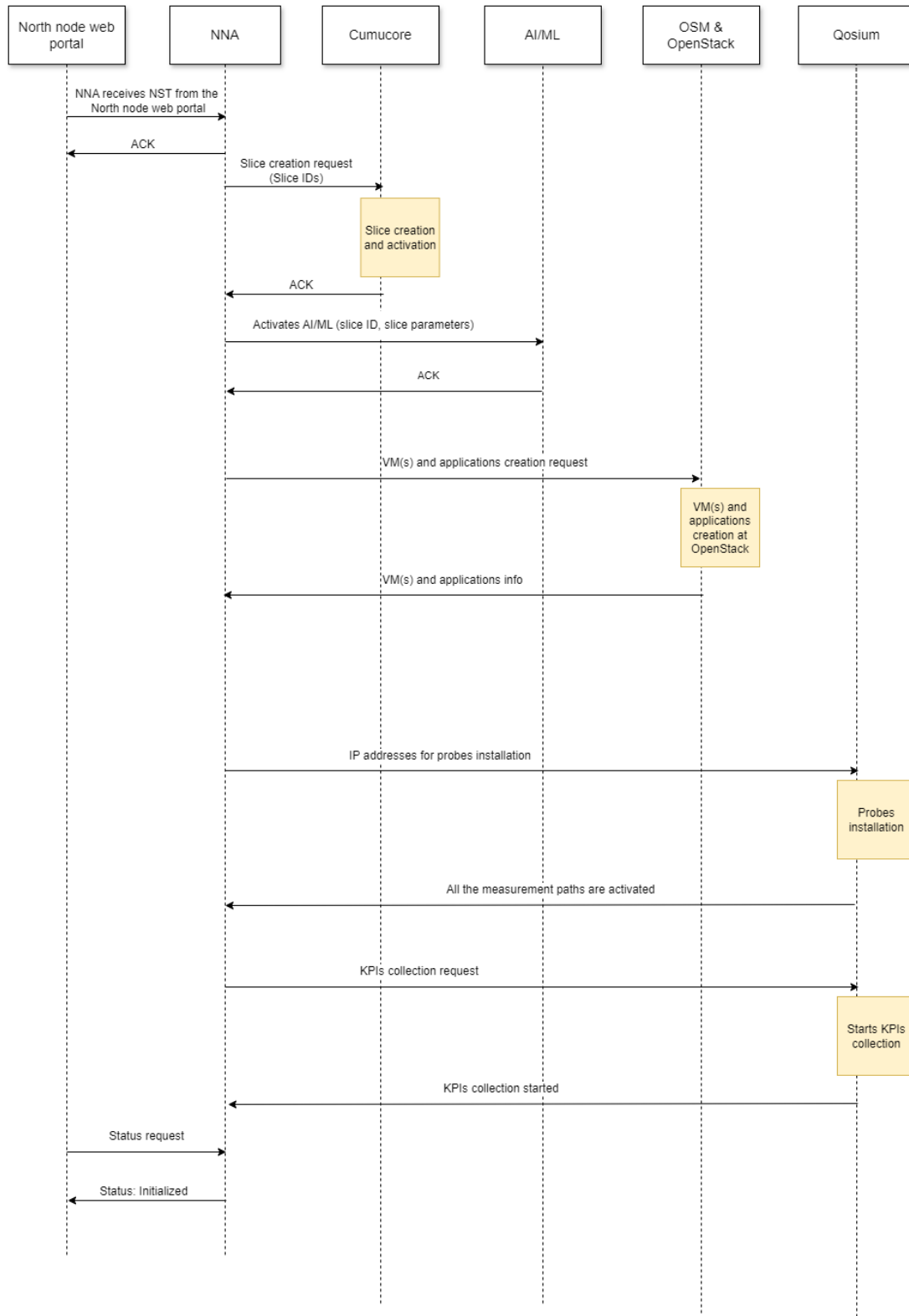


Figure 53. Initialization phase of NNA operation.

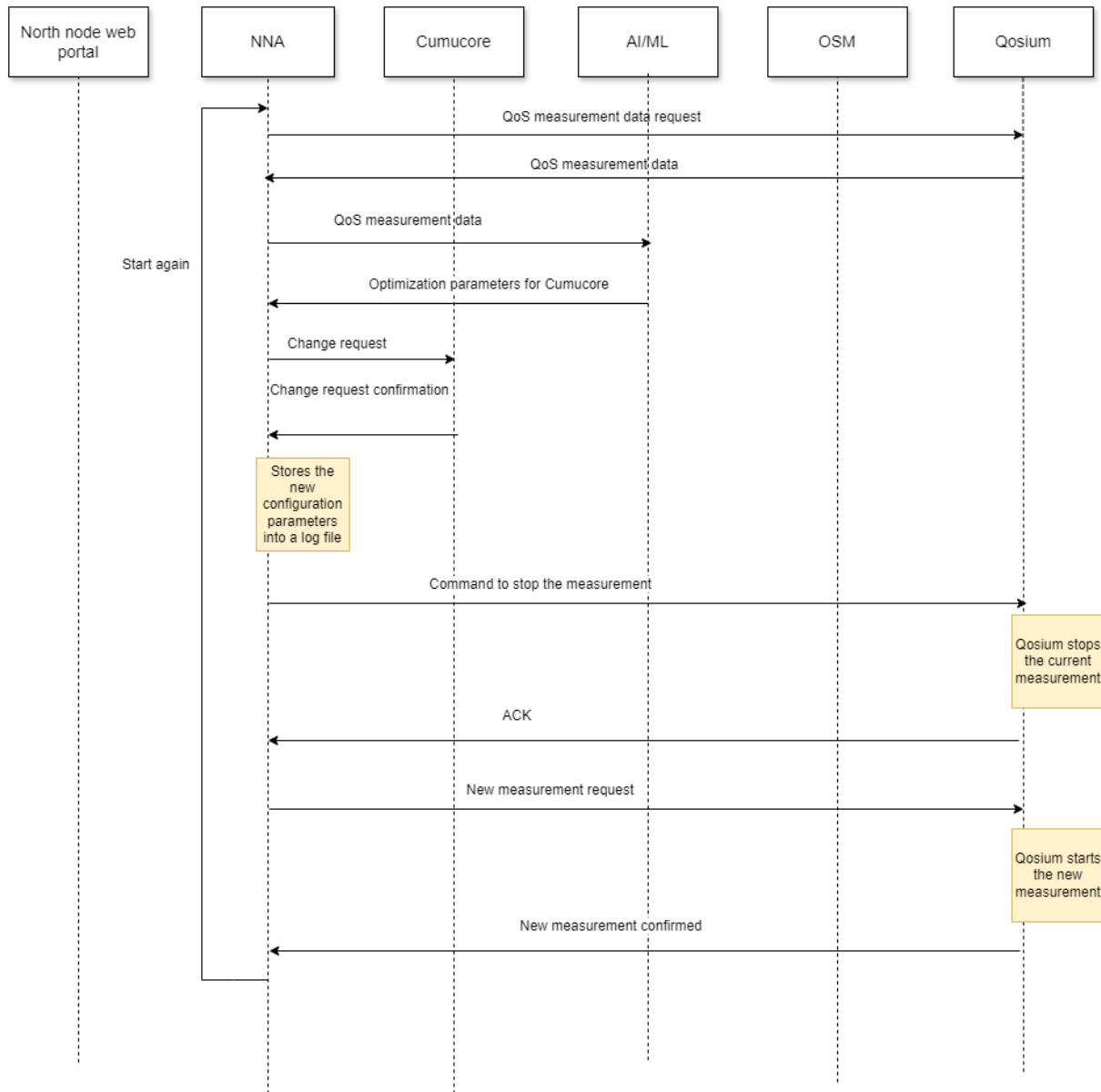


Figure 54. Execution phase of NNA operation.

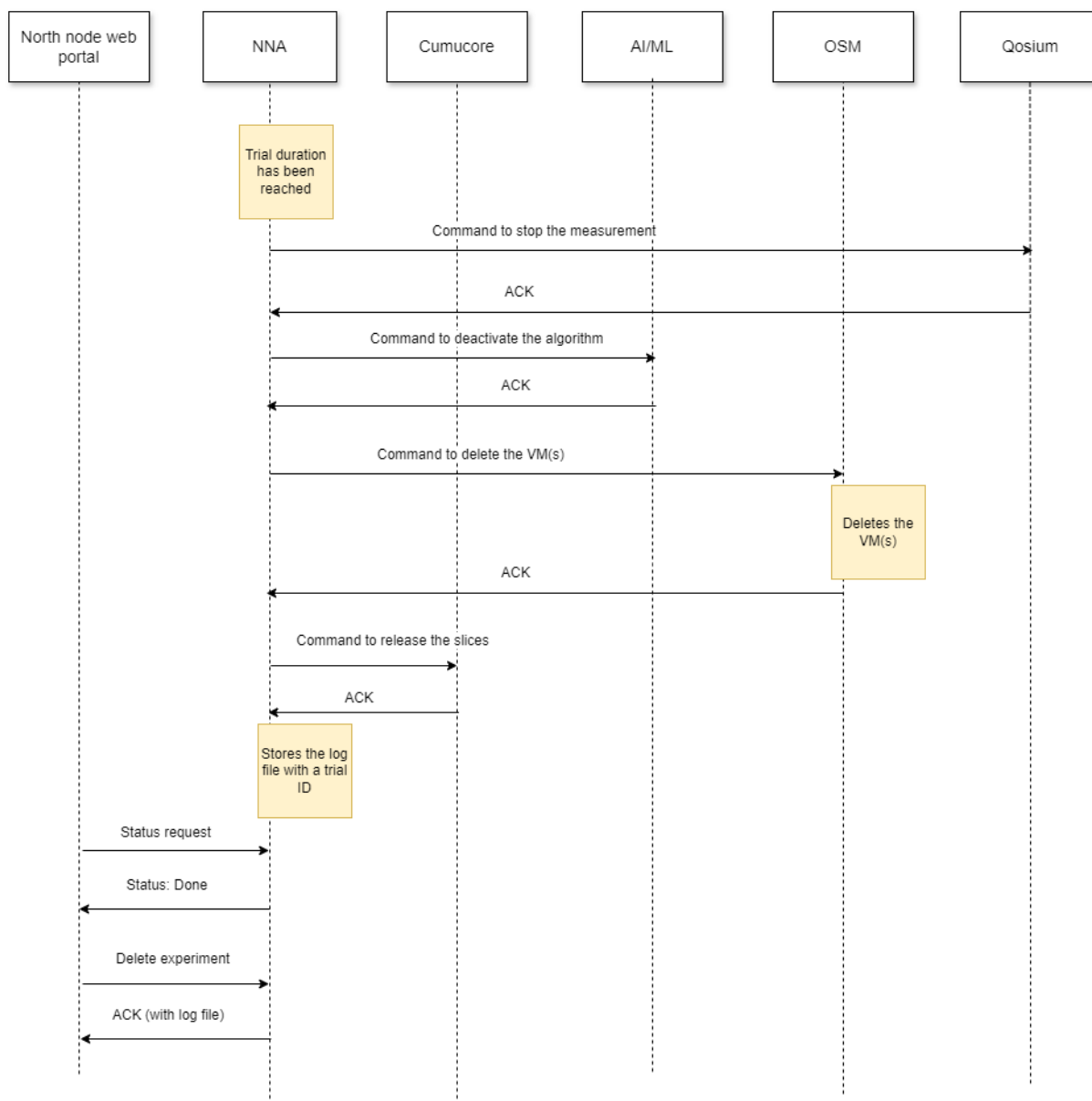


Figure 55. Termination phase of NNA operation.

5.2.3.3 North Node Network Slice Template

There are north node specific fields defined and included in NST by the north node web portal. These fields are put under “northNodeAdapterNetworkServiceTemplate” field, and they comprise “slices” array, which defines the slices and slice types to be used in a trial, and “applications” array, which comprises application names of the applications OSM should initialize in the beginning of a trial.

- **"northNodeAdapterNetworkServiceTemplate":**
 - **“slices”**: Array of slice types (“eMBB” or “uRLLC”); empty array means no slices
 - **“applications”**: Array of strings stating the applications to be instantiated at edge

6 SUMMARY

This deliverable presents the XR enabler technologies, which are developed by project and verified on 6G-XR distributed nodes - NorthNode (UOULU 5GTN and VTT 5GTN) and the SouthNode (5GBarcelona and 5TONIC). In addition, it introduces the interim deployment of trial controlled used for managing experimentation activities.

The XR enablers are categorized based on three main pillars: (1) 3GPP XR Enablers, (2) O-RAN XR Enablers and (3) 6G DISRUPTIVE XR Enablers. For each enabler the following structure is introduced

- Motivation
- Solution design with required implementation details
- Validation methodology, followed by validation results (if applicable)

After introducing the new technical enablers, this deliverable includes the trial-controller, which is used for managing and orchestrating 5G infrastructure resources during experimentation.

New enablers are validated using above-mentioned experimentation nodes, which are therefore evolving to demonstrate the performance of key Beyond 5G/6G candidate technologies, components, and architectures. Used experimentation nodes will remain valid not only in the short-term but also in the mid and long-term.

This report summarizes the interim deployment and validation results of new enablers and trial controller. Work continues and upcoming deliverable D4.3 will complement the activities by describing the final deployment results achieved in this project for new enablers and trial controller.

7 REFERENCES

- 1 P. Paymard, A. Amiri, T. E. Kolding and K. I. Pedersen, "Optimizing Mixed Capacity of Extended Reality and Mobile Broadband Services in 5G-Advanced Networks," *IEEE Access*, vol. 11, pp. 113324-113338, 2023.
- 2 "D4.1: State-of-the-art analysis and initial design of beyond 5G RAN, core, and open-source networks, disruptive RAN technologies and trial controller," [Online]. Available: <https://www.6g-xr.eu/wp-content/uploads/sites/96/2024/09/D4.1-State-of-the-art-analysis-and-initial-design-of-beyond-5G-RAN-core-and-open-source-networks-disruptive-RAN-technologies-and-trial-controller.pdf>.
- 3 "D1.1 Requirements and Use Case Specifications, 6G-XR project, June 2023.," [Online]. Available: <https://www.6g-xr.eu/wp-content/uploads/sites/96/2023/10/D1.1-Requirements-and-use-case-specifications-V1.0.pdf>.
- 4 Müller, M., Ademaj, F., Dittrich, T. *et al.* Flexible multi-node simulation of cellular mobile communications: the Vienna 5G System Level Simulator. *J Wireless Com Network* 2018, 227 (2018)
- 5 CAMARA. [Online]. Available: <https://github.com/camaraproject>. [Accessed December 2023].
- 6 CAMRA, "CAMARA-QoDAPISwagger," [Online]. Available: https://github.com/camaraproject/QualityOnDemand/tree/main/code/API_definitions. [Accessed December 2023].
- 7 Alejandro Lopez Garcia, Amr A. AbdelNabi, Daniel Camps-Mur, Miguel Catalan-Cid, Mario Montagud, "NetXRate: O-RAN enabled network assisted rate control for XR services," in *Globecom 2024*, 2024.
- 8 "D5.1: Description of sustainability experimentation framework, September 2024.," [Online]. Available: <https://www.6g-xr.eu/wp-content/uploads/sites/96/2024/09/D5.1-Description-of-sustainability-experimentation-framework.pdf>.
- 9 Kaitotek Qosium, [Online]. Available: <https://www.kaitotek.com/qosium> [Accessed 1 November 2024]
- 10 Keysight UeSIM, [Online]. Available: <https://www.keysight.com/us/en/product/P8800S/uesim-ue-emulation-ran-solutions.html> [Accessed 1 November 2024]
- 11 OpenSpeedTest, [Online]. Available: <https://github.com/openspeedtest> [Accessed 1 November 2024]
- 12 FastAPI, "FastAPI," [Online]. Available: <https://fastapi.tiangolo.com/>. [Accessed November 2024]
- 13 Accelleran, [Online]. Available: <https://acceleran.com/> [Accessed 1 November 2024]
- 14 Effnet, [Online]. Available: <https://www.effnet.com/> [Accessed 1 November 2024]
- 15 Benetel, [Online]. Available: <https://benetel.com/> [Accessed 1 November 2024]
- 16 <https://6g-xr.eu/2024/06/17/eucnc-6g-summit-2024/> [accessed November 2024]
- 17 <https://oaiibox.com/>. [Accessed November 10 2024]

18 S. P. Singh, M. J. Nokandi, M. H. Montaseri, T. Rahkonen, M. E. Leinonen and A. Pärssinen, "A 300-320 GHz Sliding-IF I/Q Receiver Front-End in 130 nm SiGe Technology," 2023 IEEE Radio Frequency Integrated Circuits Symposium (RFIC), San Diego, CA, USA, 2023, pp. 37-40.

19 [Sin2024] S. P. Singh, Radio receiver front-end ICs at the sub-THz/THz frequency range in silicon technology, Doctoral thesis, University of Oulu, Finland, p. 123, 2024.

20 3GPP TR38.901

<https://portal.3gpp.org/desktopmodules/Specifications/SpecificationDetails.aspx?specificationId=3173>

[Accessed 1 November 2024]

21 Sherif Adeshina Busari, No'elia Correia, Shahid Mumtaz, and Jonathan Rodriguez. On the Fundamental Characteristics of Intelligent Reflecting Surface Enabled MIMO Channels. IEEE Internet of Things Magazine, 5(1):67–72, 2022.

22 Shuai Zhang. Characterization and Realization of Near-Field Beamforming with RISs for mm-wave and THz Applications. In 2023 IEEE 11th Asia-Pacific Conference on Antennas and Propagation (APCAP), volume1, pages 1–2, 2023.

23 Boyu Ning, Zhongbao Tian, Weidong Mei, Zhi Chen, Chong Han, Shaoqian Li, Jinhong Yuan, and Rui Zhang. Beamforming Technologies for Ultra-Massive MIMO in Terahertz Communications. IEEE Open Journal of the Communications Society, 4:614–658, 2023.

24 H. Vulchi et al "Phase Shift Configuration for RIS-based 6G Networks using DRL Technique" IEEE CAMAD 2024